

VIRAL AND HOST GENETIC DETERMINANTS OF HEPATITIS C VIRUS  
PERSISTENCE AND INTERFERON RESISTANCE

APPROVED BY SUPERVISORY COMMITTEE

Michael Gale, Jr. Ph.D.

Wade Bresnahan Ph.D.

David Russell, Ph.D.

Iwona Stroynowski, Ph.D.

## DEDICATION

I would like to thank my mentor, Dr. Michael Gale, for his support and advice. His high expectations, challenges and encouragement for all of us created an environment in which fundamental questions about HCV biology could be asked and answered. In addition, several other members of the Gale lab in particular played key roles in my work. I collaborated extensively with Dr. Chunfu Wang on the interferon resistance project and his efforts were essential to our establishment of the HP model system. His positive attitude, persistence and dedication to science have been a true inspiration to me. Eileen Foy and Dr. Yueh-Ming Loo were invaluable contributors to the HCV persistence project and without their help (and good cheer) we would not have solved the mystery of the Huh7.5 cells. I would like to thank Dr. Takashi Fujita for his timely insights into the RIG-I pathway and for his generosity in sharing reagents. My wife Kathy has been a constant source of reassurance and understanding, especially when none of my experiments were working, and her genuine excitement about my work has helped me more than I can say. My parents, Rhea and Anne, have also been unwavering in their support over my postgraduate years. Finally, I would like to thank my friends Jason Mock, Andy Shulman and Elie Traer, with whom I share a true love of science.

VIRAL AND HOST GENETIC DETERMINANTS OF HEPATITIS C VIRUS  
PERSISTENCE AND INTERFERON RESISTANCE

by

RHEA MYERS SUMPTER, JR

DISSERTATION

Presented to the Faculty of the Graduate School of Biomedical Sciences

The University of Texas Southwestern Medical Center at Dallas

In Partial Fulfillment of the Requirements

For the Degree of

DOCTOR OF PHILOSOPHY

The University of Texas Southwestern Medical Center at Dallas

Dallas, Texas

July, 2004

VIRAL AND HOST GENETIC DETERMINANTS OF HEPATITIS C VIRUS  
PERSISTENCE AND INTERFERON RESISTANCE

Publication No. \_\_\_\_\_

Rhea Myers Sumpter, Jr. Ph.D.

The University of Texas Southwestern Medical Center at Dallas, 2004

Supervising Professor: Michael Gale, Jr., Ph.D.

## ABSTRACT

Approximately 170 million people worldwide are chronically infected with hepatitis C virus (HCV), which is an important cause of cirrhosis and hepatocellular carcinoma. HCV replicates through an error-prone process that may support the evolution of genetic variants resistant to the host cell antiviral response and interferon (IFN)-based therapy. The development of the HCV RNA replicon system has allowed the study of persistent HCV RNA replication in tissue culture. We evaluated HCV/IFN interactions within a long-term culture system of Huh7 cell lines harboring different variants of an HCV genotype 1b subgenomic RNA replicon that differed only at two sites within the NS5A coding region. A replicon with a lysine (K) insertion at HCV codon 2040 (K2040) replicated efficiently and exhibited sequence stability in the absence of host antiviral pressure. In contrast, a replicon with an leucine (L) to serine (S) point mutation at HCV codon 2198 (L2198S) replicated poorly and triggered a cellular response characterized by IFN- $\beta$  production and low-level interferon-stimulated gene (ISG) expression. When maintained in long term-culture, the L2198S RNA evolved into a stable high passage (HP) variant with 6 additional point mutations throughout the HCV protein-coding region that enhanced viral replication. The HP RNA transduced Huh7 cells with more than 1000-fold greater efficiency than its L2198S progenitor or the K2040 sequence. Replication of the HP RNA resisted suppression by IFN- $\alpha$  treatment and was associated with viral-directed reduction in host cell expression and action of ISG56, an antagonist of HCV RNA translation.

We also demonstrated that HCV subgenomic RNA replicons can be used to model the early events of HCV infection. We found that HCV RNA replicons rapidly induce the cellular antiviral response upon their transfection into host Huh7 cells and we determined that intracellular HCV double stranded RNA (dsRNA) is a potent agonist of host dsRNA-activated pathways. A Huh7 derived cell line that is highly permissive for transduction by HCV replicons is specifically defective in the activation of interferon regulatory factor (IRF)-3 by virus infection or HCV dsRNA transfection. We found that a mutation in the caspase recruitment domain (CARD) of the DExH/D-box helicase protein RIG-I, a component of the TLR3-independent intracellular dsRNA-responsive IRF-3 activation pathway, was responsible for this phenotype. Restoration of RIG-I-mediated IRF-3 activation through genetic complementation resulted in decreased permissiveness to HCV RNA replication. These results establish the RIG-I→IRF-3 pathway as a critical determinant of HCV persistence.

## TABLE OF CONTENTS

CHAPTER 1: LITERATURE REVIEW AND BACKGROUND .....	1
CHAPTER 2: MATERIALS AND METHODS .....	28
CHAPTER 3: VIRAL EVOLUTION AND INTERFERON RESISTANCE OF HCV RNA REPLICATION IN A CELL CULTURE MODEL.....	44
CHAPTER 4: RIG-I DEFINES HOST CELL PERMISSIVENESS TO HCV RNA REPLICATION .....	82
CHAPTER 5: GENERAL CONCLUSIONS AND FUTURE DIRECTIONS .....	121
BIBLIOGRAPHY .....	135
VITAE .....	164

## PRIOR PUBLICATIONS

1. **Foy, E., Li, K., C. Wang, R. Sumpter, M. Ikeda, S. M. Lemon, and M. Gale, Jr.** 2003. Regulation of interferon regulatory factor-3 by the hepatitis C virus serine protease. *Science* **300**:1145-1148.
2. **Pflugheber, J., B. Fredericksen, R. Sumpter, C. Wang, F. Ware, D. Sodora, and M. Gale, Jr.** 2002. Regulation of PKR and IRF-1 during hepatitis C virus RNA replication. *Proc Natl Acad Sci U S A* **99**:4650-4655.
3. **Wang, C., J. Pflugheber, R. Sumpter, D. Sodora, D. Hui, G. C. Sen, and M. Gale, Jr.** 2003. Alpha interferon induces distinct translational control programs to suppress hepatitis C virus RNA replication. *J Virol* **77**:3898-912.
4. **Wilson, W. K., R. M. Sumpter, J. J. Warren, P. S. Rogers, B. Ruan, and G. J. Schroepfer, Jr.** 1996. Analysis of unsaturated C27 sterols by nuclear magnetic resonance spectroscopy. *J Lipid Res* **37**:1529-55.
5. **Ye, J., C. Wang, R. Sumpter, Jr., M. S. Brown, J. L. Goldstein, and M. Gale, Jr.** 2003. Disruption of hepatitis C virus RNA replication through inhibition of host protein geranylgeranylation. *Proc Natl Acad Sci U S A* **100**:15865-15870.



## LIST OF FIGURES

Figure 1-1: Genomic organization of hepatitis C virus. ....	4
Figure 1-2: The HCV subgenomic replicon. ....	6
Figure 1-3: The innate antiviral response to dsRNA. ....	9
Figure 3-1: Assessment of protein expression and IRF-3 localization in Huh7 control and HCV replicon cell lines .....	69
Figure 3-2: Features of genetically distinct HCV replicons and Huh7 cell lines .....	70
Figure 3-3: HP adaptive mutations act synergistically to confer increased transduction efficiency of the HCV replicon RNA.....	72
Figure 3-4: HP mutations associate with IFN resistant HCV RNA replication independently of defects in IFN signaling to the ISRE .....	73
Figure 3-5: HP mutations specifically confer IFN resistance to HCV RNA replication .....	75
Figure 3-6: Suppression of ISG56 expression by the HCV HP replicon and restoration of expression in cured cells does not associate with differences in IFN receptor signaling to the ISRE .....	77
Figure 3-7: Differential ribosome recruitment by the HCV replicon RNA and alteration of the ISG56:(p48)eIF3 ratio associates with IFN resistant viral RNA replication.....	80
Figure 4-1: Activation of the host antiviral response by HCV RNA transfection.....	100
Figure 4-2: Analysis of ISRE, PKR, IKK and P38 MAPK activation in Huh7 and Huh7.5 cells .....	103
Figure 4-3: Huh7.5 cells have a defective IRF-3 response to virus and HCV dsRNA.....	105

Figure 4-4: Localization of the IRF-3 activation defect in Huh7.5 cells .....	108
Figure 4-5: RIG-I specifically complements defective virus-induced IRF-3 reporter activation in Huh7.5 cells.....	110
Figure 4-6: RIG-I restores the IRF-3 response to virus and HCV dsRNA in Huh7.5 cells	111
Figure 4-7: RIG-I controls the host response to HCV dsRNA.....	114
Figure 4-8: Identification and characterization of mutant RIG-I from Huh7.5 cells.....	116
Figure 4-9: RIG-I defines host cell permissiveness to HCV RNA replication .....	119
Figure 5-1: Differential regulation of P38 and Akt phosphorylation in Huh7 and replicon- bearing cell lines .....	129
Figure 5-2: Potentiation of IFN-induced ISG expression in IFN sensitive K2040 replicon	130
Figure 5-3: Regulation of IRF-5 localization and expression .....	131
Figure 5-4: RIG-I is alternatively spliced.....	132
Figure 5-5: HCV NS5A regulates TLR3 and TLR4 signaling.....	133

## LIST OF TABLES

Table 3-1: Primer pairs used for site directed mutagenesis.....	66
Table 3-2: IFN- $\beta$ production in control and HCV replicon-bearing cells.....	67
Table 3-3: ISGs identified in Huh7 cells and HCV replicon-bearing Huh7 cell lines by microarray analysis .....	68
Table 4-1: Primers used for PCR amplification of cDNAs for sequencing .....	98
Table 4-2: Primers used for real time PCR analysis .....	99

## **CHAPTER 1: LITERATURE REVIEW AND BACKGROUND**

### Epidemiology of hepatitis C virus

Hepatitis C virus (HCV) was identified as the major etiologic agent causing non-A, non-B (NANB) post-transfusion hepatitis in 1989 (28). Its discovery enabled the development of screening procedures for HCV-contaminated blood products and led to an 85-95% reduction in incidence of post-transfusion hepatitis after routine screening of the blood supply, beginning around 1991 (99). The primary route of transmission for HCV is parenteral, via needle sharing during intravenous drug use, with a seroprevalence rate of 50-100% among intravenous drug users, and the extremely high (~20%) seroprevalence rate in Egypt has been linked to parenteral administration of antischistosomal therapy (19). Sexual and maternal fetal transmission probably play only a minor role in HCV infection, but the likelihood of transmission increases in patients with HIV coinfection (99). However, for a significant proportion of HCV infected patients, no risk factors can be identified (19). Currently, there are an estimated 170 million chronically infected individuals worldwide, with approximately 2.7 million in the United States (99).

### Natural history of HCV infection

HCV infection leads to symptoms of acute hepatitis only in about 10% of patients (99), and it results in a chronic, lifelong infection in approximately 80% of untreated patients (19). A typical course for HCV infection involves subclinical hepatitis for 10-20 years,

followed by progression to cirrhosis in up to 20% of patients, with approximately 1% of cirrhotic patients developing hepatocellular carcinoma per year (19).

HCV has also been associated with a broad spectrum of immunological disorders, including autoimmune hepatitis, Sjögrens syndrome, Lichen planus, thyroiditis, glomerulonephritis, cryoglobulinemia and polyarteritis nodosa (115). In addition, an association has been found between HCV and B-cell lymphomas (168), some of which resolve with antiviral therapy (66). The role of HCV in these extrahepatic manifestations is poorly understood, but at least some of them could be related to the ability of HCV to infect non-hepatic cell types, especially peripheral blood mononuclear cells (168).

### HCV therapeutics

Current therapeutic regimens for HCV infection involve the use of IFN- $\alpha$  alone or in combination with the guanine nucleoside analog ribavirin (117). Unfortunately, side effects of high-dose IFN such as flu-like symptoms and severe depression often necessitate the discontinuation of therapy (116). However, the recent development of pegylated IFNs, which are slowly metabolized and thus have longer therapeutic half-lives, has allowed for maintenance of more consistent IFN levels and reduction of side effects (42). Despite improvements in combined therapy, many patients, especially those with genotype 1 HCV (see below), do not achieve a sustained virologic response (99). Due to the high failure rate of IFN-based therapy for HCV, alternative methods for treatment of HCV are needed. Several inhibitors of the HCV serine protease are currently in clinical trials and may soon

offer a third treatment option, especially for those who fail IFN-based therapy (116). However, the high mutation rate of HCV ensures that resistant variants will emerge, and mutations in the HCV protease leading to decreased inhibitor susceptibility have already been isolated in laboratory models for HCV replication (101). Thus, additional modalities will have to be devised in the future to eradicate chronic HCV infection.

### Taxonomy of HCV

HCV is classified as a member of the family *Flaviviridae*, which includes the human pathogens Yellow Fever virus, Dengue virus and West Nile virus, and is the sole member of the genus *hepaciviridae*. HCV displays a remarkable degree of sequence variability, and analysis of nucleotide sequences of the E1 envelope gene from patient samples resulted in the identification of six HCV genotypes that can be further subdivided into at least 12 HCV subtypes (23). There is no FDA approved methodology for determining HCV genotype, although several commercially available tests based on analysis of variation in the HCV 5' nontranslated region (NTR) are available (5). HCV genotyping can be a useful tool in patient management, as response rates for pegylated IFN/ribavirin treatment vary from approximately 88% for genotypes 2 and 3 to about 48% for genotypes 1 (the most common genotype infecting North Americans), 4, 5 and 6 (19). The underlying reasons for differential responsiveness to therapy between HCV genotypes are unknown.

### HCV genome and proteins

HCV is a small enveloped RNA virus with a ~9.6 kilobase positive-sense genome encoding a single viral polyprotein of 3011 amino acids (aa), which is co- and post-translationally cleaved by host proteases and the viral NS3/4A serine protease to yield at least 10 mature viral proteins. Translation of the HCV polyprotein is driven by the HCV internal ribosome entry site (IRES), a highly structured region of RNA at the 5' end of the HCV genome that allows translation without the requirement of the 5' cap structure found in most cellular mRNAs (4). The 3' nontranslated region (3' NTR) is also highly structured and is required for viral RNA replication (91).

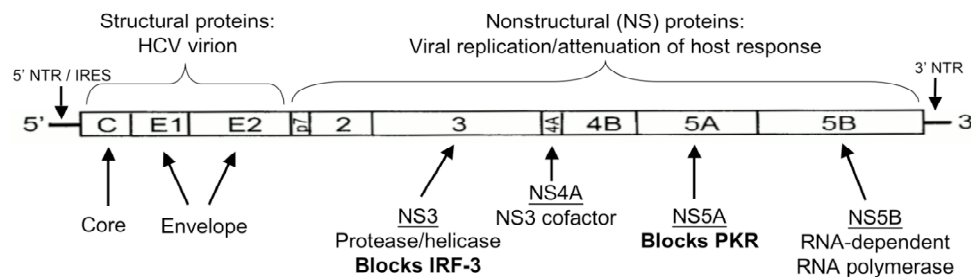


Fig 1-1: Genomic organization of hepatitis C virus.

The HCV virion contains three structural proteins: Core, which forms the viral capsid, and the viral envelope proteins E1 and E2. A host-derived lipid envelope acquired during viral egress from the infected cell surrounds HCV viral particles. In addition to their functions as components of the HCV virion, the HCV core has been proposed to regulate a wide variety of host processes (129), but these observations have yet to be confirmed in the contexts of HCV RNA replication. The nonstructural (NS) proteins p7 and NS2 are dispensable for replication, as demonstrated in subgenomic replicon studies, while the

remaining NS proteins: NS3, NS4A, NS4B, NS5A and NS5B are required for the assembly of viral replicase complexes (105).

HCV replicates in association with host endoplasmic reticulum-derived membranes and leads to the formation of characteristic “membranous webs” in the cytoplasm of the host cell (132), which can also be induced by the ectopic expression of the HCV NS4B protein alone (36). Replication of genomic viral RNA by the HCV NS5B RNA dependent RNA polymerase (RdRp) proceeds via a negative strand replicative intermediate, which is thought to represent approximately 10% of the total HCV RNA in the infected cell. Like other viral RdRps, NS5B is highly prone to errors during replication and thus HCV exists as a “quasispecies population” in the infected individual (111). In addition to their roles in viral replication, the NS3/4A protease and NS5A have been shown to antagonize the host innate antiviral response by inhibiting IRF-3 and PKR function, respectively (see below). The intrinsic ability of HCV proteins to regulate the host antiviral response combined with the high mutation rate of HCV may result in selection of HCV variants capable of attenuating the host response and resisting the effects of IFN.

#### Model systems for HCV infection

Animal model systems have been developed for the study of HCV infection including the chimpanzee model (147) and the mouse chimeric liver model (120). The chimpanzee model has been particularly useful for examining the events following initial infection with HCV, because infection in humans is often subclinical and patients are typically infected for



many years before diagnosis. In addition, *in vitro* transcribed RNA from several infectious cDNA clones of genotype 1 HCV have been successfully used to establish productive infection in chimpanzees, allowing for consistency between studies (13, 90). Important observations from these studies include the robust induction of interferon stimulated genes (ISGs) early in the course of infection, indicating that HCV replication has the capacity to stimulate the host antiviral response, while in the context of persistent infection the IFN response is blunted, suggesting that HCV also encodes mechanisms to attenuate the host response (153, 165).

The mouse chimeric liver model is the only small animal model currently available for HCV infection. It involves the use of transgenic mice that express uroplasminogen activator (uPA) under control of a liver-specific albumin promoter (120). UPA is highly toxic to hepatocytes, resulting in involution of the mouse liver, which can then be replaced with human liver explants. These mice can then be infected with HCV, which establishes persistent infection in the human hepatocytes. Unfortunately, this model has not yet been made widely available, limiting its utility.

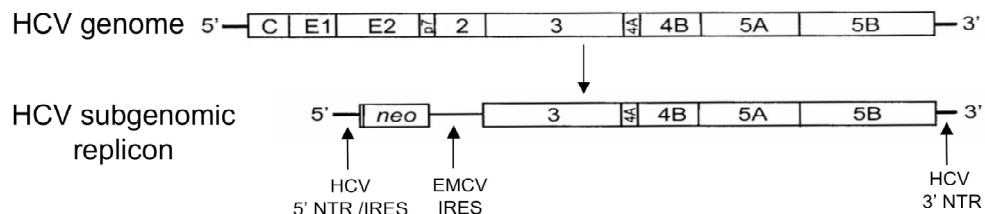


Fig 1-2. The HCV subgenomic replicon

HCV cannot currently be propagated in tissue culture. For this reason, HCV replicons have become the system of choice for investigating HCV replication and interaction with the innate antiviral response. In this system, host hepatoma (Huh7) cells are transduced with a bicistronic RNA construct in which the HCV IRES drives translation of the selectable marker neomycin phosphotransferase (Neo) and the encephalomyocarditis virus (EMCV) IRES drives translation of a subgenomic HCV RNA sequence encoding the nonstructural proteins NS3 through NS5B. HCV replicons encoding the full-length HCV polyprotein have also been developed, but they do not produce infectious virus (77). It was quickly recognized that the prototype HCV genotype 1B-derived coding region usually acquired one or more adaptive mutations during the selection process (16, 93). When these adaptive mutations were reintroduced into the original sequence, they often resulted in an increased frequency of stable transduction, although combinations of several adaptive mutations that arose independently from each other actually decreased viral fitness (93). To date, the majority of adaptive mutations described have been localized in the NS3 and NS5A coding regions, but the only adaptive mutations for which functional data have been obtained are those that increase the processivity of the NS5B RNA polymerase (27). Our group has found that HCV subgenomic replicons with distinct adaptive mutations in NS3 and NS5A varied widely in their replicative fitness and ability to control the host antiviral response (40, 133). In particular, the NS5A from a highly fit replicon mutation was able to regulate PKR to a more efficiently than the NS5A from a less fit variant, even though they each differed by only a single amino acid from the prototype sequence (133). Several groups have investigated the interferon (IFN) sensitivity of HCV replicons and have found them to be

exquisitely sensitive to IFN- $\alpha$  treatment, with IC<sub>50</sub> doses of approximately 2 IU/mL (12), well below the peak serum IFN level of 10-12 IU/mL achieved in patients undergoing IFN therapy (86).

### Interferon

Interferons (IFNs) are a family of cytokines composed of two groups: the type I interferons (IFN- $\alpha$  and IFN- $\beta$ ) and type II IFN (IFN- $\gamma$ ) (151). In addition, several IFN homologs such as IFN- $\lambda$  (92) and IFN- $\omega$  (1) have been identified, but their functions are not well understood. 14 distinct IFN- $\alpha$  genes, encoding 12 unique protein products, have been identified (131), while there is a single IFN- $\beta$  locus. IFN biology has been the subject of intense investigation, leading to the elucidation of signal transduction pathways involved in the sensing of virus inside infected cells, the subsequent induction of type I IFNs and the signal transduction mechanisms leading to the upregulation of hundreds of interferon stimulated genes (ISGs) and the induction of an “antiviral state” (143). The functions of the vast majority of ISGs in contributing to the antiviral state remain to be defined, as do the individual roles of the various type I IFNs. The innate response to viral infection is a critical component of host defense to viral infection and represents the first line of host defense once viruses have invaded the cell.

## The innate antiviral response

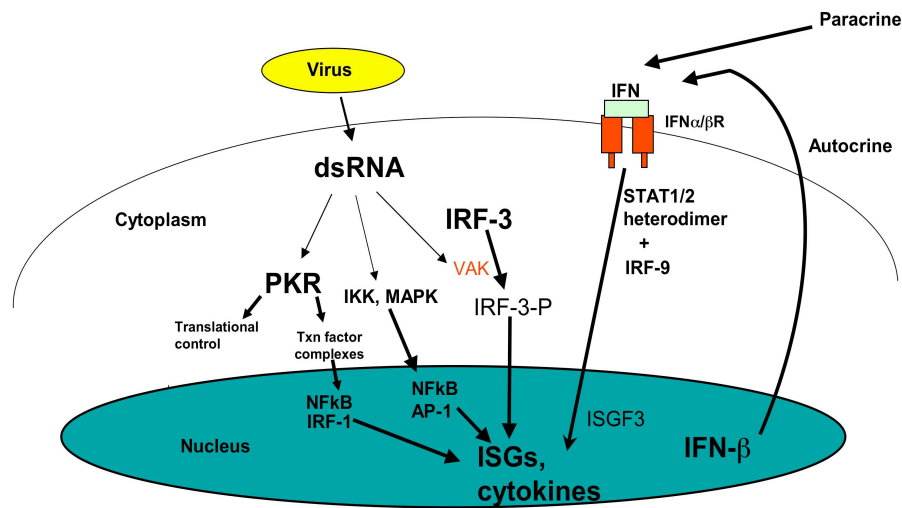


Fig 1-3: The innate antiviral response to dsRNA.

Viral replication often leads to production of double-stranded RNA (dsRNA), which is a pathogen associated molecular pattern (PAMP) (119) that is recognized by several distinct sensors within the host cell. Activation of dsRNA-sensing pathways leads to reduced permissiveness of the infected cell for viral replication and results in the production of cytokines (such as IL-6 and IFN- $\beta$ ) and chemokines (such as RANTES) that both induce the antiviral state in neighboring cells and recruit immune effector cells to the site of infection to initiate the adaptive immune response (48). In addition to dsRNA, viral components such as measles nucleocapsid (N) protein (163) and herpes simplex virus CpG DNA (108) also appear to be PAMPs, and have been shown to activate the host response upon their introduction into host cells. I will focus on host dsRNA-responsive pathways, as they are critical for host defense against HCV in our model systems.

### *2'-5' OAS*

2'-5' oligoadenylate synthetases (2-5OAs) are a family of 3 enzymes (in humans) that all catalyze the synthesis of 2'-5' linked oligomers of adenosine upon activation by direct recognition of dsRNA through double stranded RNA binding motifs (DSRBMs) (135). Oligoadenylate polymers then activate RNase L, a latent cytoplasmic RNase that cleaves cellular and viral RNAs 3' of UU and UA dinucleotide motifs (139). Importantly, RNase L also specifically cleaves the 28S ribosomal RNA, resulting in the inhibition of translation of surviving viral and cellular mRNAs (80). RNase L-deficient mice are more susceptible to lethal infection with RNA viruses such as encephalomyocarditis virus (EMCV) (188), demonstrating an important role for this pathway in host antiviral defense.

### *PKR*

PKR is a dsRNA-activated serine/threonine kinase with important roles in both translational and transcriptional responses to viral infection (177). PKR directly recognizes dsRNA through tandem DSRBMs and autophosphorylates upon dsRNA binding (37). Activated PKR then phosphorylates eIF2 $\alpha$ , a component of the multisubunit eIF2 translation initiation factor, which is responsible for bringing tRNA charged with the initiator methionine (Met) to the 40S ribosomal subunit during translation initiation (176). Formation of the eIF2-Met-tRNA complex requires hydrolysis of GTP bound by eIF2, and eIF2-GDP is then recycled to eIF2-GTP by the guanine nucleotide exchange factor eIF2B (166). Since the concentration of eIF2-GTP is limiting for translation initiation, a reduction of in the available eIF2-GTP pool leads to a dramatic decrease in protein translation (121). Phosphorylation of

eIF2 $\alpha$  on serine 51 by PKR results in an increased affinity of eIF2B for eIF2-GDP, leading to the functional sequestration of eIF2 from the translation initiation machinery and subsequent reduction in both host and viral protein synthesis (155). PKR is also important for cellular apoptosis in response to viral infection (31), due to its ability to induce host translational shutoff (34), and PKR-deficient mice are more susceptible to lethal infection by the RNA viruses VSV and influenza, demonstrating the importance of PKR in host defense against viral infection (7).

In addition to its important role in translational control, PKR is also important for the activation of the transcription factors NF $\kappa$ B and IRF-1 (96) as well as the mitogen activated protein kinases (MAPKs) P38 and JNK in response to extracellular signals such as bacterial lipopolysaccharide (LPS) (53, 177) or the synthetic dsRNA poly inosine:cytosine (poly(I)(C)), as will be discussed below.

### *IRF-1*

Interferon regulatory factor (IRF)-1 is the prototype member of the IRF family of transcription factors. As its name implies, was the first interferon regulatory factor discovered (43). IRF-1 has the same DNA binding specificity as IRF-2, its closest homolog (60), but while both IRF-1 and IRF-2 recognize the same promoter elements, they have opposing roles in the regulation of transcription, due to the fact that IRF-1 contains a C-terminal transcriptional activation domain, which is lacking in IRF-2 (60). Upregulation of IRF-1 by a variety of stimuli, including viral infection, poly(I)(C), IFN- $\alpha/\beta$ , IFN- $\gamma$  (the most

potent IRF-1 inducer known), IL-6 or TNF- $\alpha$  results in its C-terminal phosphorylation and redistribution throughout the nucleus, where it displaces IRF-2 from positive regulatory domain (PRD) I elements (94). The kinase activity of PKR has been shown to be necessary for IRF-1 activation in the context of poly(I)(C) and IFN- $\gamma$  treatment (96). While IRF-1 by itself is a relatively weak transcriptional activator, it cooperates with other transcription factors, such as NF $\kappa$ B (164), to activate transcription of IRF-1 target genes. IRF-1 is an ISG, and it also stimulates its own transcription via a positive regulatory domain I (PRDI) element in its promoter (123). Interestingly, IRF-2 is also an IRF-1 target gene (61), and, because it has a much longer half-life than IRF-1, its upregulation results in the eventual shutoff of the IRF-1 transcriptional response (94).

Although IRF-1 was initially identified as an IFN- $\beta$  promoter binding protein, it is not required for the induction of type I IFNs in response to viral infections (114). While mice deficient in IRF-1 are more susceptible to lethal infection with EMCV, they are able to clear other viral infections as well as wild-type controls (88). The importance of IRF-1 in the host antiviral response therefore appears to be virus-specific. IRF-1 is also critical for the establishment of a TH<sub>1</sub> response, and immune effector cells from IRF-1-deficient mice are defective in their responses to TH<sub>1</sub> cytokines such as IL-12 (159). In addition to its role in the antiviral response, IRF-1 has been definitively shown to be a tumor suppressor (161), thus, in the context of a persistent viral infection, it is likely that inhibition of IRF-1 activity could contribute to carcinogenesis (47).

### *IRF-3*

IRF-3 plays an indispensable role in the induction of IFN- $\beta$  in response to virus infection. It is a constitutively expressed transcription factor that is localized primarily in the cytoplasm, where it is thought to exist in an “autoinhibited” state due to interaction between the C-terminus and N-terminal DNA binding domain (103). Unlike IRFs 1, 5, 7 or 9, IRF-3 is not an ISG (8). IRF-3 is activated by diverse stimuli, including DNA damaging agents (87), measles virus nucleocapsid (N) protein (163), viral infection (186) and dsRNA treatment (174), resulting in phosphorylation of kinase targets in the N-terminus, central proline rich region or C-terminus (144). In the case of viral infection or dsRNA treatment, several serine and threonine residues in the C-terminal region of IRF-3 are phosphorylated, releasing IRF-3 from autoinhibition, after which it dimerizes and translocates to the nucleus (102). IRF-3 then binds to a specialized subset of interferon stimulated response element (ISRE) sites similar to the IFN- $\beta$  PRDIII site and associates with the histone acetyltransferases CBP/p300 to promote transcription of IRF-3 target genes, including IFNs  $\beta$  and IFN- $\alpha$ 1 (IFN- $\alpha$ 4 in mice) (130, 173). Studies of site-directed IRF-3 mutants have demonstrated that phosphorylation of IRF-3 on several residues, including serines 385 and 386 (124), as well as and four serines and one threonine in the 396-405 region occurs during IRF-3 activation in response to virus or dsRNA (185). Two I kappa kinase (IKK)-related kinases, TANK binding kinase 1 (TBK1) and IKK $\epsilon$ , were recently identified by several groups as putative “virus-activated kinases” (VAKs) that are capable of mediating the activation of IRF-3 when overexpressed (38, 145). TBK1-deficient mouse embryo fibroblasts (MEFs) do not activate IRF-3 in response to infection with Sendai virus or



dsRNA treatment (118), indicating that TBK1 is a critical component of the VAK, whereas a role for IKK $\epsilon$  in IRF-3 activation during viral infection remains to be established.

In addition to type I IFNs, a subset of genes that are activated directly by IRF-3 has been described. These genes are induced in response to viral infection or dsRNA treatment without the requirement of IFN production and include ISG56 and chemokine RANTES (CCR5) (56). ISG56 is a tetratricopeptide repeat (TPR) motif-containing protein that binds to the P48 subunit of the translation initiation factor eIF3 and thus inhibits translation of host and viral proteins (59, 75). Our group has demonstrated that HCV IRES-mediated translation is especially sensitive to inhibition by ISG56 (170), and the importance of RANTES in the recruitment of immune effector cells, including T cells, monocytes, natural killer (NK) cells and dendritic cells is well known (6). Future work on the roles of other IRF-3 target genes will give greater insight into the role of these proteins in mediating the IRF-3-dependent host response.

The importance of IRF-3 in control of viral infection was made clear by studies of IRF-3 knockout mice, which exhibit increased susceptibility to a variety of viral infections. MEFs from IRF-3-deficient mice are almost completely devoid of IFN- $\beta$  induction in response to virus or dsRNA (141). Due to the loss of IRF-3-mediated early type I IFN production, the subsequent IRF-7/IFN- $\alpha$  amplification loop (described below) is also abolished (141).

There are distinct pathways for IRF-3 activation in response to dsRNA, depending on the manner in which the cell encounters the stimulus. In response to extracellular dsRNA, toll-like receptor (TLR) 3-mediated signaling is utilized (3), whereas the DexH/D box helicase RIG-I is critical for IRF-3 activation in response to intracellular dsRNA (184). TLR3 is a member of the TLR family of PAMP recognition molecules that are responsible for the activation of host signaling pathways in response to bacterial products such as peptidoglycan, lipopolysaccharide (LPS), flagellin and lipoproteins, viral single-stranded RNAs (ssRNAs) and unmethylated CpG DNA (2). TLRs contain a conserved cytoplasmic toll/interleukin (IL)-1 homology domain (TIR) that recruits downstream adapter molecules upon ligand recognition (35). All TLRs have in common the use of the adapter molecule MyD88, which upon activation signals through the well-characterized IL-1 pathway by activating IL-1 receptor associated kinases (IRAKs) 1 and 4, ultimately leading to the activation of NF $\kappa$ B and AP-1 family transcription factors and resulting in the upregulation of proinflammatory cytokines (128). In addition to this conserved pathway, TLR3 and TLR4 also utilize the adapter molecule TRIF to signal the activation of NF $\kappa$ B and IRF-3 and appear to be unique among TLRs in their ability to induce IFN- $\beta$  (67). In addition, a dependence on PKR has been demonstrated for some aspects of TLR3 and TLR4 signaling, although it is not yet clear if its kinase activity is required (177). This raises the intriguing possibility that inhibition or sequestration of PKR could attenuate TLR signaling. It is not known exactly where TLR3 senses viral dsRNA, as it has been reported to reside both on the surface of cells and inside intracellular vesicles of the endocytic pathway (113), and a definitive role for TLR3 in the host antiviral response has yet to be established. Curiously, TLRs 7, 8 and 9,

which mediate strictly MyD88-dependent responses to uridine-rich viral ssRNAs (in the case of TLR7/8) or unmethylated CpG DNA (TLR9), also have the capacity to activate IFN- $\alpha$  transcription (30) through a mechanism that remains to be characterized but may involve one or more IRFs.

After its identification as a dsRNA pattern recognition molecule (3), it seemed likely that TLR3 would represent the primary sensor responsible for activating IRF-3 and IFN- $\beta$  production in response to viral dsRNA. However, the topology of the TLR3, with its cytoplasmic signaling domain and extracellular or intravesicular dsRNA-recognition domain, was difficult to reconcile with its putative role in recognition of intracellular viral pathogens. In addition, both TLR3- and TRIF-null mouse embryo fibroblasts (MEFs) respond to viral infection by activating IRF-3 and producing IFN- $\beta$  (184), implying the existence of an additional sensor responsive to intracellular dsRNA. One such sensor, RIG-I was recently identified and appears to fill this role (184). RIG-I belongs to the DExH/D RNA helicase family, which has 58 members in the human genome that perform diverse functions from RNA splicing to translational control (136). RIG-I is one of the few RNA helicases that contains a caspase recruitment domain (CARD). Other CARD-containing proteins, such as NOD1 and NOD2, have previously been identified as intracellular pattern recognition molecules for bacterial products (24). NOD1 and NOD2 interact with the CARD-containing kinase RIP2 to signal the activation of NF $\kappa$ B and MAPKs and activate a similar pattern of cytokine expression as observed for TLRs (78). RIG-I shares this ability to activate NF $\kappa$ B in response to dsRNA or virus infection, but, unlike NOD1 and NOD2, it also activates IRF-3,

leading to the induction of IFN- $\beta$  (184). The role of RIG-I in the induction of MAPK signaling has not yet been investigated.

### *IRF-5*

Relatively little is known about the functions of IRF-5 in the antiviral response, as it was discovered only recently. IRF-5 is normally expressed only at low levels, if at all, in most tissues, but its expression can be induced by IFN treatment (11). Like IRF-3, it is normally localized to the cytoplasm in the absence of viral infection, but redistributes to the nucleus in infected cells (10). Interestingly, infection with VSV and NDV results in the activation of IRF-5, while infection with SenV does not, indicating either specificity in the response for certain viruses, or perhaps inhibition of IRF-5 by SenV (11). Presently, it is unknown whether the virus-activated pathways leading to the activation of IRF-5 are distinct from the IRF-3 and IRF-7 response pathways, and the viral trigger for IRF-5 activation has not been identified. However, since SenV infection results in activation of both IRF-3 and IRF-7, but not IRF-5, it is possible that at least some components of the IRF-5 activation pathway are unique. Overexpression of IRF-5 during viral infection results in a shift in the profile of IFN- $\alpha$  subtypes produced by infected cells, favoring the production of IFN- $\alpha$ 8 (8), which has the most potent antiviral activity of any IFN- $\alpha$  (39). In addition, virus-activated IRF-5 induces the expression of several chemokines, including RANTES, which may be important for recruitment of components of the adaptive immune response during viral infection (10). IRF-5 interacts with both IRF-3 and IRF-7 to form heterodimers, but while IRF-3/5 heterodimers are competent to bind DNA, IRF-5/7 heterodimers are not functional

(9). This difference is probably due to the location of interaction domains responsible for heterodimer formation. The heterodimerization domains that mediate IRF-3/5 interaction are located in the C-termini of both molecules, leaving the N-terminal DNA binding domains free to bind promoters, while IRFs 5 and 7 interact at their N-termini, precluding DNA binding (9). Thus, IRF-5 may help to tailor IFN- $\alpha$  subtype-specific responses for distinct viruses, depending on what other IRFs are expressed and activated. The study of IRF-5 is still in its early stages, but the results obtained thus far suggest that it may play an important role in the host response to certain viral infections.

### *IRF-7*

IRF-7 is usually expressed at low levels, if at all (except in lymphoid cells) but its expression is induced by IFN treatment (107). Thus, the induction of IFN- $\beta$  and IFN- $\alpha$ 1 by IRF-3 results in the upregulation of IRF-7, where it localizes to the cytoplasm in uninfected cells (125). If virus/dsRNA is present, IRF-7 is activated by phosphorylation of a cluster of C-terminal serines homologous to those mediating IRF-3 activation in the same context (110). Indeed, IRF-7 phosphorylation appears to also be mediated by TBK1 and, perhaps preferentially, IKK $\epsilon$  (145). Upon activation, IRF-7 homodimerizes or heterodimerizes with IRF-3 and translocates to the nucleus, where it plays an essential role in the amplification of the host antiviral response by inducing the transcription of IFN- $\alpha$  genes, as demonstrated by studies of IRF-7-deficient MEFs (141). Interestingly, IRF-7 is constitutively expressed at high levels in plasmacytoid dendritic cells, which have been shown to mediate high-level production of IFN- $\alpha$  during virus infection (85).

### *IRF-9/Type I IFN signaling*

IRF-9 (also called P48 or ISGF3 $\gamma$ ) is a component of the transcription factor interferon stimulated gene factor (ISGF) 3, along with STAT1 and STAT2, and is required for the binding of ISGF3 to interferon stimulated response elements (ISREs) in the promoters of type I IFN target genes (151). After IFN treatment, STAT1 and a heterodimer of STAT2/IRF-9, which are preassociated with the cytoplasmic tail of the type I IFN receptor, are rapidly phosphorylated by the tyrosine kinase Jak1 (112, 151). The ISGF3 heterotrimer then translocates to the nucleus to activate ISG transcription by binding to ISRE sites in the promoters of ISGs.

Type I IFN induces several other signaling pathways besides ISGF3-mediated signaling. For example, activation of STAT3 in response to type I IFN has been reported by several groups (154, 181). Activated STAT3 dimerizes, then translocates to the nucleus, where it binds to gamma activated sequence (GAS) elements to induce transcription (100). The mitogen activated protein kinases ERK and P38 (see below), as well as a number of other alternative signaling pathways are also activated by type I IFNs (134). Although the reasons for the disparity in antiviral activities of IFN- $\alpha$  subtypes is at present unknown, differences in the activation of alternative type I IFN signaling pathways as well as ISGF3-mediated signaling should be considered as a possible explanation.

### *MAP kinases*

Mitogen activated protein kinases (MAPKs) mediate cellular responses to stress, cytokines and growth factors (26). In mammalian cells, there are three distinct and evolutionarily conserved MAPK pathways, extracellular regulated kinase (ERK), c-Jun N-terminal kinase (JNK) and P38 MAPK (142). MAPK activation follows an evolutionarily conserved pathway in which MAP 3 kinases (MAPKKK) phosphorylate MAP 2 kinases (MAPKK), which are dual specificity kinases that in turn phosphorylate the MAPKs that mediate cellular responses on threonine (T) and tyrosine (Y) residues in a conserved TXY motif (82, 97). One example of a MAPK cascade is the activation of P38 by extracellular dsRNA or LPS (via TLR 3 and 4, respectively), which requires TAK1 (MAP 3 kinase)→MKK3/6 (MAP 2 kinase)→P38 (MAP kinase) (82). Activated P38 then regulates diverse cellular processes in part by phosphorylating transcription factors of the AP-1/ATF family, which subsequently induce the transcription of proinflammatory cytokines such as IL-6 (97). P38 has also been implicated in the serine phosphorylation of STAT1 and STAT3, which, while not directly affecting their ability to bind DNA, is an important determinant of their ability to induced the transcription of certain genes (54). The translation of certain mRNAs that contain AU-rich regions in their 3' NTRs, such as those encoding the cytokines IL-1 and TNF- $\alpha$ , is also enhanced by activated P38 (97). The MAPK JNK2 has been shown to be essential for the induction of IFN- $\beta$  in response to virus infection or intracellular dsRNA, probably due to its role in activating the transcription factors c-Jun and ATF-2, which heterodimerize and bind to the PRDIV element of the IFN- $\beta$  enhanceosome (29),

although the mechanism by which JNK is activated under these circumstances remains obscure.

### *NFκB*

One of the many facets of nuclear factor kappa B (NFκB) biology is its part in the host response to virus infection (140). In mammals, NFκB consists of a family of five transcription factors, namely Rel (c-Rel), RelA (p65), RelB, NFκB1 (p50) and NFκB2 (p52) (84). All NFκB family members contain a Rel homology domain (RHD), which is responsible for the homo- or heterodimerization, nuclear translocation and DNA binding activity of NFκB family members in response to a bewildering array of stimuli including cytokines such as IL-1 and TNFα, as well as TLR activation and virus infection (84). NFκB1 and NFκB2 are initially translated as the larger precursor proteins p105 and p100, respectively (137). While the proteolytic processing of NFκB1 to p50 is unregulated, the p100→p50 processing event is inducible and results in the preferential release of p50/RelB heterodimers (84). NFκB family members are normally held in an inactive state in the cytoplasm by IκB proteins, such as IκBα. IκBα, in turn, is a substrate for signal-dependent phosphorylation on serines 32 and 36 by the I kappa kinase (IKK) complex, which consists of IKKα and IKKβ along with the noncatalytic regulatory subunit IKKγ (NEMO) (51). Serine 32/36 phosphorylated IκBα is a substrate for ubiquitin-dependent proteolysis, and its destruction liberates sequestered NFκB transcription factors, unmasking their RHDs and resulting in their dimerization, nuclear translocation and activation of NFκB target genes (137). IKKα is dispensable for the classical activation pathway in response to most stimuli,



but is absolutely required for p100→p50 signal dependent proteolysis (84). IKK $\beta$ -mediated NF $\kappa$ B activation and subsequent binding of NF $\kappa$ B to the PRDII element of the IFN- $\beta$  promoter is required for the induction of IFN- $\beta$  in response to virus infection (29). In addition, many ISGs and cytokines contain NF $\kappa$ B binding sites in their promoters.

Besides IKKs  $\alpha$  and  $\beta$ , the IKK-like (“noncanonical”) kinases TBK1 and IKK $\epsilon$  are also capable of activating NF $\kappa$ B when overexpressed (38, 145). However, they phosphorylate I $\kappa$ B $\alpha$  on only one of the two critical serine residues (serine 36) necessary for its ubiquitination, and thus degradation of I $\kappa$ B $\alpha$  is not observed during TBK1- or IKK $\epsilon$ -mediated NF $\kappa$ B activation (84). In contrast to IKK $\beta$ , a role for virus-induced NF $\kappa$ B activation has not been established for the noncanonical IKKs.

#### Viral antagonism of the innate antiviral response

In order to establish productive infection in the host, viruses have evolved diverse strategies to counteract the antiviral response (48), and mutant viruses defective in their ability to block the host response are often attenuated (14, 49). Viral evasion represents a fascinating example of convergent evolution. In some cases viruses arrive at almost exactly the same solution, albeit with widely divergent proteins, while in others they achieve similar effects by targeting components in a host pathway in distinct ways. Studies of viral interference with host response pathways have led to identification of the key components responsible for defense against viral infection.

Several viruses encode proteins that sequester dsRNA and thus block OAS, PKR and IRF-3-mediated responses. Viral proteins that fit this model include the influenza virus NS1 and vaccinia virus E3L proteins (172, 179). By targeting the most upstream portion of the host dsRNA response, these viral proteins and RNAs inhibit multiple host dsRNA-activated pathways. Another example of a general suppression of the host response is provided by the VSV M protein, which blocks the export of cellular mRNAs from the nucleus, preventing the production of cytokines and ISGs (169). In addition, several structured viral RNAs, including adenovirus VAI, Epstein-Barr virus EBER and HIV TAR RNAs, act as inhibitors rather than activators of the dsRNA response (139).

Other viral proteins block selected components of the antiviral response using an impressive array of strategies. The vaccinia virus K3L is capable of inhibiting PKR activity because its N-terminal region is homologous to the region of eIF2 $\alpha$  containing serine 51, thus allowing it to act as a competitive inhibitor or perhaps a pseudosubstrate for activated PKR (148). Herpes simplex virus ICP34.5 protein, on the other hand, binds to protein phosphatase 1 $\alpha$  (PP1 $\alpha$ ) and stimulates the dephosphorylation of eIF2 $\alpha$  (62). The V-proteins (C-proteins in the case of Sendai virus) of paramyxoviruses such as SV5 and mumps virus attenuate type I interferon signaling by binding to STAT1 and recruiting ubiquitin ligases, resulting in the proteasome-mediated degradation of STAT1 (72). Adenovirus E1A blocks IFN signaling both by inhibiting STAT1 mRNA transcription and blocking the ability of activated STAT1 to induce ISG expression (106). Human herpesvirus 8 (Kaposi's sarcoma virus) encodes four IRF homologs (vIRF1-4), which appear to act as dominant negative

isoforms of cellular IRFs 1, 3 and 7 and also antagonize the activities of p300 and PKR (8). These are only a few examples of survival strategies used by viruses, and a common theme that has emerged from the study of virus-host interaction is that in order to be successful, viruses must evolve the ability to attenuate the host response.

### Antagonism of the host response by HCV

#### *E2*

The sequence encoding the E2 envelope protein of HCV is the most highly variable region of the HCV genome (63). Since E2 is found on the surface of the virion, its variability may reflect evolution in response to selective pressure from neutralizing antibodies (175). A highly conserved region of E2, however, is homologous to the C-terminal catalytic loop domain of PKR, including several of the sites involved in PKR autophosphorylation along with a region homologous to the serine 51 PKR phosphorylation site of eIF2 $\alpha$ . This region has been termed the PKR-eIF2 $\alpha$  phosphorylation homology domain (PePHD) (162). PePHD regions from genotypes 1A and 1B, which are refractory to IFN therapy, more closely resemble the PKR and eIF2 $\alpha$  sequences than those from the IFN-sensitive genotypes 2 and 3 (63). However, role for the PePHD in viral persistence and resistance to IFN therapy has not yet been established.

#### *NS3/4A*

HCV NS3/4A is a multifunctional protein complex that contains serine protease, NTPase and helicase activities. In addition to its role in viral polyprotein processing, it has

been reported to modulate the activities of protein kinase A (PKA) and protein kinase C (PKC) (20), but the functional relevance of these observations is not understood. Our group has shown that NS3/4A blocks the activation of IRF-3, resulting in inhibition of IFN- $\beta$  induction in response to viral infection (40). While the NTPase and helicase activities of NS3/4A are dispensable for IRF-3 inhibition, the serine protease activity of NS3/4A is required. NS3/4A-mediated IRF-3 inhibition causes a loss of IRF-3 phosphorylation in response to viral infection, suggesting that the putative target of proteolytic cleavage is necessary for IRF-3 phosphorylation. The HCV protease has fairly strict substrate specificity for *trans*-cleavage events (89), thus it is likely that this cellular factor contains a conserved NS3 target site. Pharmacological inhibition of NS3/4A thus both blocks viral replication by inhibiting the cleavage of the HCV polyprotein and restores IRF-3 activation in response to HCV dsRNA. Therefore, the efficacy of HCV protease inhibitors currently in clinical trials could be partly due to their “dual efficacy” in targeting an essential step in HCV replication and restoring the host response to viral infection (40).

### *NS5A*

Although HCV NS5A does not encode any known enzymatic activities, it is capable of binding to the PKR dimerization domain and thus inhibiting the activation of PKR in response to dsRNA (44). It exists as both a basally phosphorylated and hyperphosphorylated isoforms (83), but the functional significance of these modifications is not understood. A correlation between IFN resistance and mutations in the “Interferon Sensitivity Determining Region” (ISDR) of NS5A, which overlaps with its PKR binding domain (PKRBD), has been

described in studies from a number of laboratories [reviewed in (63)]. Distinct HCV NS5A coding regions isolated from infected patients have differential abilities to regulate PKR activity, due to mutations in the PKRBD of NS5A that affect its association with PKR (45). Stable overexpression of NS5A results in oncogenic transformation of NIH3T3 cells in a mouse tumorigenesis model, but this phenotype was observed only for NS5A isolates that can regulate PKR, suggesting that PKR inhibition by NS5A may contribute to the development of hepatocellular carcinoma (47).

In addition to its ability to block PKR, NS5A has been reported to interact with the adapter protein Grb2 by homophilic interactions between Src homology 3 (SH3) domains in Grb2 and a highly conserved C-terminal SH3 domain in NS5A (160). This results in an inhibition of epidermal growth factor (EGF)-mediated activation of extracellular regulated kinases (ERK) 1 and 2, and may contribute to HCV-induced carcinogenesis (64). NS5A has also been shown to interact with the P85 subunit of phosphoinositol 3 kinase (PI3K), leading to increased activation of antiapoptotic cellular pathways (64, 152). Modulation of these signaling pathways by NS5A may also contribute to viral persistence and the propensity of HCV to induce oncogenic transformation.

### Summary

Modulation of the host antiviral response is a key feature of virus infection. In order to replicate and spread, viruses must redirect cellular processes to evade the antiviral strategies of the host. HCV is remarkably successful at evading these defenses as evidenced

by its persistent infection of hundreds of millions of people worldwide. Understanding how HCV triggers, regulates and counteracts the host antiviral response is essential for developing new approaches to combat the current HCV pandemic.

## CHAPTER 2: MATERIALS AND METHODS

### Cell culture and viruses

Huh7 and Huh7.5 cells were propagated in Dulbecco's Modified Eagles Medium (DMEM) supplemented with 10% fetal bovine serum, 200  $\mu$ M L-glutamine, and Sigma antibiotic/antimycotic solution. Huh7-L2198S cells, Huh7-K2040 cells and Huh7-HP cells respectively containing the L2198S, K2040 or HP subgenomic HCV RNA replicon were described previously (40, 170, 183). 293T/Neo, 293T/TLR3 and 293T/TLR4 cell lines were gifts from Dr. K. Fitzgerald. Stable replicon and 293T cell lines were maintained in DMEM supplemented with 200  $\mu$ g/mL G418. The presence of the specific adaptive mutation within the replicon RNA of the stable cell lines was verified by nt sequence analysis as described below. Low passage isolates of each cell line (corresponding to approximately 8 population doublings) were expanded and stored frozen for further analysis. To initiate long-term study, Huh7-K2040 and Huh7-L2198S cells were thawed and cultures were concurrently initiated and maintained for the study duration. For IFN, anisomycin, poly(I)(C), LPS or IL-1 treatment of cells, medium was removed from cell cultures and replaced with pre-warmed medium containing the indicated concentration of IFN- $\alpha$ 2a (PBL Laboratories), anisomycin (Sigma), poly(I)(C) (Amersham), LPS (from *E. coli*; a gift from Dr. R. Munford) or IL-1 (R & D Systems).

For the generation of cured cell lines, we transiently cultured Huh7-derived replicon cell lines for 2 weeks or longer in medium containing 100 units/ml (U/ml) of IFN $\alpha$ 2a. We

verified that the cells were cured of the HCV replicon RNA and that they were sensitive to G418 selection as previously described (40).

Sendai virus (SenV; Cantell strain) was obtained from ATCC. Vesicular stomatitis virus (VSV) was a gift from Dr. P. Marcus.

#### Nucleotide sequence analysis: cellular mRNAs

The nucleotide sequence of TBK1, IKK $\epsilon$ , TRIF and RIG-I from Huh7 and Huh7.5 cells was determined as follows: Total cellular RNA was extracted from Huh7 and Huh7.5 cells with Trizol reagent using the manufacturer's protocol (Invitrogen). The recovered RNA was resuspended in water and 1  $\mu$ g of RNA was reverse transcribed with Omniscript (Qiagen) reverse transcriptase (RT) for 1.5 h using an oligo dT oligonucleotide primer (Ambion) and the manufacturer's protocol. 10% of the RT reaction was then used in each PCR reaction (ExTaq, Takara) to amplify full-length cDNAs. PCR conditions were 1 min at 95°C, 30 sec at 60°C and 2 min 30 sec at 68°C for 45 cycles. The amplified DNA was then purified by agarose gel electrophoresis and was extracted from the gel using the QIAquick kit (Qiagen) and the manufacturer's protocol. DNA fragments were sequenced directly by automated sequencing and complete ORF sequences for each mRNA were assembled using Vector NTI software (Informax). Primers used for cDNA amplification are listed in Table 4-1.



### Nucleotide sequence analysis: HCV replicons

The nucleotide sequence of the each HCV replicon was determined as follows: Total cellular RNA was extracted from replicon-bearing cells with Trizol reagent using the manufacturer's protocol (Invitrogen). The recovered RNA was resuspended in water and 1 µg of RNA was reverse transcribed with Omniscript (Qiagen) reverse transcriptase (RT) for 1.5 h using the HCV specific primer: 8081a: 5' GCCAGTATCAGCACTCTCTG 3' and the manufacturer's protocol. 10% of the RT reaction was then used in each PCR reaction (Advantage 2, Clontech) to amplify 4 overlapping fragments using the primer pairs 1844s: 5' TACATGGTGTAGTCGAGGTT 3' / 3575a: 5' TCTCCTGCCTGCTTAGTCTGG 3'; 3086s: 5' ACTCAATGCTGTAGCATATTA 3' / 5112a: 5' AACCTCCACGTACTCCTCAGC 3'; 4711s: 5' TCACTCAGCTGCTGAAGAGG 3' / 6572a: 5' ACGATAAGGCGAGCTGGCTTG 3'; or 6071s: 5' TACCGTAAGCGAGGAGGCTAG 3' / 8052a: 5' GCGGCTCACGGACCTTTCACA 3'. PCR conditions were 1 min at 95°C, 30 sec at 60°C and 2 min 30 sec at 68°C for 40 cycles. The amplified DNA was then purified by agarose gel electrophoresis and was extracted from the gel using the QIAquick kit and the manufacturer's protocol (Qiagen). DNA fragments were then sequenced directly by automated sequencing and complete replicon sequences were assembled using Vector NTI software (Informax).

### Site directed mutagenesis and reconstruction of the HP replicon

Nt substitutions identified within the evolved HP replicon sequence were reintroduced into a previously assembled prototype Con1 HCV replicon sequence, pHCV

1bpt (40). Each mutation was individually introduced by site directed mutagenesis using the QuickChange<sup>TM</sup> XL Site-Directed Mutagenesis Kit (Stratagene). The mutagenic primers used in this procedure are listed in Table 3-1. For subcloning and assembly of the reconstructed HP sequence, an interval spanning the PmeI to the Eco47III restriction sites was first amplified using the primer pair PmeIs: 5' AGTTTAAACAGACCACAACGG 3'/Eco47IIIa: 5' ACGACGGCTGGGAGGAGCAAG 3' and the Advantage 2 HF PCR kit (Clontech) from a replicon RNA template to obtain a DNA fragment containing the Q1737R mutation. The PCR product was ligated into pCR2.1 (Invitrogen) to yield pCR2.1 Q1737R. Following site-directed mutagenesis of the Con1 DNA, a restriction fragment spanning the BsrGI/BspEI sites and containing the K1609E mutation was inserted into the corresponding sites of pCR2.1 Q1737R to yield pCR2.1 K1609E/Q1737R. A DNA fragment corresponding to the PmeI to AccI restriction sites of the Con 1 sequence and containing the P1115L mutation was then cloned into the corresponding sites of pCR2.1 K1609E/Q1737R to yield pCR2.1 HP 5'. pCR2.1 HP 5' was then digested with BsrGI and Eco47III restriction enzymes and the resulting DNA fragment was subcloned into pHCV 1bpt to yield pHCV 1bpt HP 5'. In parallel, fragments containing the P2007A, L2198S, S2236P, and K2040 mutations engineered into the Con1 sequence were subcloned individually into a pHCV 1bpt recipient to respectively yield pHCV 1b P2007A, pHCV 1b L2198S, pHCV 1b S2236P, and pHCV 1b K2040. An Eco47III/MluI DNA restriction fragment containing the P2007A mutation was then subcloned into pHCV1b L2198S to yield pHCV1b P2007A/L2198S, and then a XhoI/MunI DNA restriction fragment from the engineered Con1 sequence containing the S2236P mutation was subcloned into pHCV1b P2007A/L2198S to yield pHCV 1b HP

NS5A. A BsrGI/Eco47III DNA restriction fragment from pCR2.1 HP 5' was then subcloned into pHCV 1b HP NS5A to yield pHCV 1b HP 5' + HP NS5A. Finally, a MunI/BspCI DNA restriction fragment containing the V2971A mutation engineered into the Con1 sequence was subcloned into pHCV1b HP 5' + NS5A to yield pHCV1b HP. At each step of the replicon assembly process we verified the resulting nt sequence of each product by DNA sequence analysis.

#### Assessment of replicon RNA transduction efficiency

10 µg of pHCV 1b pt and derived plasmids were linearized with ScaI, purified, and 4 µg of the digested DNAs were used to program an *in vitro* transcription reaction using T7 RNA polymerase. After incubation for 5 hr, the transcription reactions were terminated and were extensively treated with DNaseI following the manufacturer's protocol (Ambion) and the DNA-free replicon RNA was recovered by lithium chloride precipitation. 900 ng of replicon RNA were transfected into  $2.5 \times 10^5$  Huh7 cells that were plated into the well of a 6-well dish. RNA transfection was conducted using the Transmessenger reagent and the manufacturer's protocol (Qiagen) and all transfections were performed in triplicate. 3 hr post transfection cells were released from the culture well by trypsinization and 90% of the recovered cells were plated into a 10 cm culture dish containing 7 ml of pre-warmed DMEM containing 400 µg/ml G418. The transfection efficiency of each transfected cell culture was determined by co-transfecting cells with 100 ng of purified, *in vitro* transcribed luciferase polyA RNA prepared from pCDNA3.1 luc polyA and subsequently conducting a luciferase assay on cell extracts prepared from the lysate of the remaining 10% of cells. After 3 weeks

of G418 selection cell colonies were visualized by staining the cells with Coomassie brilliant blue (0.6g/liter in 50% methanol/10% acetic acid). Colonies from replicate plates were counted to determine relative transduction efficiency of the corresponding HCV replicon RNA.

Transduction efficiency is expressed as the percent of initially transfected cells that were stably transduced and was normalized for relative transfection efficiency as determined by luciferase assay. Cell clones harboring distinct replicons were isolated by cylinder cloning and expanded for further characterization. A negative control ( $\Delta$ NS5B or  $\Delta$ 5B) replicon was produced by digesting pHCV1b with BglII, which liberates a ~1 kb region containing the active site of NS5B, followed by religation. *In vitro* transcribed RNA from an isogenic replicon containing a previously identified adaptive mutation (R2884G, a gift from Dr. R. Bartenschlager) was used as a positive control in all transduction experiments.

For measurement of initial HCV RNA replication efficiency,  $4 \times 10^4$  Huh7 or Huh7.5 cells were plated per well of a 24 well plate. 24 hr later the cells were mock transfected or transfected with HCV replicon RNA transcribed from pHCV1b  $\Delta$ 5B luc or pHCV 1b HP luc. 3 hr post transfection, cells were harvested for luciferase assay to determine relative transfection efficiencies or replated into 6 well dishes for monitoring of HCV RNA replication. Cells were harvested at the indicated times and extracts were subjected to luciferase assay in triplicate according to the manufacturer's protocol (Luciferase Reporter Assay System; Promega). Luciferase activity was quantified using a BioRad luminometer.

HCV RNA replication efficiency is expressed as the fold increase in luciferase activity from HP luc transfected samples versus  $\Delta$ 5B luc controls, normalized for transfection efficiency.

### RNA expression analysis

Northern blot analysis of RNA levels was performed exactly as described previously (40) using specific cDNA probes corresponding to the full-length open reading frames of HCV NS3, OAS1, ISG6-16, ISG56, ISG15, SenV-N, RIG-I or glyceraldehyde 6-phosphate dehydrogenase (GAPDH). Signal strength of the hybridized probe was quantified by phosphorimager analysis. For RT-PCR analysis of RNA levels, 5  $\mu$ g of total cellular RNA was treated with DNase I (DNAfree, Ambion) for 1 hr at 37°C and 1  $\mu$ g of the DNA-free RNA was used as a template for reverse transcription in a reaction containing Omniscript reverse transcriptase (Qiagen) primed with an oligo dT oligonucleotide primer and the HCV-specific primer 1942a: 5' GCGTCTGTTGGGAGTAGGCCG 3'. PCR reactions were conducted in triplicate for the amplification of IFN- $\beta$  and GAPDH cDNAs using the respective primer pairs and amplification conditions described previously (41). Primers used for the amplification of IRF-5 were IRF-5s: 5' GACCCCTCTGCCCCATGAACCAGT 3'/IRF-5a: 5' AACCCAGAGGTAGGACCCTGCA 3'. Quantitative real time PCR analyses were performed with an ABI Prism Sequence Detection system (ABI) in the presence of SYBR green using cDNA representing 10 ng of input RNA per reaction with all reactions conducted in triplicate. Real time primer pairs are listed in Table 4-2.

For microarray expression analysis cultures of Huh7, Huh7-L2198S, Huh7-K2040 or Huh7-HP cells were seeded with  $1 \times 10^6$  cells each in 100 mm dishes containing DMEM without G418. The cells were allowed to recover for 24 hr after which the culture medium was removed and replaced with DMEM alone or containing 10 U/ml IFN $\alpha$ 2a. After a further 24 hr the cells were harvested and total RNA was isolated using the Trizol reagent (Invitrogen) followed by a second RNA purification step using RNeasy columns and the manufacturers protocol (Qiagen). Biotinylated, single-stranded anti-sense RNAs were prepared from 25  $\mu$ g of template RNA and probes were hybridized to an Affymetrix human GeneChip<sup>®</sup> (Hu95A) containing 12626 probe sets for known genes, according to the manufacturer's protocol (Affymetrix, Santa Clara, CA). The DNA arrays were scanned using an Affymetrix confocal scanner (Agilent). Gene expression comparison files were generated using MAS 5.0 software (Affymetrix), and clustering analysis was performed in GeneSpring<sup>®</sup> software version 4.0.4 (Silicon Genetics). Gene expression levels within direct comparison tests between control Huh7 cells and Huh7 cells harboring the different HCV replicons were considered to be significantly different if the change in the hybridization signal (calculated average difference for the relevant probe set) was greater than or equal to 2.0.

#### Plasmids and DNA transfection

Plasmid DNA was prepared using the endotoxin free midiprep kit (Sigma) followed by extensive extraction with equal volumes of phenol and chloroform to remove residual impurities from the DNA. The extracted DNA was subjected to ethanol precipitation and

was resuspended in ultrapure water. Purified plasmid DNA was transfected using Lipofectamine 2000 transfection reagent (Invitrogen). pCMV-IRF-3 5D was a gift from Dr. J. Hiscott. pIRF-3-EGFP was a gift from Dr. A. Garcia-Sastre. pIRF-5-EGFP was a gift from Dr. P. Pitha. pEF Bos Flag-TBK1, -IKK $\epsilon$  and -TRIF plasmids were gifts from Dr. K. Fitzgerald. pEF Bos vector control and pEF Bos Flag-RIG-I, -RIG-I N and -RIG-I C plasmids were gifts from Dr. T. Fujita. Full length RIP2 was amplified from cDNA derived from Huh7 cells using the primers RIP2s:

5' AAGCTTATGAACGGCGAGGCCATCTGCAG 3'/RIP2a:

5' GAATTCCCATGCTTTTATTTTGAAGTAAATTTAAAGATGG 3', then digested with HindIII/EcoRI and ligated into pFlag CMV-2 (Sigma) to yield pFlag RIP2. pEF Bos Flag-RIG-I T55I and -RIG-I N T55I were created using the Quickchange™ kit from Stratagene with the mutagenic primers T55Is: 5'

GCCCAATGGAGGCTGCCATACTTTTCTCAAGTTCC 3'/T55Ia: 5'

GGAAGTTGAGAAAAAGTATGGCAGCCTCCATTGGGC 3'. pF3-EGFP was constructed by ligating a HindIII/XbaI fragment from pEGFP (Clontech) into pF3-Luc (a gift from Dr. J. Hiscott). pDsRed was purchased from Clontech. pFlag-NS5A 1b-1 has been described previously (46).

For dual luciferase assays,  $2 \times 10^4$  cells were plated into the well of a 48 well plate. 24 hr later the cells were cotransfected with a cocktail of luciferase reporter plasmids that included 50 ng of pIFN- $\beta$ -luc (a gift from Dr. Z. Chen) or pISRE-luc (Stratagene) and 12.5 ng of pCMV-Renilla (Promega) and allowed to recover for 24 hr. Cells were harvested at the

indicated times and extracts subjected to the dual luciferase assay as according to the manufacturer's protocol (Dual-Luciferase® Reporter Assay System; Promega). Luciferase activity was quantified using a BioRad luminometer.

### RNA synthesis and transfection

Endotoxin-free plasmid DNA for *in vitro* transcription was prepared exactly as described above. All *in vitro* transcripts were synthesized with the T7 Megascript kit (Ambion) and the manufacturer's protocol, followed by extensive treatment with Turbo DNase I (Ambion). The creation of pHCV 1b ΔNS5B, L2198S, HP and K2040 subgenomic replicon templates and their *in vitro* transcription has been described above. Luc polyA RNA was transcribed from pCDNA3.1 luc polyA, which was constructed by ligating a HindIII/EcoRI fragment from pSP6 luc polyA into pCDNA3.1 and the plasmid template was linearized with EcoRI. pSP6 luc polyA was constructed by ligating a HindIII/XbaI fragment from pGL3 basic (Promega) into pSP6 polyA (Promega). HCV 5' NTR-luc RNA was transcribed from pHCV 1bpt luc, which was constructed by ligating firefly luciferase into the AscI/PmeI sites of pHCV 1bpt and the plasmid template was linearized with PmeI. Firefly luciferase was amplified with Advantage 2 HF (Clontech) from pISRE luc (Stratagene) using the primers Luc AscI: 5' GGCGCGCCATGGAAGACGCCAAAACATA 3'/Luc PmeI: 5' GTTTAACTTACACGGCGATCTTTCCGCC 3' and the manufacturer's protocol. PCR conditions were 1 min at 95°C, 1 min 30 sec at 60°C and 30 sec at 68°C for 40 cycles. Δ5B luc and HP luc RNAs transcribed from pHCV 1b Δ5B luc and pHCV 1b HP luc, which were created in the same manner as pHCV 1bpt luc, and the plasmid templates were linearized



with ScaI. EMCV IRES-luc RNA was transcribed from pIRES luc, which was constructed by ligating firefly luciferase into pIRES (Clontech) digested with SmaI and the plasmid template was linearized with NotI. HCV ss1 RNA was transcribed from pCDNA3.1 HCV 1bpt NS3/4A and the plasmid was linearized with SgrAI. HCV ss2 RNA was transcribed from pCDNA3.1 HCV 1bpt NS5A and the plasmid was linearized with EcoRI. HCV 5' NTR (IRES) and 3'NTR were transcribed directly from the PCR products T7 HCV 5' NTR and T7 HCV 3' NTR, which were amplified from pHCV 1bpt using the primers T7 HCV 5' NTRs 5' GTAATACGACTCACTATAGGGCCAGCCCCCTGATGGGGGCGACA 3' /pHCV 1bpt 520a 5' TCGGTGCAATCCATCTTGTTTC 3' and T7 HCV 3' NTRs 5' TAATACGACTCACTATAGGGAGATGAAGGTTGGGGTAAACACTC 3' /HCV 3' NTRa 5' ACATGATCTGCAGAGAGGCCA 3', respectively. PCR conditions were 1 min at 95°C, 30 sec at 60°C and 30 sec at 68°C for 40 cycles. The amplified DNA was purified by agarose gel electrophoresis and extracted from the gel using the QIAquick kit and the manufacturer's protocol (Qiagen). RNA was transfected using the Transmessenger RNA transfection reagent (Qiagen) and the manufacturer's protocol.

### Protein analysis

For evaluation of protein expression, cell extracts were prepared and immunoblot analysis was conducted exactly as described previously (170), except that RIPA buffer (10 mM Tris, 150 mM NaCl, 0.02% NaN<sub>3</sub>, 1% Na-deoxycholate, 1% Triton X-100, 0.1% SDS) was used for cell lysis. Primary antibodies used for immunoblot analysis included a well-characterized anti-HCV patient serum (obtained with informed consent through Dr. W. Lee)

(133), anti-PKR monoclonal antibody 71/10, (a gift from Dr. A. Hovanessian), rabbit polyclonal anti-ISG56 (a gift from Dr. G. Sen), rabbit polyclonal anti-ISG15 (a gift from Dr. A. Haas), rabbit polyclonal anti-IRF-3 (a gift from Dr. M. David), rabbit polyclonal anti-ISG56 (a gift from Dr. G. Sen), rabbit polyclonal anti-RIG-I (a gift from Dr. T. Fujita), rabbit polyclonal anti-VSV (a gift from Dr. M. Whitt), rabbit polyclonal anti-SenV (a gift from Dr. I. Julkunen), monoclonal anti-TBK1 (Imgenex), monoclonal anti-IKK $\epsilon$  (Imgenex), rabbit polyclonal anti-phospho-Ser51-eIF2 $\alpha$  (Cell Signaling Technologies), monoclonal anti-eIF2 $\alpha$  (Research Genetics), rabbit polyclonal anti-phospho-Thr180/Tyr182-P38 (Cell Signaling Technologies), rabbit polyclonal anti-P38 (Cell Signaling Technologies), rabbit polyclonal anti-phospho-Ser473-Akt (Cell Signaling Technologies), rabbit polyclonal anti-IkB $\alpha$  (Santa Cruz), monoclonal anti-Flag (Sigma) and goat polyclonal anti-actin (Santa Cruz). Proteins were detected with a secondary antibody coupled to horseradish peroxidase and were visualized by chemiluminescence.

For immunofluorescence,  $2 \times 10^4$  cells were cultured and treated on chamber slides then fixed and probed with polyclonal rabbit anti-IRF-3 serum or monoclonal anti-Flag serum and FITC-conjugated or Rhodamine donkey anti-rabbit secondary antibodies exactly as described (40). Following antibody staining, the nuclei were stained with DAPI. Cells were visualized by fluorescence microscopy using a Zeiss Axiovert digital imaging microscope in the UT Southwestern Pathogen Imaging Facility.

PKR kinase assay was performed exactly as described in (44) and IRF-3 dimerization assay was performed exactly as described in (184).

For measurement of secreted IFN- $\beta$  within cultures of mock or poly(I)(C)-transfected cells, culture medium was collected from the cells 24 hr post transfection, centrifuged to remove cell debris, and the amount of IFN- $\beta$  within the cell-free supernatant was quantified using an antigen capture assay from Research Diagnostics as described previously (41).

#### Polyribosome distribution analysis

Analysis of ribosome-HCV RNA association and corresponding protein content in Huh7 cells harboring HCV replicon quasispecies was conducted following a modification of the methods of Ruan, Brown, and Morris (138) and as previously described (170). Huh7-L2198S or Huh7-HP cells were cultured in two 15 cm dishes each at approximately 70-80% confluency in medium lacking G418 and in the presence or absence of 100 U/ml IFN $\alpha$ 2a for 24 hr. We have previously demonstrated that a cell culture density of 80% confluency does not affect the steady-state HCV RNA level present in each replicon cell line (170). Prior to cell harvest the culture media was replaced with pre-warmed media containing 100  $\mu$ g/ml cyclohexamide (CHX) and incubated for 15' at 37°C. Cells were rinsed with pre-warmed PBS containing 100  $\mu$ g/ml CHX (PBS/CHX), the solution was removed, and cells were released from the dish by incubation in a pre-warmed trypsin/CHX solution. Cells were washed from the culture dish with 10 ml PBS/CHX containing 1mM PMSF and were pooled into a tube containing and additional 5 ml of ice cold PBS/CHX. Tubes were subjected to

centrifugation at 1000 x g for 5 min at 4 °C, the supernatant discarded, and the cell pellet washed once with 10 ml ice cold PBS/CHX. Cell pellets were resuspended in 750 µl of ice-cold low salt buffer [LSB; 20 mM Tris (pH 7.5), 100 mM NaCl, 30 mM MgCl<sub>2</sub>] and tubes were placed on ice for a total time of 3 min. to allow cell swelling. After adding 250 µl of detergent buffer (LSB supplemented with 1.2% Triton N-101), cell suspensions were transferred into an ice cold 7 ml Dounce homogenizer and homogenized with 7 strokes of the pestle. The homogenate was transferred to an ice-cold micro centrifuge tube and subjected to a 1 min. centrifugation at 10,000 x g at 4 °C. The supernatant was then collected and transferred to an ice cold recipient tube containing 100 µl of LSB supplemented with 1 mg of heparin and containing a final concentration of 1.5 M NaCl. The lysate mixture was layered carefully on top of a 0.5 M-1.5 M sucrose gradient prepared in a 14 x 95 mm polyallomer centrifuge tube. Gradients were centrifuged for 2 hr at 36,000 rpm using a Beckman SW40 rotor. Afterwards, 12 x 1 ml fractions were collected in a top to bottom manner from each gradient tube using an ISCO density gradient fractionator (ISCO, Inc.). Fractions were monitored for optical density using a wavelength of 254 nm. All fractions were collected into micro centrifuge tubes containing 100 µl 10% SDS, after which 220 µg proteinase K was added to each tube. In some experiments proteinase K was omitted from the collection tubes to facilitate protein recovery from the respective fractions. Tubes were incubated for 30 min. at 37°C and RNA was extracted from each using the Trizol reagent and the manufacturer's protocol (Gibco). We conducted a parallel assessment of ribosome-associated proteins by extracting and collected the protein constituents of each fraction. Proteins were extracted from the organic phase of the Trizol reagent as described in the

manufacturer's protocol (Invitrogen). The extracted proteins were precipitated in 100% ethanol, dried, and rehydrated in Triton X-100 lysis buffer. For RNA extraction, purified RNA was resuspended in 30  $\mu$ l RNase-free water. The integrity of the recovered RNA was confirmed by running 10  $\mu$ l of each sample on a standard 1% agarose gel and visualizing the ethidium bromide-stained ribosomal RNA (rRNA) bands. The distribution of the 18S and 28S ribosomal RNAs associate with the presence of the 40S and 60S ribosomal subunits respectively (158), and monitoring the rRNA band distribution in this manner allowed us to confirm the ribosome subunit and polysome distribution of our fractionation procedure.

The gradient distribution (ribosome association) of actin and HCV RNAs was assessed by RT-PCR using the Titanium one-step RT-PCR kit (Clontech) and 1  $\mu$ l of total RNA isolated from each gradient fraction using the primer pairs  $\beta$ -actin\_s: 5' TTGTTACCAACTGGGACGACATGG 3'/ $\beta$ -actin\_a: 5' GATCTTGATCTTCATGGTGCTAGG 3', and the previously published KY78 and KY80 primers for HCV RNA amplification (187). PCR amplification was conducted for a total of 25 cycles, which we have confirmed represents the mid-linear stage of the amplification cycle under the conditions used (170). HCV and actin RT-PCR products were analyzed by agarose gel electrophoresis and digital imaging of the ethidium bromide-stained gel.

#### Poly(I)(C) pulldown assay

Poly(C)-coated agarose beads (Sigma) were resuspended in 50 mM Tris pH 7.0, 50 mM NaCl and collected by centrifugation at 1000 x g. Beads were washed several times in

50 mM Tris pH 7.0, 200 mM NaCl. To make poly(I)(C)-coated beads, poly(I)-coated beads were resuspended in 2 volumes of 2 mg/mL poly(I) (Sigma) in 50 mM Tris pH 7.0, 150 mM NaCl then rocked gently overnight at 4°C and collected by centrifugation. Beads were then equilibrated in 50 mM Tris pH 7.0, 150 mM NaCl and stored at 4°C.

For poly(C) and poly(I)(C) pulldown assays, poly(C) or poly(I)(C)-coated beads were equilibrated in binding buffer (50 mM Tris pH 7.5, 150 mM NaCl, 1 mM EDTA, 1% NP-40) as a 5-10% slurry, then combined with an equal volume of whole cell extract containing 3-20 µg protein (cells lysed in binding buffer supplemented with protease and phosphatase inhibitors), and 25 units/mL RNAsin and rocked for 1 hr at 4°C (for competition experiments, pulldown reactions were supplemented with 10-50 µg/mL of the indicated competitor RNAs). Beads were centrifuged at 1000 x g and rinsed 3 times with binding buffer, then resuspend beads in 3-5 volumes of 1X SDS-PAGE sample buffer. Samples were then boiled for 5 min., centrifuged at 13,000 x g for 30 seconds and loaded immediately onto SDS-PAGE gels for immunoblot analysis.

## **CHAPTER 3: VIRAL EVOLUTION AND INTERFERON RESISTANCE OF HCV RNA REPLICATION IN A CELL CULTURE MODEL**

### **Introduction**

In this study we examined the relationship between viral sequence variation and the host response to HCV RNA replication in a cell culture model of HCV persistence. Because HCV cannot be efficiently propagated in cultured cells, we focused our studies on evaluating these properties within cell lines harboring genetic variants of an HCV 1b subgenomic RNA replicon derived from the previously published Con1 prototype sequence (an infectious genotype 1B molecular clone) (105). The HCV NS3-NS5B coding region within the replicon RNA mediates viral RNA replication in Huh7 hepatoma cells (105). Various studies have identified adaptive mutations throughout the HCV protein-coding region of the replicon RNA, thereby verifying the potential for genetic diversification and adaptation of the HCV RNA through a process of error-prone replication (104, 189). Among these mutations functional significance has been conclusively assigned only for those that increased the processivity of the NS5B RdRp (27), though mutations identified within the NS3 and NS5A regions corresponded with enhanced replication (16, 104) and differential control of the host response (40, 133). We have extensively characterized a variety of HCV RNA replicon variants with respect to their resistance to IFN treatment and their interactions with host cell antiviral response pathways. We identified a pair of replicons derived from the Con1 sequence that each differed by only a single aa residue within the NS5A coding region. Both

replicon variants were sensitive to the antiviral actions of IFN, and although initial culture adaptation of the respective replicon RNA was conferred by a single point mutation (a leucine to serine substitution at HCV aa position 2198 or a lysine insertion at HCV aa position 2040, both of which lie in the NS5A protein-coding region), the two variants impart dramatically different properties with respect to their regulation of the host response. We have previously demonstrated that L2198S mutation abrogates the NS5A-PKR interaction, and cells harboring this replicon exhibit increased levels of active PKR and viral RNA-induced potentiation of IRF-1 and NF $\kappa$ B DNA binding activity (41, 133). We utilized long-term cultures of these replicon systems as a model with which to evaluate how the pressures from the host cell antiviral response may influence viral genetic adaptation, the response to IFN-based therapy and overall viral fitness associated with persistent HCV replication. Our results provide evidence that the host cell antiviral response exerts selective pressure for viral sequence evolution that can impact the overall fitness and IFN sensitivity of HCV replication.

## Results

### *Viral fitness associates with the host response to HCV RNA replication*

We examined the host response in low passage isolates of Huh7 cell lines harboring either the K2040 or L2198S HCV replicon RNA. These cell lines, respectively termed Huh7-K2040 and Huh7-L2198S, were both derived from the same pool of parental Huh7 cells transduced with the prototype Con1 subgenomic HCV RNA replicon sequence (133). Evaluation of HCV RNA levels in the low-passage cell lines by quantitative real time RT-



PCR and Northern blot analysis demonstrated that the level of HCV RNA differed by approximately 10-fold between each line and was higher in Huh7-K2040 cells (see Figs 3-2 and 3-4). We have previously shown that Huh7-K2040 cells are refractory to transfected dsRNA and fail to activate IRF-1 or NF- $\kappa$ B due to an NS5A-imposed block in PKR-dependent signaling (41, 133). To further characterize the host response to HCV RNA in these cells, we evaluated the influence of each replicon on the activation state of IRF-3. As shown in Fig 3-1A, the nuclear, active form of IRF-3 was not observed in parental Huh7 cells or Huh7-K2040 cells. However, nuclear IRF-3 was detected, albeit at a low frequency, in Huh7-L2198S cells. Within a given culture of Huh7-L2198S cells we routinely observed nuclear IRF-3 in 5-7% of the total cells examined. Therefore, under conditions of low HCV protein abundance, the HCV NS3/4A protease renders an incomplete block to IRF-3 activation. IRF-3 is a component of the IFN- $\beta$  enhancosome that assembles to promote IFN production (55), and we sought to determine if the differential regulation of these components influenced IFN synthesis. We therefore measured IFN- $\beta$  levels in supernatants collected from cultures of control or replicon-bearing cells alone or treated with dsRNA. In the absence of transfected dsRNA, a low level of IFN- $\beta$  was detected in the culture media collected from Huh7-L2198S cells but not in media collected from cultures of control human diploid fibroblasts (B52 cells), parental Huh7 cells or Huh7-K2040 cells (Table 3-2). Transfection of cells with dsRNA induced IFN- $\beta$  production in all cultures, but this response was limited to only a low level of IFN production in cells harboring the K2040 replicon. Huh7 control cells and HCV replicon-bearing cells were responsive to IFN treatment, and the basal IFN- $\beta$  production in Huh7-L2198S cells associated with increased levels of PKR and

an induction of ISG56 and ISG15 expression that was not apparent in control or Huh7-K2040 cells (Fig 3-1B). In particular, ISG56 and ISG15 are IRF-3 target genes (56) and their low level of expression in Huh7-L2198S cells is consistent with the basal nuclear, active state of IRF-3 in these cells. Thus, HCV RNA replication fitness corresponded with the extent of a cellular antiviral response characterized by differential regulation of IRF-3 action, IFN- $\beta$  production and ISG expression.

#### *HCV RNA sequence evolution*

In order to evaluate the impact of an active host response upon HCV persistence, we subjected the low passage isolates of Huh7-K2040 and Huh7-L2198S cells to continuous long-term culture and we monitored IFN- $\beta$  and ISG expression as well as viral RNA sequence within the cultured cells. In Huh7-K2040 cells the absence of IFN- $\beta$  and ISG expression associated with HCV RNA sequence stability, and the sequence of the this replicon remained stable and unchanged over a 16-month culture period. In contrast, after 6-months of culture we identified 12 nt substitutions in the replicon sequence derived from Huh7-L2198S cells. The mutations were not clustered within any single site but instead were scattered throughout the NS coding region. 6 of the mutations were synonymous and 6 others each conferred aa changes that also were scattered throughout the HCV NS protein coding region. The aa changes included 2 mutations in the NS3 and NS5A regions, and single changes within the NS4B and NS5B regions (Fig 3-2A). We termed the evolved high passage replicon sequence and replicon-bearing cells HP and Huh7-HP, respectively. Viral RNA sequence analysis confirmed that the adaptations within the HP replicon remained

stable and unchanged upon continuous culture, indicating that an evolutionary equilibrium had been reached. Quantitative PCR assessment of viral RNA levels demonstrated a 10-fold increase of viral RNA in the Huh7-HP cells compared to the Huh7-L2198S cells, and the former approximated the viral RNA levels observed in the Huh7-K2040 cells (Fig 3-2A). Immunoblot analysis demonstrated a concomitant increase of viral protein abundance in Huh7-HP cells relative to Huh7-L2198S cells, and this similarly approximated the levels observed in Huh7-K2040 cells (Fig 3-2B). We also evaluated IRF-3 localization and IFN- $\beta$  mRNA expression within cells harboring the HP replicon and their progenitor low passage Huh7-L2198S or Huh7 control cells. The active, nuclear form of IRF-3 was observed at a low frequency in cultures of Huh7-L2198S cells but not in parallel cultures of Huh7-HP cells (Fig 3-2C), and this corresponded to the pattern of IFN- $\beta$  mRNA expression, which was only observed in the Huh7-L2198S cells (Fig 3-2D). Taken together, these results demonstrate that HCV RNA sequence evolution occurred concomitantly with host pressures associated with active IRF-3 and IFN- $\beta$  and ISG expression during persistent HCV RNA replication.

*The evolved HP adaptations are synergistic and confer increased viral replication fitness*

To determine how the adaptations within the HP replicon sequence influence the initiation and fitness of HCV RNA replication, we systematically introduced the mutations alone or in sets into an assembled prototype Con1 replicon (40). Huh7 cells were then transduced with purified RNA transcribed *in vitro* from various Con1 cDNA templates containing the HP mutations. As controls, we included transduction analyses of replicon RNA corresponding to the prototype Con1 sequence alone or harboring the adaptive

mutations L2198S, K2040 or R2884G. As has been previously reported by others, G418 selection of cells transduced with a negative control Con1 replicon that has a deletion in the NS5B RdRp active site ( $\Delta$ NS5B) failed to produce cell colonies (Fig 3-3), while transduction with the prototype Con1 sequence produced cell colonies only as a rare event and the R2884G adaptive mutation, which increases the processivity of the NS5B RdRp (27), produced cell colonies with comparative high efficiency (104). The L2198S mutation alone rendered only a slight improvement in transduction efficiency over the Con1 prototype replicon, consistent with the poor replication properties of this progenitor sequence (133). The set of HP mutations in the NS3 and NS4B coding regions (P1115L/K1609E/Q1737R) supported cell colony formation at an improved and approximately equal frequency as the K2040 replicon. The set of three NS5A mutations (P2007A/L2198S/S2236P) did not increase transduction efficiency when compared with the L2198S progenitor sequence, but when the NS5A, NS3 and NS4B mutations were combined the combination was synergistic and increased transduction efficiency approximately 300-fold over the L2198S progenitor (Fig 3-3, compare panels 3 and 5-7). The NS5B mutation (V2971) affected transduction efficiency only when combined with the NS3 and NS4B mutations to render a further 4-fold increase in cell colony selection (Fig 3-3, panel 8). In general we found that the synergistic effects of combined HP mutations also rendered large, more robust cell colonies that even outgrew cells transduced with the R2884G control replicon sequence. These results identify the HP replicon as a highly fit variant and demonstrate that the HP mutations function synergistically to initiate and support HCV RNA replication.

Since the HP replicon sequence evolved under constant pressure from IFN and innate immune processes conferred by the host cell, we focused our efforts on evaluating HCV RNA replication fitness in the context of the host cell IFN response. When treated with IFN $\alpha$ 2a for 24 hr, Huh7 cells initiate a host response that severely limits the replication of culture adapted HCV replicon RNA (57, 170). Consistent with this, Northern blot analysis demonstrated the acute sensitivity to IFN of the L2198S and K2040 HCV replicon variants, and each exhibited an IC<sub>50</sub> of <10 units /ml (U/ml) IFN $\alpha$ 2a (Fig 3-4A). In contrast, the level of HP replicon RNA was comparably resistant to IFN action and only began to significantly decay after treatment of Huh7-HP cells with IFN doses above 100 U/ml. To determine if this difference in IFN sensitivity among the HCV replicons was due to cellular or viral-mediated defects in IFN receptor signaling, we measured the activity of an IFN-responsive luciferase reporter gene under control of an ISRE. As shown in Fig 3-4B, IFN-induced signaling to the ISRE was intact in all cell lines and was only slightly reduced in the Huh7-L2198S cells. Moreover, immunoblot analysis confirmed that IFN signaled the increased expression of PKR, an ISRE-containing IFN-responsive gene (95) to approximately equal levels (data not shown). Thus, IFN resistance of the HP replicon is not attributed to a general disruption of IFN signaling or ISGF3 action in the host cell.

#### *HP mutations direct viral resistance to IFN*

To determine if the HP replicon resistance to IFN action was mediated by viral-directed processes, we transduced naïve Huh7 cells with the reconstructed HP replicon RNA and selected and expanded clonal cell lines and cell populations for further analysis. As

controls, we transduced cells with K2040 replicon RNA for the parallel selection of clonal cell lines and populations harboring the K2040 sequence. As shown in Fig 3-5A, the HP replicon RNA within a distinct cell population and clonal cell lines exhibited approximately equal and low IFN sensitivity as the original HP replicon in the Huh7-HP cells. In contrast, IFN treatment of control cultures harboring the K2040 replicon RNA induced a marked decay in viral RNA level and this high sensitivity to IFN was maintained between clonal cell lines. When we interrogated the same blot with an ISG6-16-specific probe (Fig 3-5A, middle panel), we found that ISG6-16 was expressed in all cell lines in an IFN and dose-dependent manner, confirming that the cells responded to IFN.

We similarly evaluated the effect of IFN treatment on HCV nonstructural protein expression from the replicon RNA within Huh7-L2198S cells, clonal Huh7-HP cell lines and a Huh7-HP cell population (Fig 3-5B). Over a 48 hr treatment period the HCV nonstructural protein abundance within Huh7-L2198S cells decayed in a dose-dependent manner, consistent with the acute sensitivity of this replicon RNA to IFN action. In contrast, the abundance of HCV nonstructural proteins expressed from the HP replicon RNA remained relatively unchanged at IFN doses below 50 U/ml and only began to decay at IFN doses greater than 100 U/ml. Parallel analyses revealed that PKR levels accumulated in a dose-dependent manner in the IFN-treated cell lines and showed that the cells responded equally well to the IFN treatment. Thus, the IFN-resistant phenotype is a consistent feature associated with the HP replicon RNA that is not attributed to global defects in IFN signaling or clonal variation among cell lines.

*Regulation of ISG56 expression*

To determine if the HP replicon conferred differential regulation of ISG expression we conducted microarray analysis to evaluate global gene expression levels in cells cultured in the absence or presence IFN $\alpha$ 2a for 24 hr. Pharmacological studies have determined that serum level of IFN is approximately 10-12 U/ml within 2 hrs after the administration of IFN in patients undergoing therapy with recombinant IFN $\alpha$  preparations (86), and to maintain physiologic relevance we treated cells with 10 IU/ml of IFN. Our analyses included assessment of gene expression in the parental Huh7 control cells and Huh7-K2040, Huh7-L2198S and Huh7-HP cells. Overall, the global gene expression profiles of replicon-bearing cells gave distinct signatures associated with the level of viral RNA replication in each cell line, and Huh7-K2040 cells exhibited a similar global signature as Huh7-HP cells, each of which were distinct from Huh7 and Huh7-L2198S cells (these results will be presented elsewhere).

We focused our analyses on expression profiling of ISGs, and we identified a subset of genes whose expression was regulated in response to IFN treatment. As shown in Table 3-3, this includes a variety of canonical ISGs identified in other studies (32, 50). Comparison of the ISG profile among the various cell lines identified a deficit in ISG56 expression that was specific to Huh7-HP cells. Immunoblot analysis of extracts from IFN-treated cells confirmed that ISG56 protein expression was significantly reduced in Huh7-HP cells compared to control Huh7 cells and Huh7-L2198S cells over a 24-72 hr time course of IFN

treatment (Fig 3-6A). Since ISG56 expression is induced to peak levels early after IFN treatment, we also evaluated gene expression by Northern blot analysis over an acute induction time course after IFN treatment of control Huh7 cells, Huh7-HP cells and Huh7-K2040 cells as well as in clonal cell lines derived from naïve Huh7 cells transduced with the reconstructed HP or K2040 replicon RNA. As shown in Fig 3-6B, IFN-induced ISG56 expression within Huh7 and Huh7-K2040 cells was first apparent by 4 hrs post-treatment and reached peak levels beginning at 8 hrs and continuing through 12 hrs after which the mRNA declined to a final low level at 24 hr post-treatment. ISG56 mRNA was not detected in Huh7-HP cells until 8 hr post IFN-treatment and then continuously declined throughout the 12 and 24 hr treatment time points. Similar results were obtained when we examined ISG expression within clonal cell lines harboring the reconstructed HP or K2040 replicon RNA. We consistently observed a deficit in ISG56 mRNA expression within cells harboring the HP replicon but the kinetics and abundance of ISG56 expression within IFN-treated cells harboring the K2040 replicon were similar to control Huh7 cells. By comparison IFN-induced ISG6-16 expression was not significantly different among cell lines and both analyses revealed that the mRNA reached peak levels in each at 12 hrs post-treatment (Fig 3-6B, middle panel).

To extend these results we also evaluated protein levels in the various cell lines or their counterparts that were cured of the HCV replicon after continuous high-dose IFN treatment. As shown in Fig 3-6C, when compared to control Huh7 cells and Huh7-K2040 cells, the protein levels of ISG56 were attenuated in Huh7-HP cells and clonal cell lines



transduced by the reconstructed HP RNA. Importantly, the expression levels of ISG56 returned to normal when the Huh7-HP cells were cured of the HCV replicon RNA (see Fig 3-6C left panel, lanes 7-9). Analysis of the IFN-induced expression of a synthetic ISRE-luciferase promoter reporter construct or an ISG56-luciferase promoter reporter construct in the transfected cells demonstrated that this pattern of ISG56 expression did not correlate with differences in IFN signaling to the ISRE and ISG56 promoter, which was variable between cell lines (Fig 3-6D). Taken together, these results indicate that 1) the kinetics of ISG56 induction and overall peak levels of expression were specifically attenuated by one or more viral products present in the Huh7-HP cells, and 2) this regulation was not a result of viral regulation of IFN receptor signaling to the ISRE.

*Differential ribosome association of HCV RNA and correlation with ISG56 levels*

ISG56 is a translational regulator whose actions contribute to suppression of HCV IRES translation and viral RNA replication by disrupting translation initiation and ribosome recruitment to template RNA in IFN-treated cells (75, 170). We therefore sought to determine if the differential levels of ISG56 expression conferred an altered association of HCV replicon RNA with ribosomes. To evaluate the ribosome association of the HCV replicon, we conducted polyribosome distribution analysis of the L2198S and HP replicon RNA from cells cultured in the absence or presence of IFN. This approach separates RNA-ribosome complexes based upon their physical density that is defined by the relative number of ribosomes bound to a specific RNA but it does not discriminate between ribosome recruitment by the viral IRES elements encoded within the HCV replicon RNA (170). As

shown in Fig 3-7, in the absence of IFN the L2198S RNA was primarily associated with low mass polysomes. IFN treatment caused the L2198S RNA to redistribute into fractions corresponding to an association with a single 80S ribosome or the 40S ribosomal subunit/translation preinitiation complex. In contrast the HP replicon RNA was found predominantly distributed within high mass fractions of increasing polysome complexity regardless of IFN treatment.

ISG56 physically associates with the p48 subunit of eIF3 (58) and both proteins are co-distributed in the cell to the sites of translating RNAs where they localize primarily with translation initiation complexes (75, 170). We therefore evaluated the relative levels of ISG56 and eIF3 within proteins extracted from pooled gradient fractions corresponding to the 40S ribosome/preinitiation and 80S translation initiation complex (fractions 1 and 2, respectively) of the IFN-treated cells shown in Fig 3-7A. Immunoblot analysis demonstrated that ISG56 and its interacting partner, the p48 subunit of eIF3 [(p48)eIF3 (58)], were co-distributed in the pooled fractions from each cell line but the relative amount of ISG56 that co-fractionated with (p48)eIF3 in Huh7-HP cells was comparably reduced. Densitometric quantification of the protein levels revealed an ISG56:(p48)eIF3 ratio of 1.4 in Huh L2198S cells that was essentially identical to the ratio consistently observed in similar gradient fractions recovered from control Huh7 cells (see ref 170). By comparison we derived an ISG56:(p48)eIF3 ratio of 0.6 from the same fractions recovered from Huh7-HP cells (Fig 3-7C). Thus, polyribosome retention and IFN-resistant viral RNA replication of the HP RNA

corresponded with a specific deficit of ISG56 expression and co-fractionation with eIF3 within translation initiation complexes from IFN-treated Huh7-HP cells.

## Discussion

Molecular epidemiology studies have demonstrated that viral sequence evolution is a characteristic of HCV infection in human patients, and that virus persistence largely associates with the outgrowth of a highly fit viral sequence whose stability is influenced by host immune pressures (146). The present study provides further evidence that selective pressure of the host response can drive the incorporation of viral adaptive mutations. Our results demonstrate that these mutations can result in the enhancement of HCV RNA replication fitness through processes that involve suppression of one or more components of the host response and IFN programs against HCV.

### *An in vitro system to model virus/host parameters of acute to chronic HCV progression*

Our model system of study utilized genetically defined HCV subgenomic RNA replicons that differed at single sites in the NS5A coding region that have been shown to significantly influence viral replication fitness (133). The K2040 HCV replicon was maintained as a single dominant sequence even in long-term culture while, in contrast, the L2198S replicon evolved into the HP variant during the same culture period. The evolved HP replicon is effective at blocking virus-induced IRF-3 activation (40), and we found the basal level of active IRF-3 and IFN- $\beta$  expression observed in cells harboring the progenitor L2198S sequence were completely suppressed in Huh7-HP cells. This indicates that the HP replicon gained the advantage of completely blocking the IRF-3 component of the host response. These observations provide strong support for the concept that HCV replication fitness and persistence are in part dependent upon viral-directed processes that control the

host response to infection. Our HCV replicon systems now provide an *in vitro* model from which to characterize and contrast virus/host interactions in the dynamic context of the innate host response triggered by HCV RNA replication.

*HCV RNA replication has the capacity to induce a host response that includes IRF action, IFN- $\beta$  production and ISG expression*

The basal level of IFN- $\beta$  and ISG expression in Huh7-L2198S cells indicates that HCV RNA replication has the capacity to induce a host response that includes IRF effector function, IFN production and ISG expression. It has been suggested that virus infection triggers this response through the engagement of toll-like receptors (TLRs) on the cell surface and intracellular vesicles or that it may be activated independently of TLRs through specific intracellular signaling events that remain largely undefined (2, 68). Viral RNA and dsRNA in general serve as potent inducers of the host response and can stimulate the activation of IRF-1, IRF-3, PKR and other antiviral effectors (143). Huh7 cells lack a TLR3 response to external dsRNA (98), and coupled with the fact that the HCV replicons are strictly intracellular we conclude that TLR signaling from external cellular receptors is not likely to participate in triggering the host response to HCV products or viral RNA in our replicon model. Instead, our data suggest that in this context HCV RNA replication triggers the host response exclusively through intracellular events that include but are not limited to signaling IRF-3 and IRF-1 transcription effector function.

We have found that the HCV NS5A protein and NS3/4A protease can respectively antagonize IRF-1 and IRF-3 transcription effector function and that these factors are differentially regulated in Huh7-K2040 and Huh7-L2198S cells (40, 133). In the case of IRF-1, the differential levels of IRF-1 DNA-binding activity and target gene expression within Huh7-K2040 and Huh7-L2198S cells was attributed to the differential regulation of PKR and PKR-dependent signaling conferred by the corresponding mutation within the NS5A protein encoded by the respective HCV replicon RNA. When compared to control Huh7 or Huh7-L2198S cells, we found significantly reduced levels of PKR activity in Huh7-K2040 cells (170) and in Huh7-HP cells (R.S. and M.G. unpublished observations). Since the K2040 and HP replicons are respectively sensitive and resistant to IFN, we cannot assign regulation of PKR activity alone as the sole cause for the IFN-resistant phenotype of the HP replicon. However, our data further support the concept that NS5A sequence is an important contributor to HCV replication fitness. In particular, the L2198S mutation locates to a region of NS5A where departure from the prototype Con1 sequence has been shown to significantly influence the initiation of HCV RNA replication (16). It is likely therefore, that this mutation supported HCV RNA replication at the expense of releasing a level of viral control over the host response, which resulted in its inefficient replication in part through the antiviral actions of this response. Here we showed that IRF-3 was a component of the host response to HCV RNA replication and that the active, nuclear isoform of IRF-3 was present at a low but significant frequency in cultures of Huh7-L2198S cells but not in Huh7-K2040 cells. The sequence of the NS3-4A coding region is identical within the corresponding replicons, suggesting that the single aa differences in NS5A likely influenced viral control of IRF-3

indirectly by affecting overall viral protein and NS3/4A abundance. This conferred a complete block to IRF-3 activation by the K2040 replicon but only a partial block by the L2198S replicon. This idea is supported by the relationship between viral RNA and NS3/4A protein abundance, which has negatively correlated with IRF-3 activation status here and in our previous studies (40). IRF-3 activation is signaled through the virus-stimulated activation of the TBK1 or IKK $\epsilon$  protein kinases (38, 145), and our results suggests that 1) HCV RNA replication has the capacity to induce host cell signaling events that direct the activation of one or both of these IRF-3 kinases to trigger a level of IRF-3 activation, and 2) HCV control of these processes is dependent upon the relative abundance of viral protein antagonists of the host response (like NS5A and NS3/4A) and indirectly upon overall viral RNA replication efficiency.

*The host response to HCV replication provides selective pressure for viral adaptive mutations*

The error-prone RdRp of HCV provides remarkable adaptability that allows the virus to continually evade host immune challenges. Several studies have now linked viral genetic adaptation with evasion of the adaptive immune response and to the outcome of IFN-based therapy for HCV infection [for examples see (146, 178)]. Such studies have identified host immune pressure as a potent driving force for the fixation of HCV adaptive mutations to indicate that such mutations may contribute to overall viral fitness. The current study supports this notion and provides direct evidence that antiviral pressure from the host cell contributes to HCV sequence evolution and the fixation of viral adaptive mutations. We base

this statement on three key observations. First, the replication of the K2040 replicon associated with the absence of a host response while the poor replication of the L2198S replicon associated with an active host response in the Huh7-L2198S cells. Second, the L2198S replicon acquired 6 additional adaptive mutations over the 6 month culture period while the K2040 replicon sequence was stable during this same period and has remained stable over a several month follow-up period. Third, the HP replicon that evolved from the L2198S sequence remains stable, is highly fit and efficiently suppressed the host response that was initially ongoing in the cell.

The evolved HP sequence retained the initial L2198S mutation in NS5A but gained mutations throughout the NS coding region. The effect of these mutations was synergistic toward initiating viral RNA replication and for supporting stable, high level viral RNA replication and protein expression, possibly reflecting a temporal relationship in the order by which these adaptations were incorporated into the replicon genome. Their positions throughout the NS coding region suggest that the HP mutations could affect the processivity of the RdRp, the enzymatic actions of the NS3 protease/helicase and/or the overall assembly and action of the viral replicase. A search of the HCV sequence database ([www.hcv.lanl.gov](http://www.hcv.lanl.gov)) revealed that of the total set of adaptive mutation in the HP sequence only the P1115L mutation (located in the NS3 coding region) has been identified in viral RNA isolated from human patients. Thus, the particular complement of HP mutations could be unique to cultured cells but clearly represent a defined outcome of HCV sequence evolution. The fixation of the L2198S mutation in the evolved HP replicon indicates that



sequence evolution took place around this initial adaptation, possibly to complement the deficiencies in controlling the host response imposed by the initial adaptation at codon 2198 (133). In support of this idea, we found that the HP mutations rendered an IFN-resistant phenotype (discussed below). This strongly suggests that the HP sequence evolution was not a stochastic process but rather was directed by the antiviral pressures of the host cell response to HCV RNA replication. The fact that the evolved HP replicon achieved control of this host response and resistance to the IFN response indicates that one or more shared element(s) of these responses applied the major pressure behind the HP sequence evolution.

#### *Viral regulation of ISG56 expression and resistance to IFN therapy*

Our results demonstrate that the evolved HP replicon is resistant to the antiviral actions of IFN and that this is associated with a deficit in IFN-induced ISG56 expression. We found that IFN resistance was a property conferred by the adaptive mutations in the replicon RNA and not by adaptations of the host cell. This conclusion is based upon the observations that the reconstructed HP RNA mediated IFN-resistant replication after transduction of naïve Huh7 cells, and that viral resistance to IFN was a property associated with clonal cell lines and cell populations harboring the HP replicon. In contrast, the K2040 replicon retained its IFN-sensitive phenotype after transduction and selection of the reconstructed K2040 RNA in naïve Huh7 cells. Since the K2040 and HP RNA were maintained at approximately equal abundance in the respective cell lines (see Fig 3-2), we do not attribute this difference in IFN sensitivity to replicon copy number distinctions that could have affected the viral RNA decay rates after IFN treatment. Despite the differences in IFN sensitivity among the HCV

replicons, our transfection and microarray studies, respectively, did not reveal any significant differences in the IFN-induced activation of either an ISG56 promoter-reporter gene, an ISRE reporter gene or the overall profile of ISGs between control Huh7 cells and cells harboring the different replicons. Thus, HCV replicons and the replicon-encoded NS proteins in general do not affect IFN-receptor signaling events in this context. Instead, our microarray analyses identified a specific defect in the expression of ISG56 within Huh7-HP cells. This characteristic of ISG56 regulation was conferred by the HP replicon upon transduction of naïve Huh7 cells with the HP RNA but normal levels of IFN-induced ISG56 expression were restored when the Huh7-HP cells were cured of the replicon upon prolonged high-dose IFN treatment. We conclude that ISG56 regulation was conferred by viral disruption of cellular processes that control the expression of this ISG.

The linkage of IFN resistant HCV RNA replication with a deficit in IFN-induced ISG56 expression indicates that one or more HP mutation directs the control of ISG56 expression, perhaps by modulating IFN and/or viral responsive signaling events that influence ISG56 expression. ISG56 has been defined as an IRF-3 target gene (56), and we speculate that HCV control of IRF-3 could be a factor that affects ISG56 levels. By this model viral regulation of secondary signaling events that regulate ISG56 expression could be a key element by which the one or more viral NS proteins suppress its expression. HCV adaptive mutations in the NS3 coding region, and to a larger extent the NS5A coding region, have associated with viral resistance to IFN *in vivo* (69, 178) but their relationship to ISG56 has not been addressed. It remains possible that the HP mutations within the NS3, NS5A or

other NS proteins direct the control of ISG56 expression by modulating the yet to be defined host pathways that control ISG56 expression.

Within the IFN response, ISG56 confers a level of control to HCV RNA translation through processes that are dependent upon its interaction with the p48 subunit of eIF3 to directly affect ribosome recruitment to the viral RNA (170). When compared to Huh7-L2198S cells, we found a substantial reduction in the relative abundance of ISG56 from Huh7-HP cells that co-distributed with eIF3 within sucrose gradient fractions isolated from our polysomes distribution studies. Overall, the basal and IFN-induced levels of ISG56 expression in Huh7-L2198S cells respectively corresponded to an association of the L2198S RNA with low mass polysomes and their disassembly upon IFN treatment. However, the HP RNA was maintained in high mass polyribosome complexes that were retained in the presence of IFN, indicating that the distinct polysomes profiles of the L2198S and HP RNA were attributed, at least in part, to the respective level and action of ISG56 in the host cell. We have found that the IFN sensitivity of the K2040 replicon corresponded with high induction of ISG56 and a concomitant disassembly of ribosome-viral RNA complexes (170). Our results, taken together, suggest that viral control of ISG56 expression supports IFN resistant HCV RNA replication by removing a layer of control from the IFN-induced block to the translation initiation process.

In summary, our results show that HCV RNA replication can trigger a host response that includes IRF activation, IFN production and ISG expression, and that antiviral pressures

from this response can drive selection of viral adaptive mutations that confer resistance to IFN action. Our studies define the control of viral RNA translation mediated by ISG56 as an important component of the host response to HCV whose targeted suppression may contribute viral persistence and host response evasion.

Table 3-1. Primer pairs used for site directed mutagenesis.

<b>Mutation</b>	<b>Primer pair</b>
P1115L	5' GGCAAGCGCCCCTCGGGGCGCGTTC 3' 5' GAACGCGCCCCGAGGGGCGCTTGCC 3'
K1609E	5' GGGACCAAATGTGGGAGTGTCTCATACGGC 3' 5' GCCGTATGAGACACTCCCACATTTGGTCCC 3'
Q1737R	5' GCAATCGGGTTGCTGCGAACAGCCACCAAGC 3' 5' GCTTGGTGGCTGTTTCGCAGCAACCCGATTGC 3'
P2007A	5' CGATTGCCGGGAGTCGCCTTCTTCTCATGTC 3' 5' GACATGAGAAGAAGGCGACTCCCGGCAATCG 3'
L2198S	5' GGGGATCTCCCCCCTCCTCGGCCAGCTCATCAGC 3' 5' GCTGATGAGCTGGCCGAGGAGGGGGGAGATCCCC 3'
S2236P	5' GACGGTTGTCCTGCCAGAATCTACCGTGTC 3' 5' GACACGGTAGATTCTGGCAGGACAACCGTC 3'
V2971A	5' CCAGCTGGTTCGCTGCTGGTTACAGCGG 3' 5' GACACGGTAGATTCTGGCAGGACAACCGTC 3'
K2040	5' CACCGGACATGTGAAAAAAAAACGGTTCCATGAGGATCGTGG 3' 5' CCACGATCCTCATGGAACCGTTTTTTTTTCACATGTCCGGTG 3'

Table 3-2. IFN- $\beta$  production in control and HCV replicon-bearing cells.

Cells	Treatment	
	-dsRNA	+dsRNA <sup>1</sup>
B52	-	324.7 (163.9) <sup>2</sup>
Huh7	-	314.2 (95.8)
Huh7-K2040	-	26.7 (8.1)
Huh7-L2198S	116 (13.6)	253.6 (53.4)

<sup>1</sup>Cells were mock-transfected (-dsRNA) or transfected with poly(I)(C) (+dsRNA) 24 hr prior to assessing IFN- $\beta$  levels from culture media.

<sup>2</sup>pg/ml (+/- S.D.)

Table 3-3. ISGs identified in Huh7 cells and HCV replicon-bearing Huh7 cell lines by microarray analysis.

Gene Name	Acc. No <sup>2</sup> .	Fold change <sup>1</sup>			
		Huh7	L2918S	HP	K2040
OASI (p40/46)	X04371	< 2	3.2	< 2	< 2
MxA	NM_002462	2.3	7.0	7.0	9.9
ISG1-8U	NM_021034	3.0	3.0	4.6	7.5
Phospholipid-scramblase	AB006746	2.5	2.6	2.1	2.8
ISG6-16	NM_002038	15.0	7.5	27.8	8.0
ISG9-27	NM_003641	6.5	3.7	5.3	6.5
ISG56	M24594	3.2	2.8 <sup>3</sup>	< 2	4.3
ISG15	M13755	11.3	5.2 <sup>3</sup>	11.3	9.2
ISG54	N63988	< 2	2.3	< 2	< 2
P44	D28915	< 2	2.3	< 2	2.3

<sup>1</sup>Fold change (p<0.005) of mRNA level within cells cultured in the presence of 10 U/ml of IFN $\alpha$ 2a for 24 hr as compared to the same cells cultured in the absence of IFN.

<sup>2</sup>Gene sequence accession as designated by the Genbank database.

<sup>3</sup>Fold-change represents an increase from a preexisting basal level of expression (as determined by Northern blot analysis) and does not adequately reflect the comparably high abundance of ISG56 and ISG15 mRNA in Huh7-L2198S cells cultured in the absence of IFN.

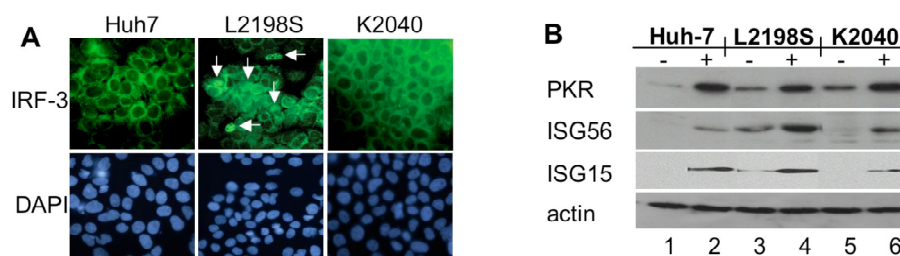


Fig 3-1. Assessment of protein expression and IRF-3 localization in Huh7 control and HCV replicon cell lines. (A) Huh7 control cells (left panel set), Huh7-L2198S cells (middle panel set) or Huh7-K2040 cells (right panel set) cultured on chamber slides were fixed and probed with polyclonal rabbit anti-IRF-3 serum and a FITC-conjugated donkey anti-rabbit secondary antibody (upper panels). Following antibody staining, the nuclei were stained with DAPI (lower panels). IRF-3 and nuclei were visualized by fluorescence microscopy using a Zeiss Axiovert digital imaging microscope in the UT Southwestern Pathogen Imaging Facility. The white arrows point to nuclear IRF-3 in Huh7-L2198S cells, which amounted to 5-7% of the cells in a given culture. Magnification was 40X. (B) Immunoblot analysis of interferon-stimulated gene (ISG) expression. Huh7 control, Huh7-L2198S or Huh7-K2040 cells were cultured for 24 hr alone (-; lanes 1, 3, and 5) or in the presence of 10 U/ml IFN $\alpha$ 2a (+; lanes 2, 4, and 6). 20  $\mu$ g of total cellular protein were then separated on a 10% SDS-PAGE gel and subjected to immunoblot analysis of PKR, ISG56 and ISG15 protein levels. In this and other immunoblot experiments we confirmed that equal amounts of protein were loaded in each lane of the gel by stripping the blot and reprobing it with an antiserum to actin (lower panel).



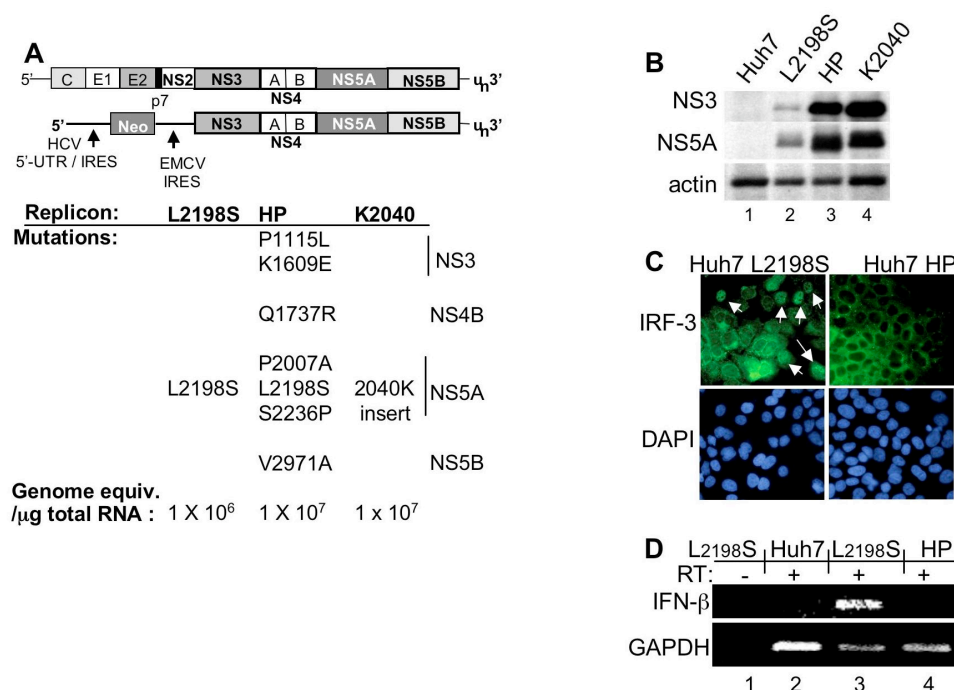


Fig 3-2. Features of genetically distinct HCV replicons and Huh7 cell lines. (A) Schematic structural representation of full-length HCV genome (upper) and the HCV subgenomic RNA replicon (lower). The regions corresponding to the 5' NTR/IRES, 3' NTR, and core (C), envelope (E1, E2), p7 and nonstructural protein coding regions are indicated. Also shown is the position of the EMCV IRES in the HCV replicon RNA. Below this are listed the three HCV replicons examined in this study and their corresponding adaptive mutations. Aa positions refer to the HCV Con1 polyprotein sequence (105). HCV replicon RNA genome equivalents were determined by quantitative RT-PCR and are expressed per microgram of total cellular RNA (bottom of Fig). (B) HCV protein level in extracts from Huh7 (lane 1), Huh7-L2198S (lane 2), Huh7-HP (lane 3) or Huh7-K2040 cells (lane 4) were assessed by resolving 20 μg total cellular protein by denaturing gel electrophoresis (10% SDS-PAGE)

followed by immunoblot analysis using an HCV-specific antiserum to detect the NS3 and NS5A proteins. The abundance of actin was monitored as an internal control (lower panel).

(C) The subcellular localization of IRF-3 in Huh7-L2198S and Huh7-HP cells was determined by anti-IRF-3 immunostaining and immunofluorescence microscopy exactly as described in the legend to Fig 3-1B. Nuclei (lower panels) were visualized by DAPI stain of the fixed cells. The white arrows point to cells with the nuclear isoform of IRF-3. (D) IFN- $\beta$  (upper panel) and GAPDH mRNA expression (lower panel) in total RNA isolated from Huh7-L2198S cells (lanes 1 and 3) or Huh7-HP cells (lanes 2 and 4) were detected by standard RT-PCR assay using primers specific for IFN- $\beta$  or GAPDH. RT above each lane refers to the presence or absence of reverse transcriptase in the reaction mix.

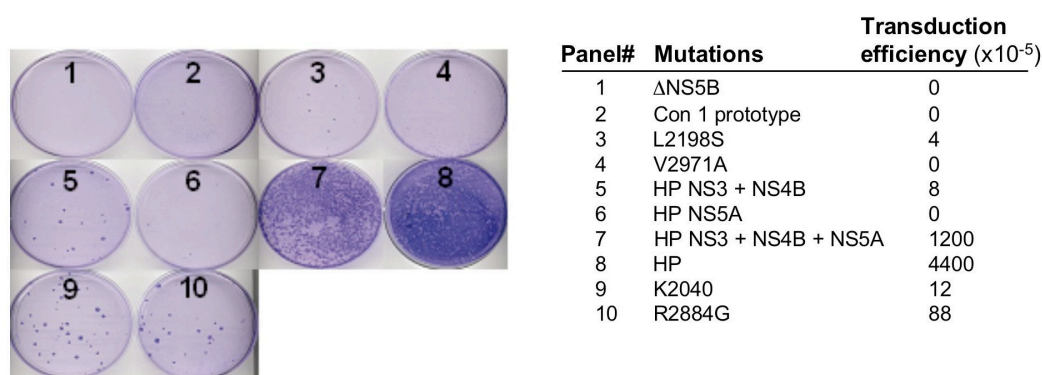


Fig 3-3. HP adaptive mutations act synergistically to confer increased transduction efficiency of the HCV replicon RNA. The specific adaptive mutations identified in the L2198S, HP or K2040 HCV replicon were reintroduced into the parental HCV replicon cDNA as described in Materials and Methods. Huh7 cells were transfected with 900 ng of DNA-free *in vitro* transcribed replicon RNA plus 100 ng luciferase polyA RNA for monitoring and normalization of transfection efficiency. The numbered panels show the cell colonies that were recovered after three weeks of G418 selection and correspond to the average transduction efficiency (derived from triplicate experiments) and the corresponding replicon mutation(s) listed below the panel set. Transduction efficiency is expressed as the average number of stably transduced cell colonies per  $10^5$  cells plated and was controlled for transfection efficiency as determined by luciferase assay.

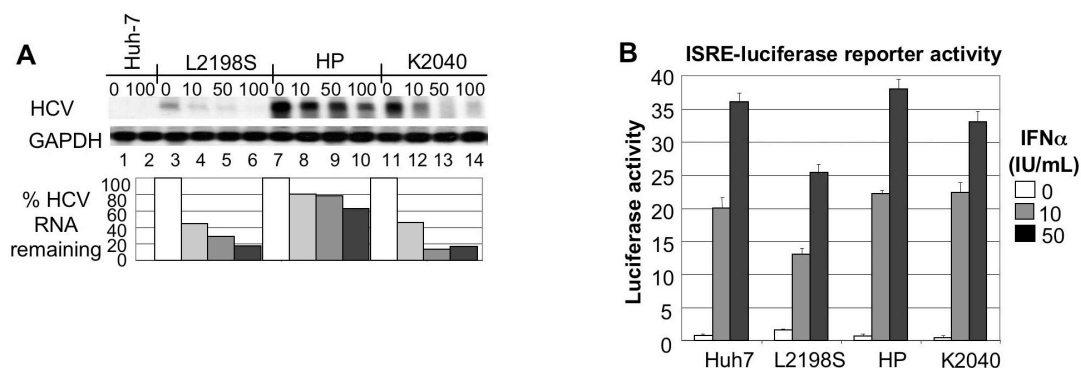


Fig 3-4. HP mutations associate with IFN resistant HCV RNA replication independently of defects in IFN signaling to the ISRE. (A) Control Huh7 cells (lanes 1 and 2) and HCV replicon-bearing Huh7-L2198S cells (lanes 3-6), Huh7-HP cells (lanes 7-10) or Huh7-K2040 cells (lanes 11-14) were cultured in the absence of G418 in medium containing 0, 10, 50 or 100 U/ml IFN $\alpha$ 2a for 24 hr after which the cells were harvested and extracts prepared for RNA evaluation. 5  $\mu$ g of total RNA was subjected to Northern blot analysis using probes specific for HCV or GAPDH. The relative HCV and GAPDH signal strength were then quantified by phosphorimager analysis and a HCV/GAPDH RNA ratio for each lane was calculated. The percentage of HCV RNA remaining relative to GAPDH for each IFN dose was determined by dividing the resulting HCV:GAPDH ratio from the IFN-treated samples by the ratio value derived from each untreated control and is expressed in the bar graph as percent HCV RNA remaining. (B) Control Huh7 cells or replicon-bearing cell lines were transfected in triplicate with a plasmid encoding the ISRE-firefly luciferase reporter construct and a second plasmid encoding the *Renilla* luciferase reporter protein expressed from a constitutive CMV promoter. 24 hr later the culture medium was replaced with fresh medium containing 0, 10 or 50 U/ml IFN $\alpha$ 2a and the cells were cultured for a further 8 hr, harvested

and extracts were subjected to the dual luciferase reporter assay. ISRE-luciferase values were normalized against the *Renilla* luciferase value. The graph shows the average relative ISRE-dependent luciferase values and standard deviation from a total of three experiments.

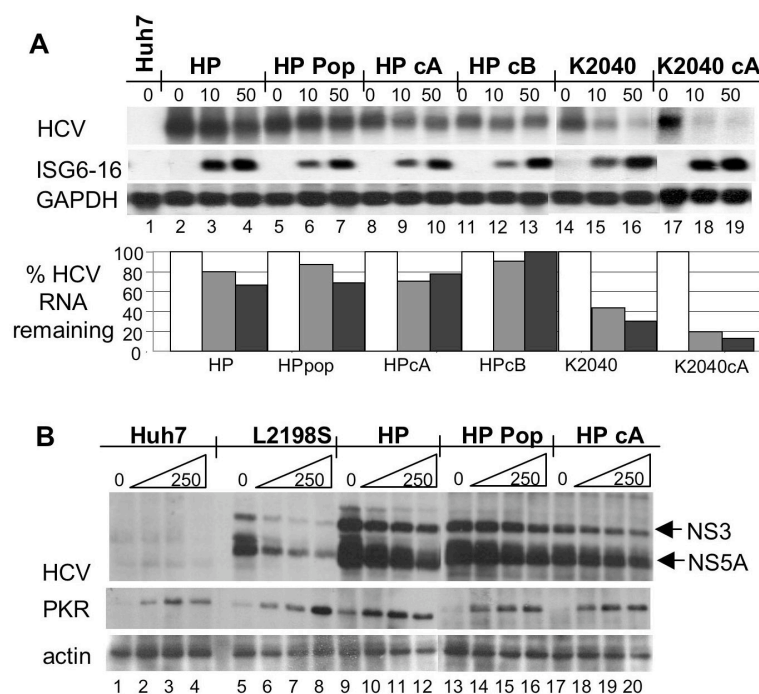


Fig 3-5. HP mutations specifically confer IFN resistance to HCV RNA replication. (A) Total RNA from cells cultured for 24 hr in medium alone or in the presence of increasing concentrations of IFN $\alpha$ 2a was subjected to Northern blot analysis of HCV RNA, ISG6-16 and GAPDH mRNA levels. Lanes show control Huh7 cells cultured in medium alone (lane 1) and HCV replicon cells cultured in 0, 10 or 50 U/ml IFN $\alpha$ 2a. Lanes 2-4 show the original Huh7-HP cells. Lanes 5-13 show a cell population (HP pop, lanes 5-7) and clonal cell lines (respectively HP cA, lanes 8-10 and HP cB, lanes 11-13) that were derived from naïve Huh7 cells transduced with the reconstructed HP replicon RNA. The original Huh7-K2040 cells (K2040, lanes 14-16) and a clonal cell line from naïve Huh7 cells transduced with the reconstructed K2040 replicon RNA (K2040 cA, lanes 17-19) were included for comparison. The percentage of HCV RNA remaining in the IFN-treated cells is shown in the bar graph and was derived as described in the legend to Fig. 3-4. (B) HCV protein, PKR and actin

abundance were evaluated by immunoblot analysis of extracts prepared from cells cultured in medium alone or with increasing amounts of IFN $\alpha$ 2a for 48 hr. Shown are Huh7 cells (lanes 1-4), Huh7-L2198S cells (lanes 5-8), Huh7-HP cells (lanes 9-12); lanes 13-20 show a cell population (HP pop, lanes 13-16) and a clonal cell line (HP cA, lanes 17-20) that were derived from naïve Huh7 cells transduced by the reconstructed HP replicon RNA. The panels show NS3 and NS5A expression (denoted by arrows; upper panel), PKR (middle panel) and actin expression (lower panel). Each lane set represents IFN doses (from left to right) of 0, 10, 100 and 250 U/ml IFN $\alpha$ 2a.

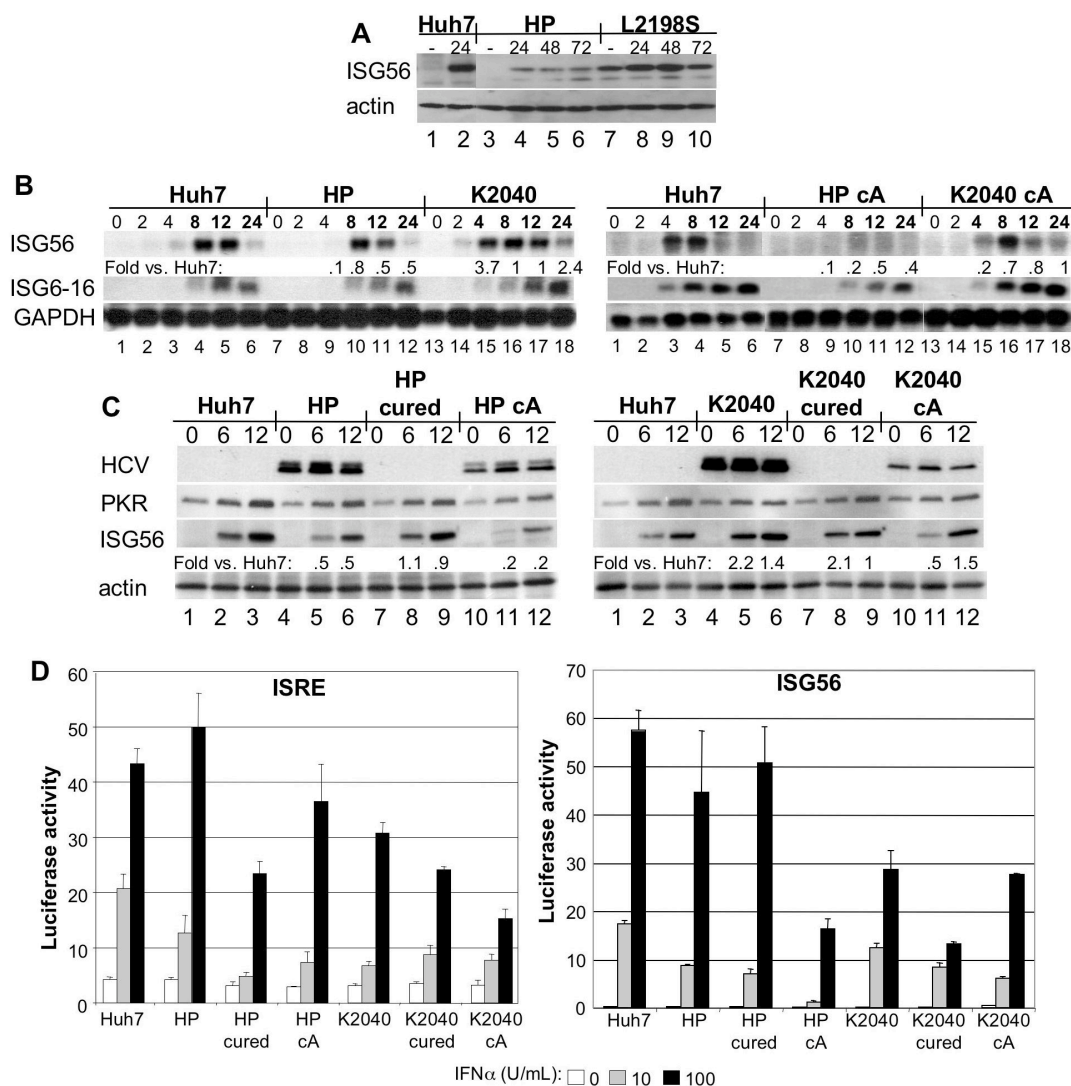


Fig 3-6. Suppression of ISG56 expression by the HCV HP replicon and restoration of expression in cured cells does not associate with differences in IFN receptor signaling to the ISRE. (A) Immunoblot analysis of ISG56 and actin expression in control Huh7 cells (lanes 1 and 2), Huh7-HP cells (lanes 3-6) and Huh7-L2198S cells (lanes 7-10). Cells were cultured in medium alone (-) or containing 10 U/ml IFN $\alpha$ 2a for 24, 48, or 72 hr as shown above the corresponding lane. (B) 5  $\mu$ g of total RNA from cells cultured in medium alone or



containing 10 U/ml IFN $\alpha$ 2a were subjected to Northern blot analysis using cDNA probes specific for ISG56, ISG6-16 or GAPDH. Cells were harvested at 0, 2, 4, 8, 12 or 24 hr post-IFN treatment as indicated above each lane. The left panel set shows a comparison of control Huh7 cells (lanes 1-6) Huh7-HP cells (lanes 7-12) and Huh7-K2040 cells (lanes 13-18). The right panel set shows a comparison of control Huh7 cells (lanes 1-6) with clonal cell lines derived from naïve Huh7 cells transduced with the reconstructed HP replicon RNA (HP cA, lanes 7-12) or the reconstructed K2040 replicon RNA (K2040 cA, lanes 13-18). The fold-difference in ISG56 level in replicon cells compared to Huh7 control cells for each time point is shown below the corresponding lane and was quantified as described in the legend to Fig 3-4. (C) Immunoblot analysis of NS5A, PKR, ISG56 and actin abundance in cells cultured for 0, 6 or 12 hr in the presence of 10 U/ml IFN $\alpha$ 2a. The left panel set shows protein expression in control Huh7 cells (lanes 1-3), Huh7-HP cells (lanes 4-6), Huh7-HP cells devoid of the HCV replicon (HP cured, lanes 7-9) and a clonal cell line derived from naïve Huh7 cells transduced with the reconstructed HP replicon RNA (HP cA, lanes 10-12). The right panel set: control Huh7 cells (lanes 1-3), Huh7-K2040 cells (lanes 4-6), Huh7-K2040 cells devoid of the HCV replicon (K2040 cured, lanes 7-9) and a clonal cell line derived from naïve Huh7 cells transduced with the reconstructed K2040 replicon RNA (K2040 cA, lanes 10-12). To generate cell lines devoid of the HCV replicon the Huh7-HP and Huh7-K2040 cells were cultured continuously in the presence of high dose IFN $\alpha$ 2a as described in Materials and Methods. The fold difference in ISG56 protein level in replicon cells compared to Huh7 control cells for each time point is shown below the corresponding lane and was determined by quantitative densitometry of the respective ISG56 and actin bands.

(D) IFN signaling to an ISRE-promoter luciferase construct (left panel) or an ISG56-promoter luciferase construct (right panel) was measured in control Huh7 cells, Huh7-HP cells (HP), Huh7-HP cells devoid of the HCV replicon (HP cured), Huh7-HP cA cells (HP cA), Huh7-K2040 cells (K2040), Huh7-K2040 cells devoid of the replicon RNA (K2040 cured) or Huh7-K2040 cA cells (K2040 cA). Triplicate cultures of each cell line were co-transfected with a plasmid encoding a *Renilla* luciferase construct expressed from a constitutive CMV promoter and a second plasmid encoding the IFN-inducible ISRE or ISG56 promoter/enhancer firefly luciferase reporter construct. Cells were cultured in medium containing 0, 10, or 100 U/ml of IFN $\alpha$ 2a for 8 hr, harvested and subjected to the dual luciferase assay. Bars show the average relative firefly luciferase activity and standard deviation of values normalized for *Renilla* luciferase activity between each sample.

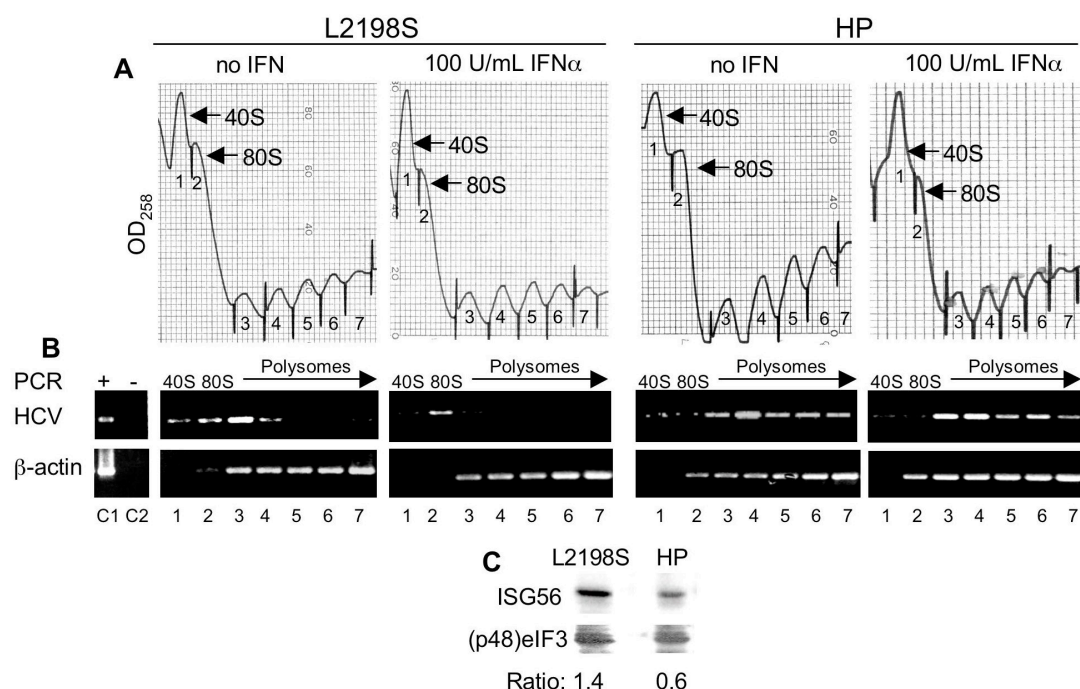


Fig 3-7. Differential ribosome recruitment by the HCV replicon RNA and alteration of the ISG56:(p48)eIF3 ratio associates with IFN resistant viral RNA replication. Huh7-L2198S cells (left panel set) or Huh7-HP cells (right panel set) were cultured in medium alone or containing 100 U/ml IFN $\alpha$ 2a for 16 hr. Cell extracts were prepared for polyribosome distribution analysis and RNA-protein complexes were separated by ultracentrifugation through a sucrose density gradient. Gradient fractions were collected and simultaneously monitored for their optical density at 258 nm (OD<sub>258</sub>). (A) The relative density of each fraction from the respective gradient is shown in the panel set and the gradient positions of the template-associated 40S ribosome, 80S ribosome and polyribosomes are indicated. (B) The gradient distribution of the HCV replicon RNA and  $\beta$ -actin were monitored by RT-PCR analysis on an equal volume of total RNA isolated from each fraction. Panel sets correspond to the gradient OD<sub>258</sub> profile shown above each set and were derived from an ethidium

bromide-stained agarose gel of the resolved RT-PCR products as indicated. Lane numbers shown beneath each gel image correspond to fraction number shown in the respective OD<sub>258</sub> profile. Lanes C1 and C2 on the far left show control RT-PCR products from a reaction containing RNA from sucrose gradient fraction 4 derived from Huh7-HP cells cultured without IFN. (C) Proteins were extracted from sucrose gradient fractions 1 and 2 containing 40S and 80S ribosome associated RNA from the IFN treated Huh7-L2198S cells (left) or Huh7-HP cells (right) shown above. The abundance of ISG56 and eIF3 were measured by immunoblot analysis and quantitative densitometry of the products shown to derive the indicated ISG56:(p48)eIF3 ratio. The eIF3 panel shows the p48 eIF3 subunit, which is an interacting partner with ISG56 (75). Comprehensively similar results were obtained from cells cultured in the presence or absence of 10 U/ml IFN $\alpha$ 2a (data not shown).

## **CHAPTER 4: RIG-I DEFINES HOST CELL PERMISSIVENESS TO HCV RNA REPLICATION**

### Introduction

In addition to viral genetic determinants of HCV persistence, defects in cellular factors responsible for mediating the induction of an antiviral state in response to viral dsRNA might increase susceptibility to persistent HCV infection. Several Huh7 derived cell lines that are highly permissive for transduction by HCV replicons have been identified (17), but their response to dsRNA had not yet been characterized. DsRNA is a pathogen-associated molecular pattern (PAMP) found in highly structured regions of single stranded RNA viral genomes, including HCV, and is an intermediate in the replication of many viruses. Activation of IRF-3 and subsequent IFN- $\beta$  production in response to extracellular dsRNA is known to require TLR3 in a signaling cascade involving the adaptor protein TRIF and the kinase TBK1 (118, 180). Several groups have suggested the existence of a TLR3- and TRIF-independent dsRNA response pathway that recognizes dsRNA motifs in the cytoplasm of the host cell, but the identity of the host factor(s) involved in this pathway was not defined in these studies (68, 70). Recently, Yoneyama, et. al. have shown that RIG-I, a DExH/D-box helicase containing a caspase recruitment (CARD) domain, recognizes dsRNA and can mediate IRF-3 activation and IFN- $\beta$  induction in response to viral infection or dsRNA transfection in a TLR3-independent manner (184).

In this study, we investigated the cellular response to HCV RNA and its impact of the permissiveness of host Huh7 cells to HCV RNA replication. We demonstrate that structured regions of the HCV RNA genome are potent inducers of the cellular antiviral response and identify the HCV 5' nontranslated region (5' NTR)/internal ribosome entry site (IRES) and 3' NTR as agonists for host dsRNA activated pathways. Defective RIG-I-mediated IRF-3 activation in response to HCV dsRNA results in increased permissiveness of Huh7 cells to HCV RNA replication. These results illustrate the central importance of the regulation of IRF-3 signaling for the establishment of persistent HCV RNA replication.

## Results

### *Activation of the host antiviral response by HCV RNA.*

The efficiency of HCV RNA replication is dependent in part on viral adaptive mutations or host differences that confer differential ability to initiate replication and overcome the cellular antiviral response that is triggered by viral RNA (40, 133). To determine how the host response may influence the initiation of HCV RNA replication, we examined the expression of a variety of ISGs in human hepatoma (Huh7) cells transfected with *in vitro* transcribed RNA encoding different HCV subgenomic RNA replicons. Each replicon contained distinct adaptive mutations that confer differential replication and transduction properties (157). As shown in Figure 4-1A, the expression of ISG6-16, ISG56, and ISG15 was induced by 12 hr after transfection of Huh7 cells with HCV subgenomic replicons L2198S, HP, or K2040 in addition to the replication deficient mutant  $\Delta$ 5B, while no response was observed in mock transfected cells. HCV replicon RNA therefore has the capacity to stimulate a host response independent of HCV RNA replication in Huh7 cells.

The single-stranded HCV RNA genome contains defined regions of secondary structure including the 5' NTR/IRES (22) and the 3' NTR (18). In addition, computer modeling has revealed regions of predicted RNA secondary structure in the HCV protein coding region as well as regions marked by nonstructured linear domains (167). To determine the relative contributions of these regions of the HCV genome towards triggering the host antiviral response, we transfected Huh7 cells with purified, *in vitro* transcribed RNA spanning the highly structured HCV 5' NTR/IRES or 3' NTR. As controls, we included an

analysis of cells transfected with RNAs corresponding to HCV nt 3423-3772 (ss1) and 6261-6702 (ss2), which are predicted to represent nonstructured RNA domains (167). Transfection of cells with HCV 5' NTR/IRES or 3' NTR RNA induced the IFN- $\beta$  promoter element, as measured by promoter luciferase assay. In contrast, nonstructured HCV RNA failed to induce the IFN- $\beta$  promoter in transfected cells (Fig 4-1B). These results suggest that dsRNA regions of the HCV genome can trigger a host response that includes IFN- $\beta$  promoter induction and ISG expression. To verify and extend these results, we transfected Huh7 cells with purified *in vitro* transcribed RNA constructs that direct the expression of the firefly luciferase gene, thereby allowing us to monitor the overall transfection efficiency between experiments. Northern blot analysis revealed that firefly luciferase RNA appended with a polyA tail was a poor inducer of ISG expression in transfected Huh7 cells (Fig 4-1C). In contrast, HCV IRES-luciferase and EMCV IRES-luciferase RNA both induced ISG expression within 8 hr after transfection into Huh7 cells. Analysis of luciferase activity demonstrated that the cells were transfected efficiently and that the luciferase gene product itself was not responsible for induction of ISG expression, confirming that structured regions of the HCV and replicon genome activate host response pathways that lead to ISG expression in Huh7 cells. Because HCV IRES RNA represents a physiologic trigger of the host response to HCV RNA and can be monitored by luciferase assay of transfected cells, we utilized the HCV IRES luciferase RNA to model the host response in further experiments. As shown in Fig 4-1D, transfected HCV IRES luciferase or L2198S replicon RNA, but not luciferase polyA RNA, induced the expression of IFN- $\beta$  as measured by real time PCR within 8 hr after transfection. Taken together, these results demonstrate that regions of



secondary structure within the HCV RNA genome can act as agonists of cellular pathways that trigger IFN- $\beta$  and ISG expression.

*Evaluation of host response pathways in cells permissive to HCV RNA replication.*

Host pathways activated by viral RNA play important roles in controlling viral replication, and lesions in host response pathways have been shown to confer increased permissiveness to virus infection (7, 141). Previous work has identified a subline of Huh7 cells, termed Huh7.5, that exhibit a marked increase in their permissiveness to HCV RNA replication (17). We hypothesized that one or more components of the host response was defective in these cells. First, we verified the increased permissiveness of these cells to HCV RNA replication by measuring both initial HCV RNA replication and HCV replicon transduction efficiency. For measurement of initial HCV RNA replication, we utilized a transient HCV replication assay in which we transfected HCV RNA replicons engineered to express luciferase under control of the HCV IRES into Huh7 and Huh7.5 cells. As shown in Fig 4-1E (left panel), we observed an increase in initial HCV replication efficiency in the permissive Huh7.5 cells. In addition, stable transduction of Huh7.5 cells by HCV RNA replicons was more efficient in Huh7.5 cells. As shown in the right panel set of Fig 4-1E, transfection of Huh7.5 cells with L2198S and K2040 HCV replicon RNAs resulted in a greater than 70-fold enhanced transduction efficiency when compared to Huh7 cells. We hypothesized that the increased permissiveness of Huh7.5 cells to HCV RNA replication might result from a specific defect in the host response initiated by HCV dsRNA.

We examined Huh7.5 cells for defects in cellular signaling pathways activated by type I IFN or that directly or indirectly respond to viral RNA. No differences were observed in the response of Huh7 or Huh7.5 cells to treatment with IFN- $\alpha$ 2a over a range of IFN doses and the expression of an IFN-responsive ISRE promoter luciferase construct was induced to comparable levels in both cell lines, indicating that type I IFN receptor/Jak-STAT signaling pathway was intact in Huh7.5 cells (Fig 4-2A). We also examined virus-responsiveness of PKR, P38 MAPK and IKK pathways, each of which are activated in response to dsRNA accumulation during virus infection (7, 29). As shown in Fig 4-2B, both the kinase activity of PKR and PKR-dependent eIF2 $\alpha$  phosphorylation were induced in both Huh7 and Huh7.5 cells in response to vesicular stomatitis virus (VSV) infection. In addition, we found that VSV efficiently triggered the phosphorylation of P38 MAPK and induced the degradation of I $\kappa$ B $\alpha$  in Huh7 and Huh7.5 cells, indicating that the virus-responsiveness of the IKK and MAPK pathways remained intact in Huh7.5 cells (Fig 4-2C).

*Defective IRF-3 activation correlates with increased permissiveness to HCV RNA replication.*

Virus infection results in the activation of IRF-3 and the subsequent expression of IRF-3 target genes including IFN- $\beta$  and ISG56 (59, 141). To determine if the IRF-3 pathway was intact in Huh7.5 cells, we measured the activation of an IFN- $\beta$  promoter luciferase construct in Huh7 and Huh7.5 cells in response to either Sendai virus (SenV) or VSV infection. As shown in Fig 4-3A, infection of Huh7 cells with SenV or VSV induced the activation of the IFN- $\beta$  promoter, but neither virus triggered IFN- $\beta$  promoter induction in

Huh7.5 cells. To verify these results, we examined protein expression in Huh7 and Huh7.5 cells after various treatments that included SenV infection, IFN- $\alpha$  treatment or transfection with HCV IRES RNA. As shown in Fig 4-3B, SenV infection, IFN treatment and HCV IRES RNA transfection induced the expression of ISG56 in Huh7 cells. In contrast, Huh7.5 cells were defective in their response to SenV and HCV IRES RNA and did not induce ISG56 expression in response to either stimulus. However, the Huh7.5 cells fully responded to IFN treatment and induced ISG56 to similar levels as their IFN treated Huh7 counterparts. We also examined the subcellular distribution of endogenous IRF-3 in either cell line in response to virus infection or RNA transfection. As shown in Fig 4-3C, in resting Huh7 cells IRF-3 is distributed in a perinuclear/cytoplasmic context and, in response to virus infection, active IRF-3 redistributes to the nucleus. In addition, we found that transfection of Huh7 cells with HCV IRES -luciferase induced the nuclear redistribution of IRF-3, demonstrating that HCV RNA could directly trigger IRF-3 activation. The active, nuclear isoform of IRF-3 was not detected in Huh7 cells upon transfection with control luciferase polyA RNA. Huh7.5 cells were refractory to IRF-3 activation by SenV or HCV IRES-luciferase RNA, and IRF-3 was retained in the cytoplasm under all conditions tested.

Our results suggest that the Huh7.5 cells have a specific defect in the IRF-3 pathway that confers differential regulation of ISG expression in response to viral RNA, and this differential host response could contribute to the increased permissiveness of Huh7.5 cells to HCV RNA replication. We therefore compared the pattern of ISG expression in Huh7 and Huh7.5 cells after transfection of HCV IRES-luciferase or HCV replicon RNAs. As shown

in Fig 4-3D, Northern blot analysis demonstrated that Huh7 cells responded to HCV RNA to induce ISG expression within a 12 hr time course. Parallel analysis of transfected Huh7.5 cells confirmed that these cells were refractory to HCV RNA and as a consequence failed to induce ISG expression. Similar patterns of ISG expression were observed when cells were transfected with poly(I)(C) (data not shown). These results provide evidence to link defective IRF-3 activation to a loss of ISG expression in response to HCV RNA in Huh7.5 cells.

*Characterization of the IRF-3 response defect.*

We sought to determine the level at which the IRF-3 activation pathway was compromised in Huh7.5 cells. We first evaluated whether the IRF-3 pathway was competent to induce the nuclear translocation of a GFP-tagged IRF-3 protein when ectopically expressed in Huh7 or Huh7.5 cells. As shown in Fig 4-4A (panels 1-4 and 7-10), GFP-IRF-3 accumulated in the nucleus of Huh7 cells but not Huh7.5 cells in response to SenV infection. We verified that the lack of IRF-3 nuclear accumulation in virus infected Huh7.5 cells was not due to disruption of IRF-3 nuclear transport processes because the phosphomimetic IRF-3 5D mutant (102) was constitutively localized to the nucleus upon expression in Huh7 or Huh7.5 cells (Fig 4-4A panels 5-6 and 11-12). These results suggested that lesion(s) in Huh7.5 cells is above the level of IRF-3 itself and likely resides within one or more upstream transducers of IRF-3 activation. Therefore, we examined IRF-3 dependent signaling to an IFN- $\beta$  promoter luciferase construct. Forced expression of the VAK components, TBK1 or IKK $\epsilon$  induced the activation of the IFN $\beta$  promoter in both Huh7 and Huh7.5 cells.

Moreover, ectopic expression of the TLR adaptor protein TRIF resulted in IFN- $\beta$  promoter activation in either cell type. We confirmed that endogenous TBK1 and IKK $\epsilon$  proteins were expressed to equal levels in Huh7 and Huh7.5 cells (Fig 4-4B) and that TRIF and TLR3 mRNAs were equally abundant in both cell types (data not shown). We also sequenced the respective protein coding regions of the TBK1, IKK $\epsilon$  and TRIF mRNAs amplified from Huh7 and Huh7.5 cells. While nonsynonymous mutations were not identified, we did find several silent mutations in these mRNAs that were shared between Huh7 and Huh7.5 cells (data not shown). Huh7 cells express little, if any, TLR3 and they do not respond to extracellular dsRNA (98), suggesting that the response to intracellular HCV RNA is TLR3-independent. Thus, we concluded that signaling to IRF-3 from the level of VAK complex in response to virus infection or intracellular dsRNA is intact in Huh7.5 cells and that the lesion in the IRF-3 pathway was attributed to an undefined signal transducer or RNA recognition molecule.

*RIG-I complements the IRF-3 defect in permissive cells.*

To identify upstream signaling components that conferred responsiveness to intracellular dsRNA upon the IRF-3 pathway, we subjected Huh7.5 cells to a genetic screening/complementation assay for cDNA products that could confer virus or HCV dsRNA responsiveness to IRF-3. Recent work has identified the retinoic acid inducible gene I (RIG-I) as an intracellular pattern recognition molecule that binds intracellular dsRNA to signal the downstream activation of IRF-3 during virus infection (184). Therefore, we included RIG-I in a screen of select cDNAs that were chosen based upon previously defined roles in

activating the innate response to virus infection (38, 145). Of the subset of cDNAs screened, RIG-I was unique in conferring virus responsiveness to an IRF-3 dependent promoter element in Huh7.5 cells (Fig 4-5).

We evaluated the ability of RIG-I to complement the IRF-3 defect in Huh7.5 cells and to confer responsiveness to HCV dsRNA. Ectopic expression of RIG-I restored the induction of ISG56 expression upon either SenV infection or HCV IRES RNA transfection of Huh7.5 cells (Fig 4-6A). Moreover, the activation and nuclear translocation of the active IRF-3 isoform was dependent on RIG-I, and expression of RIG-I restored virus and dsRNA responsiveness IRF-3 as measured by its dimerization and nuclear translocation in Huh7.5 cells (Fig 4-6B and C). RIG-I is expressed at a low basal level in both Huh7 and Huh7.5 cells (Fig 4-6D and E) and its expression is increased in response to IFN treatment, as previously reported (184). However, RIG-I levels are increased in response to virus only in Huh7 cells, in keeping with the global defect in virus-induced ISG upregulation in Huh7.5 cells.

#### *RIG-I binds HCV dsRNA.*

The RIG-I cDNA encodes a 925 aa protein containing tandemly arranged amino terminal caspase recruitment domain (CARD) followed by a DExH/D-box helicase domain that binds specifically to dsRNA (see Fig 4-7A) (184). While full length wt RIG-I confers virus inducibility to the IRF-3 pathway (see Fig 4-6), the amino terminal region encoding the CARD domains directs the effector action of RIG-I and when ectopically expressed confers

constitutive activation of the IRF-3 pathway, whereas expression of the C terminal helicase domain alone directs dominant negative inhibition of virus-induced IRF-3 activation (184). We confirmed these features associated with expression of the different RIG-I domains, and found that the CARD and helicase domains, respectively, directed constitutive activation or dominant negative inhibition of an IFN- $\beta$  promoter luciferase construct in Huh7 cells after virus infection (Fig 4-7B). We also evaluated the ability of RIG-I to bind dsRNA in a pulldown assay using poly(I)(C)-agarose beads. As shown in Fig 4-7C, RIG-I was recovered from cell extracts as a poly(I)(C) binding protein. This pulldown procedure also recovered endogenous PKR, a known dsRNA binding protein, but not endogenous actin, thereby demonstrating the specificity of the assay for dsRNA binding proteins. The dsRNA binding activity of RIG-I was specifically competed by the addition of increasing concentrations of soluble poly(I)(C), HCV IRES RNA or HCV 3' NTR RNA, but not a ss region of the HCV RNA genome (Fig 4-7D).

*RIG-I is defective in permissive cells.*

The distinct domain features of RIG-I indicate that loss of function of one or both domains could potentially confer defects in dsRNA signaling to IRF-3 during virus infection and explain the phenotype of Huh7.5 cells. We therefore sequenced the entire RIG-I open reading frame from RNA isolated from Huh7 or Huh7.5 cells. A single aa change (T55I) was identified within the first CARD domain and was present only in RIG-I mRNA isolated from Huh7.5 cells (Fig 4-8A). When introduced into wt RIG-I, the T55I mutation resulted in a dominant negative effect upon RIG-I mediated activation of an IFN- $\beta$  promoter luciferase

construct in Huh7 cells (Fig 4-8B). Moreover, when introduced into a construct encoding the amino terminal CARD domains alone, the T55I mutation conferred loss of function, and the mutant protein failed to constitutively activate IRF-3 in the transfected cells (Fig 4-8 B and C). We examined the dsRNA binding properties of the T55I RIG-I mutant and found that the T55I mutation had no effect upon the ability of RIG-I to bind dsRNA (Fig 4-8D). In these experiments, the specificity of RIG-I for dsRNA was further demonstrated by the absence of a RIG-I pulldown product from ssRNA/polyC-agarose beads. Thus, the loss of function from the T55I mutation is independent from effects of differential dsRNA binding between wt and mutant RIG-I. Therefore, we attribute the inability of Huh7.5 cells to activate IRF-3 in response to dsRNA or virus infection to the T55I mutation in RIG-I and disruption of one or more signaling events directed by the RIG-I CARD domains.

*RIG-I controls permissiveness to HCV RNA replication.*

To determine if the T55I mutation in RIG-I was responsible for the increased permissiveness of Huh7.5 cells to HCV RNA replication, we evaluated the effect of RIG-I expression on initial HCV RNA replication efficiency in Huh7.5 cells. First, we demonstrated the IRF-3 target gene ISG56 was induced by HCV IRES-luc RNA transfection only in Huh7 cells (Fig 4-9A). We confirmed that ectopic RIG-I expression could rescue the host response to HCV RNA in Huh7.5 cells (Fig 4-9B, top panel set) and demonstrated that efficient RIG-I expression was maintained for at least 6 days post transfection (Fig 4-9B, bottom panel set). In parallel with these experiments, we performed an initial HCV RNA replication assay. As shown in Fig 4-9C, the RIG-I-mediated rescue of the antiviral response



results in a dramatic decrease in permissiveness for HCV RNA replication in Huh7.5 cells. These experiments identify RIG-I as a critical component of the cellular response to HCV dsRNA whose actions impart control over permissiveness to HCV RNA replication. Taken together, our results demonstrate that RIG-I plays a pivotal role in recognition of HCV dsRNA and triggers the IRF-3 component of the host response to HCV infection.

### Discussion

In this study, we demonstrate that the introduction of structured regions of the HCV RNA genome into host Huh7 cells results in activation of the host antiviral response and define the CARD-containing DExH/D box helicase RIG-I as a sensor of intracellular HCV dsRNA. We propose a model for direct activation of the antiviral response by HCV RNA (see Fig 4-9D) in which latent RIG-I specifically recognizes dsRNA structures in the HCV genome and adopts an active conformation. Active RIG-I signals to IRF-3 through as yet uncharacterized signaling intermediates, resulting in the induction of an antiviral state characterized by the induction of IFN- $\beta$  and ISGs. We hypothesize that the HCV NS3/4A serine protease targets a signaling intermediate between RIG-I and IRF-3 to block activation of the host antiviral response in the context of HCV RNA replication (these data will be presented elsewhere). The T55I point mutation in RIG-I results in specific defect in the RIG-I/IRF-3/IFN- $\beta$  arm of the response to HCV dsRNA and is responsible for the increased permissiveness of Huh7.5 cells to HCV RNA replication.

CARD-containing proteins mediate signaling events in response to a variety of intracellular and extracellular stimuli (21). Importantly, the CARD-containing proteins NOD1 and NOD2 have been shown to be involved in a TLR-independent response to intracellular bacteria by activating NF $\kappa$ B in response to bacterial products in the cytosol (25, 52, 79). RIG-I and other CARD containing DExH/D box helicase proteins may represent a family of proteins functionally similar to NODs that activate a TLR3-independent response to viruses. Unlike the CARD domains of NOD1 and NOD2, however, the RIG-I CARD is capable of inducing IRF-3 activation, suggesting that it recruits distinct signaling components (184). CARD-mediated signaling proceeds through homophilic CARD-CARD interactions between the sensor CARD and downstream signaling molecules (78) and a high degree of specificity for sensor:intermediate CARD interactions has been demonstrated in several studies (15, 171). The kinase TBK1, which does not contain a CARD, has recently been shown to be essential for virus-induced IRF-3 activation (118). Thus, the most likely scenario for RIG-I-mediated IRF-3 activation involves interaction with downstream CARD-containing proteins that ultimately results in TBK1/IRF-3 activation, although the putative signaling intermediate(s) remains to be identified. In this regard, the location of the T55I mutation in the first CARD domain of RIG-I mutant is of particular interest as it results in defective signal transduction without affecting dsRNA binding (see Fig 4-8D). We hypothesize that the RIG-I T55I mutant cannot recruit and/or signal to one or more CARD-containing downstream components and is therefore unable to transduce the dsRNA signal to IRF-3.

Huh7 cells were for some time the only cell line known to be capable of supporting stable HCV RNA replication. Although they retain the ability to respond to virus or intracellular dsRNA by activating PKR, MAPK, NF $\kappa$ B and IRF-3, they lack an intact TLR3-mediated response to dsRNA. A defect in TLR3 signaling may therefore partially explain the relative permissiveness of Huh7 cells, but the impact of this pathway on HCV RNA replication remains to be evaluated. Recently, several groups have successfully transduced HeLa cells, which have a functional TLR3 pathway, with HCV replicons (190). This will facilitate the study of TLR3-dependent signaling in the context of HCV RNA replication and expression of HCV nonstructural proteins.

Although HCV RNA subgenomes accumulate to the level of greater than 1000 copies/cell (RS and MG, unpublished data), the host antiviral response is quiescent in Huh7 cells harboring all but the most poorly adapted HCV replicons (40, 133). Similar observations have been made in the analysis of ISG expression levels in liver biopsies from chronically infected HCV patients (149). In the present study, we have shown that HCV genome itself is capable of rapidly and efficiently stimulating the host dsRNA response (see Fig 4-1), which is intact (with the exception of TLR3-mediated signaling) in Huh7 cells. Thus, Huh7 cells stably transduced with HCV subgenomic RNA replicons harbor ample stimulus for functional dsRNA-responsive pathways in Huh7 cells, including RIG-I-mediated IRF-3 activation. Current studies are focused further elucidating the mechanisms employed by HCV to antagonize HCV dsRNA-stimulated RIG-I signaling.

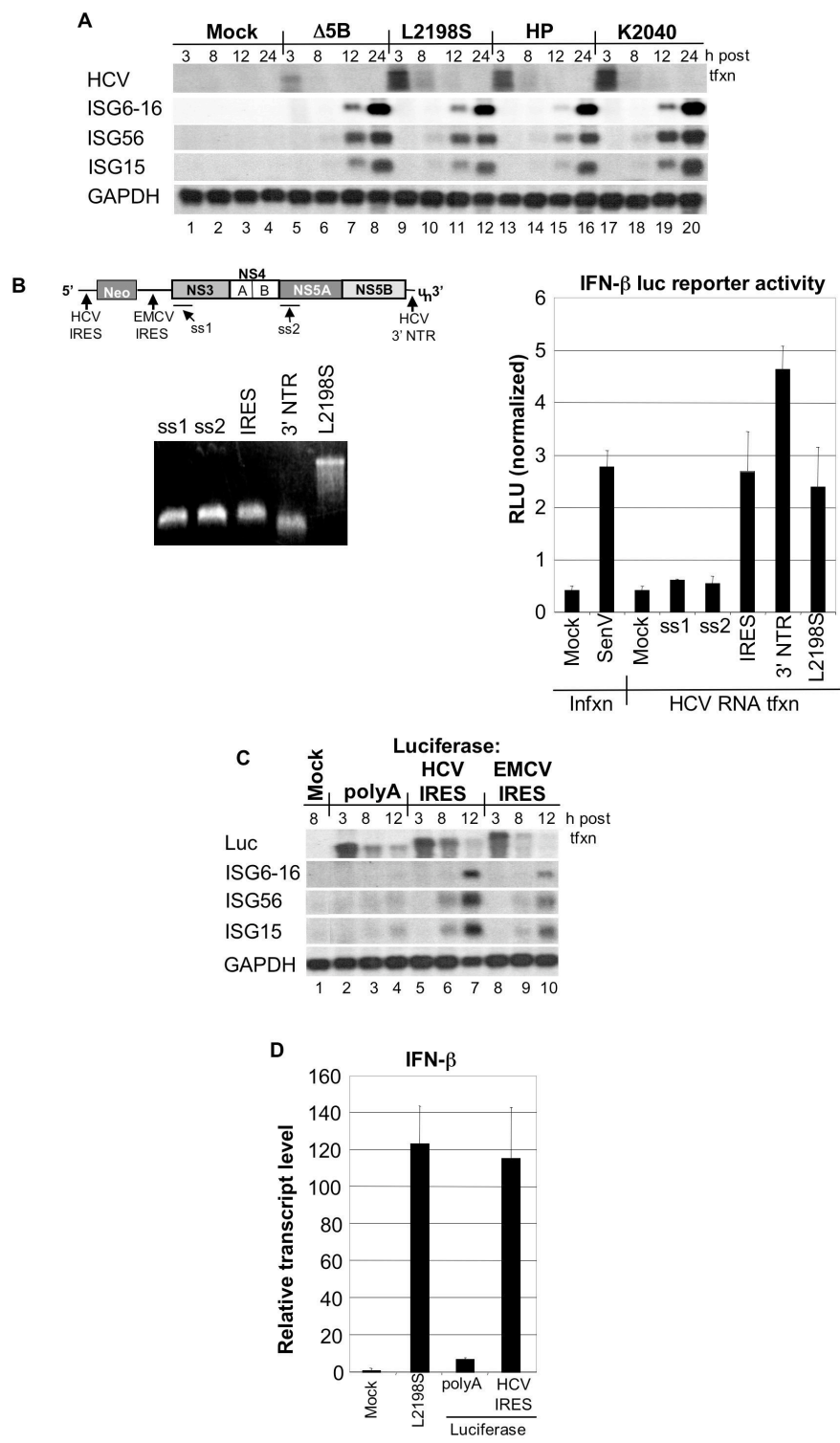
Identification of signaling pathways responsible for establishing a host response to HCV infection is of critical importance for determining the mechanisms utilized by the virus to establish persistent infection. RIG-I plays a central role in generating an antiviral state in the HCV RNA replicon model system by recognizing HCV dsRNA and activating IRF-3. Since IRF-3-mediated signaling is indispensable for the induction of IFN- $\beta$  in response to viral infection (141), control of the RIG-I/IRF-3/IFN- $\beta$  pathway is likely to be essential for the long-term maintenance of HCV RNA replication in chronic HCV infection.

Table 4-1. Primers used for PCR amplification of cDNAs for sequencing.

Gene name	GenBank ID	Sense/Antisense
TBK1	NM_013254	5' GCGGAGACCCGGCTGGTATAACAAG 3' / 5' CTATAAAGGCATTCATTTAATGCCCAAGCG 3'
IKKe	XM_375834	5' TTGGCTACCAGGAGGCTAAGAACACTGCTC 3' / 5' GGCAGTGGAAGGTAATGCTGGCGAC 3'
TRIF	NM_014261	5' TTGCAGAGGAAGAAATGGAAGTTGAAGGAGGCGACG 3' / 5' CCACCAAGACCCTTCACCCAGAAAT 3'
RIG-I	NM_014314	5' GTCCGGCCTCATTTCTCGGAAAATC 3' / 5' GGTACAAGCGATCCATGATTATACCCACTATGTTTG 3'

Table 4-2. Primers used for real time PCR analysis.

Gene name	GenBank ID	Sense/Antisense
IFN- $\beta$	NM_002176	5' CAGCAATTTTCAGTGTCTCAGAAGCT 3' / 5' TCATCCTGTCCTTGAGGCAGTAT 3'
RIG-I	NM_014314	5' GACTGGACGTGGCAAAACAA 3' / 5' TTGAATGCATCCAATATACACTTCTG 3'
ISG56	NM_001548	5' CCTGCTGGTGGTGGACAAAT 3' / 5' TGC GGCCCTTGTTATTCC 3'
GAPDH	NM_002046	5' CTGGGCTACACTGAGCACCAG 3' / 5' CCAGCGTCAAAGGTGGAG 3'



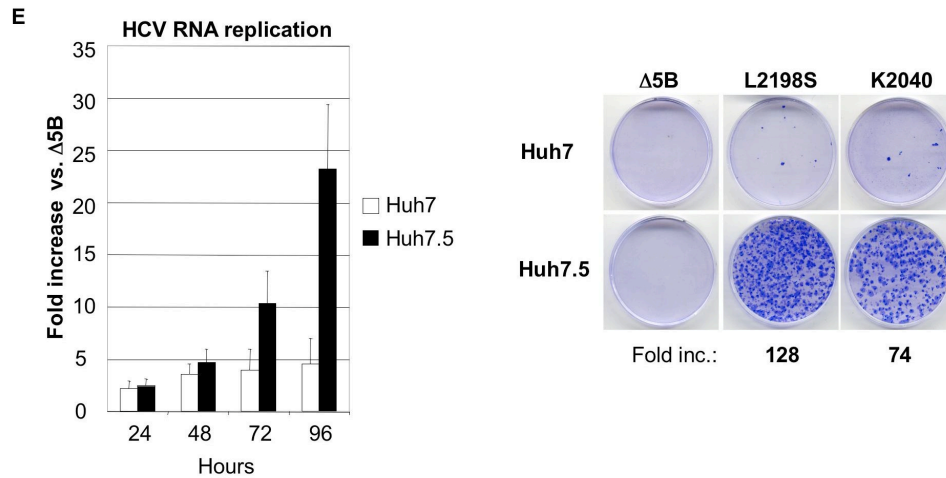


Fig 4-1. Activation of the host antiviral response by HCV RNA transfection. (A) Huh7 cells were mock transfected or transfected *in vitro* transcribed RNAs encoding either a replication-deficient HCV subgenomic replicon ( $\Delta 5B$ ) or replicons containing distinct adaptive mutations (L2198S, HP or K2040) and cellular RNA was collected at 3, 8, 12 and 24 hr post transfection. 5  $\mu$ g of total cellular RNA was subjected to Northern blot analysis using probes specific for HCV, ISG6-16, ISG56, ISG15 or GAPDH. (B) Triplicate cultures of Huh7 cells were cotransfected with inducible IFN- $\beta$  firefly luciferase and constitutive pCMV-*Renilla* plasmids followed by either infection with SenV (24 hr) or transfection with *in vitro* transcribed HCV RNAs (8 hr). Cells were then harvested and extracts were subjected to dual luciferase assay. Bars show the average firefly luciferase value and standard deviation normalized for *Renilla* expression for each sample. A schematic diagram of the HCV subgenomic RNA is depicted on the upper left, with positions of the two internal single-stranded HCV RNAs (ss1 and ss2) underlined. Integrity of all RNAs was confirmed by visualization on an agarose gel prior to transfection (lower left). (C) Huh7 cells were either mock transfected or transfected with *in vitro* transcribed luciferase RNA appended with



polyA or under control of the HCV or EMCV IRES and cellular RNA was collected at the indicated time points. Northern blot analysis was performed as in (A) above. (D) Real time PCR analysis of relative IFN- $\beta$  transcript levels was performed in triplicate on reverse-transcribed RNA from Huh7 cells 8 hr post transfection with *in vitro* transcribed HCV subgenomic replicon (L2198S), luciferase polyA or HCV IRES-luciferase RNAs. Bars show average GAPDH normalized IFN- $\beta$  transcript level and standard deviation. (E) Left panel: Huh7 and Huh7.5 cells were transfected with  $\Delta$ 5B-luc or HP-luc replicon RNAs and the initial HCV replication assay was performed as described in Materials and Methods. Bars show the average fold increase in HCV RNA replication and standard deviation for triplicate samples at each time point post HCV RNA transfection. Right panel set: Huh7 or Huh7.5 cells were transfected in triplicate with the indicated HCV subgenomic replicon RNAs and subjected to G418 selection for 3 weeks. Colonies stably transduced with HCV subgenomic replicons were then fixed, stained and counted. Representative plates for each transfection are shown. Fold increase was determined by dividing the average number of stably transduced Huh7.5 cell colonies by the number of stably transduced Huh7 cell colonies after normalizing for transfection efficiency by luciferase assay (see Materials and Methods).

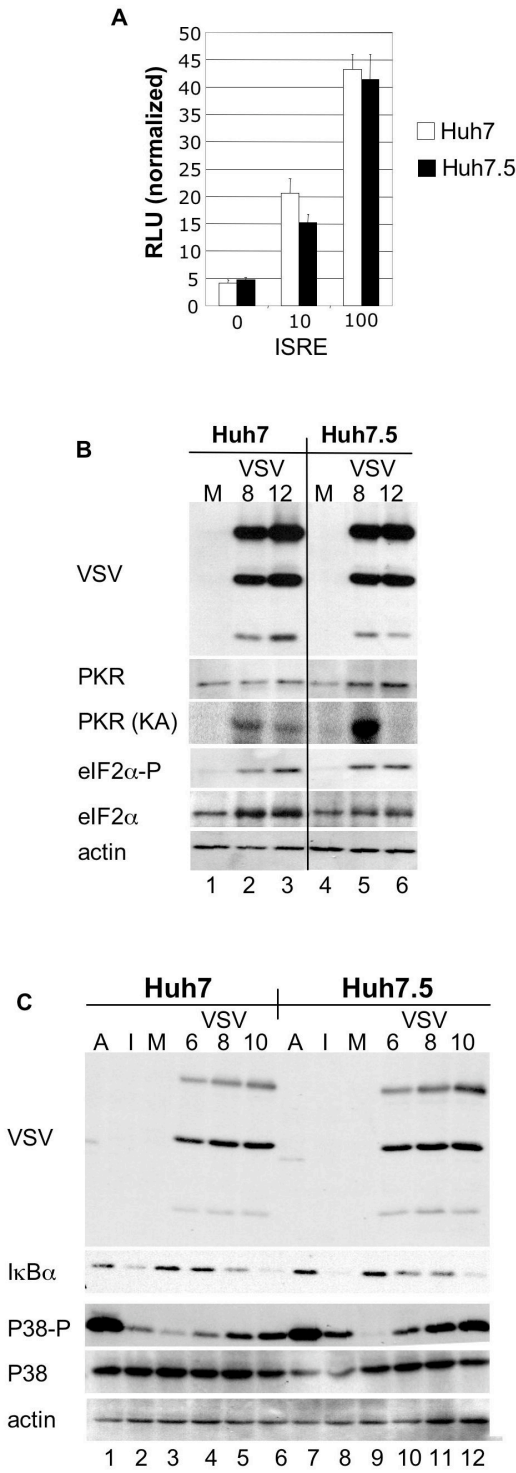


Fig 4-2. Analysis of ISRE, PKR, IKK and P38 MAPK activation in Huh7 and Huh7.5 cells.

(A) Triplicate cultures of Huh7 cells were cotransfected with inducible ISRE firefly luciferase and constitutive pCMV-*Renilla* plasmids. 24 hr post transfection, medium was removed and replaced with fresh medium containing 0, 10 or 100 IU/mL IFN- $\alpha$ 2a. Cells were harvested 8 hr post IFN treatment and extracts were subjected to dual luciferase assay. Bars show the average firefly luciferase value and standard deviation normalized for *Renilla* expression for each sample. (B) Huh7 and Huh7.5 cells were either mock infected (M) for 12 hr or infected with VSV (MOI = 10) for 8 or 12 hr. 20  $\mu$ g of total cellular protein was resolved by SDS-PAGE and subjected to immunoblot analysis with monoclonal anti-PKR or anti-eIF2 $\alpha$ , polyclonal rabbit antisera specific for VSV or phospho-Ser51-eIF2 $\alpha$  and goat polyclonal anti- $\beta$ -actin. For PKR kinase assay (KA), PKR immunoprecipitated from each sample was incubated with  $\gamma$ -<sup>32</sup>P-ATP, resolved by SDS-PAGE and visualized by autoradiography. (C) Huh7 and Huh7.5 cells were treated with anisomycin (A; 10  $\mu$ g/mL, 15 min.), recombinant IL-1 (I; 10 ng/mL, 30 min.), or mock infected (M; 12 hr) or infected with VSV (MOI = 10) for 6, 8 or 10 hr. 20  $\mu$ g total cellular protein was resolved by SDS-PAGE and subjected to immunoblot analysis with rabbit polyclonal antisera specific for VSV, IkB $\alpha$ , phospho-Thr180/Tyr182-P38, total P38 and goat polyclonal anti- $\beta$ -actin.

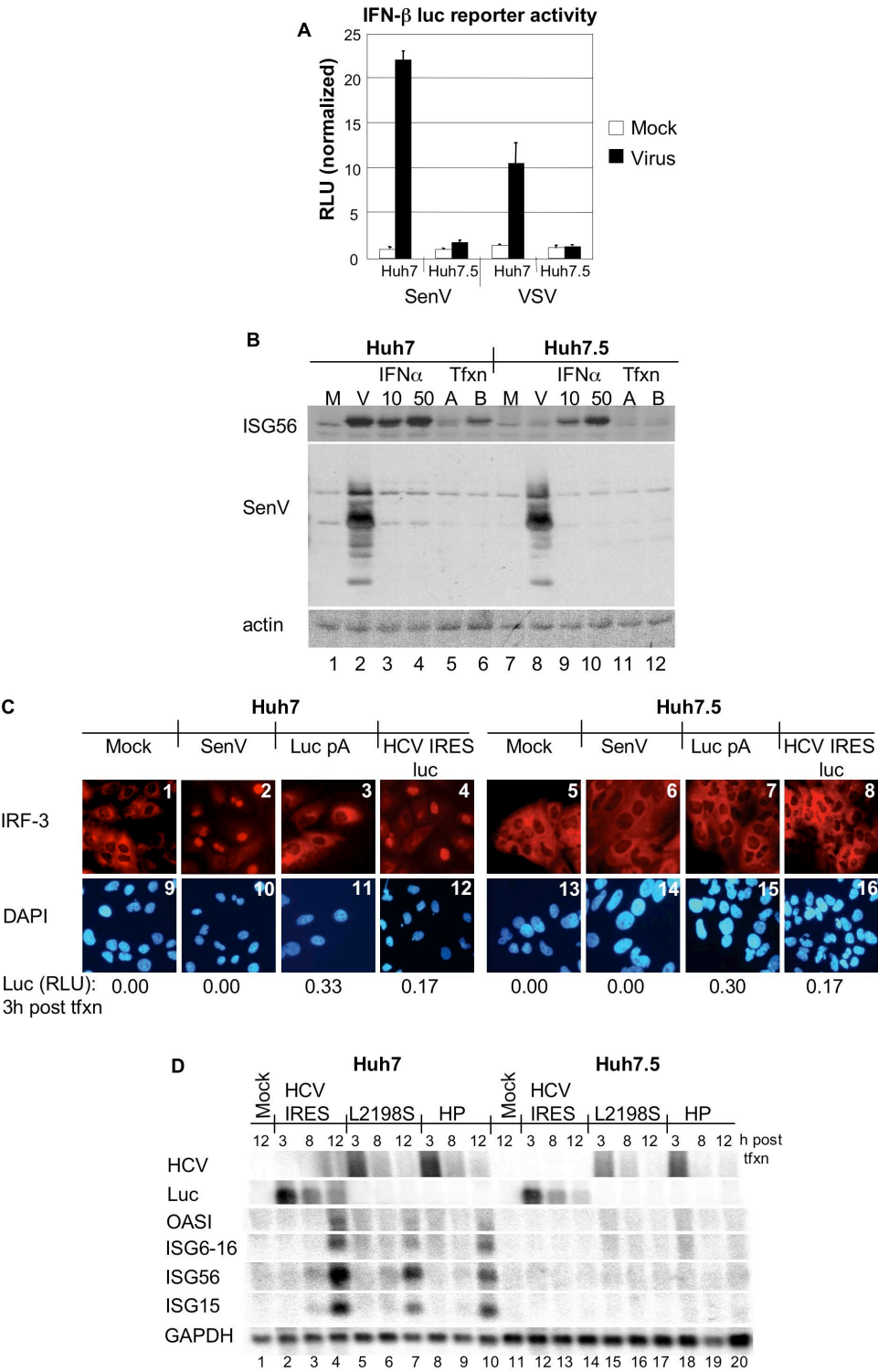


Fig 4-3. Huh7.5 cells have a defective IRF-3 response to virus and HCV dsRNA. (A)

Triplicate cultures of Huh7 and Huh7.5 cells were cotransfected with inducible IFN- $\beta$  firefly luciferase and constitutive pCMV-*Renilla* plasmids and allowed to recover for 24 hr, followed by mock infection or infection with either SenV (24 hr) or VSV (10 hr). Cells were then harvested and extracts were subjected to dual luciferase assay. Bars show the average firefly luciferase value and standard deviation normalized for *Renilla* expression for each sample.

(B) Huh7 and Huh7.5 cells were either mock infected (M; 24 hr), infected with SenV (V; 24 hr), treated with 10 or 50 IU/mL IFN- $\alpha$ 2a (10,50; 12 hr) or transfected with *in vitro* transcribed luciferase polyA (A; 8 hr) or HCV IRES-luciferase RNAs (B; 8 hr). 20  $\mu$ g of total cellular protein was resolved by SDS-PAGE and subjected to immunoblot analysis with polyclonal rabbit anti-ISG56 or SenV and goat polyclonal anti- $\beta$ -actin. Relative RNA transfection efficiency was monitored by luciferase assay (see Fig 4-3C). (C) Huh7 and Huh7.5 cells were infected with SenV (24 hr) or transfected with *in vitro* transcribed luciferase polyA or HCV IRES-luciferase RNAs (8 hr). Cells were then fixed, permeabilized and probed with rabbit polyclonal anti-IRF-3 followed by a FITC-conjugated donkey anti-rabbit secondary antibody (upper panel set). Nuclei were visualized by staining with DAPI (lower panel set). Magnification was 40X. In parallel, triplicate cultures of Huh7 and Huh7.5 cells were mock transfected or transfected with each luciferase RNA. 3 hr post transfection, cells were harvested and the lysates were subjected to luciferase assay. Average luciferase values are shown below for the parallel cultures corresponding to each panel set. (D) Huh7 and Huh7.5 cells were transfected with *in vitro* transcribed HCV IRES-luciferase

RNA or the L2198S or HP replicon RNAs and total cellular RNA was collected at 3, 8 or 12 hr post transfection. 5 µg of total cellular RNA was then subjected to Northern blot analysis using probes specific for HCV, firefly luciferase (Luc), OASI, ISG6-16, ISG56, ISG15 and GAPDH.

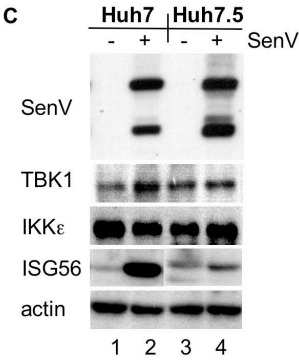
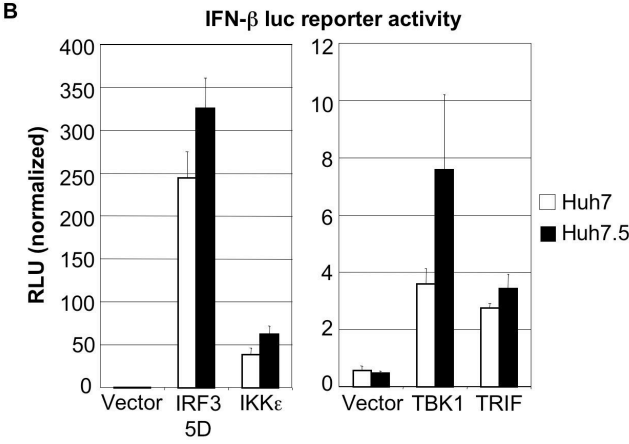
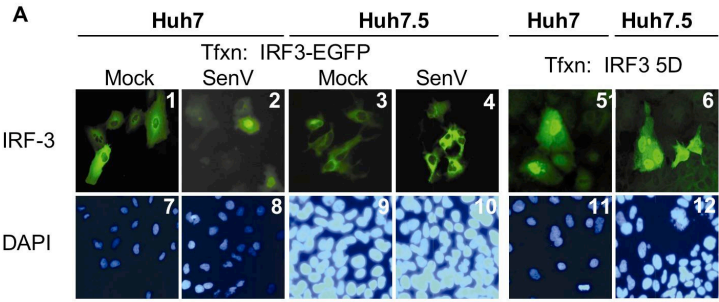


Fig 4-4. Localization of the IRF-3 activation defect in Huh7.5 cells. (A) Huh7 and Huh7.5 cells were transfected with plasmids encoding either a C-terminal EGFP-tagged IRF-3 (IRF-3-EGFP) or a constitutively active phosphomimetic IRF-3 mutant (IRF-3 5D) and allowed to recover for 24 hr. IRF-3-EGFP transfected cells were then infected with SenV (100 HAU/mL; 24 hr), fixed and permeablized. Subcellular localization of IRF-3-EGFP was assessed by direct imaging in the FITC channel (panels 1-4) and transfected IRF-3 5D was visualized by probing rabbit polyclonal anti-IRF-3 followed a FITC-conjugated donkey anti-rabbit secondary antibody (panels 5-6). Nuclei were visualized by staining with DAPI (lower panel set). Magnification was 40X. (B) Triplicate cultures of Huh7 and Huh7.5 cells were cotransfected with inducible IFN- $\beta$  firefly luciferase and constitutive pCMV-*Renilla* plasmids and plasmids directing the expression of IRF-3 5D, IKK $\epsilon$ , TBK1 or TRIF. Cells were harvested 24 hr post transfection and extracts were subjected to dual luciferase assay. Bars show the average firefly luciferase value and standard deviation normalized for *Renilla* expression for each sample. (C) Huh7 and Huh7.5 cells were mock infected (-) or infected (+) with SenV (100 HAU/mL) and cells were harvested 24 hr post infection. 20  $\mu$ g of total cellular protein was resolved by SDS-PAGE and subjected to immunoblot analysis with polyclonal rabbit antisera specific for ISG56 or SenV, monoclonal anti-TBK1 or anti-IKK $\epsilon$  and goat polyclonal antiserum specific for  $\beta$ -actin.



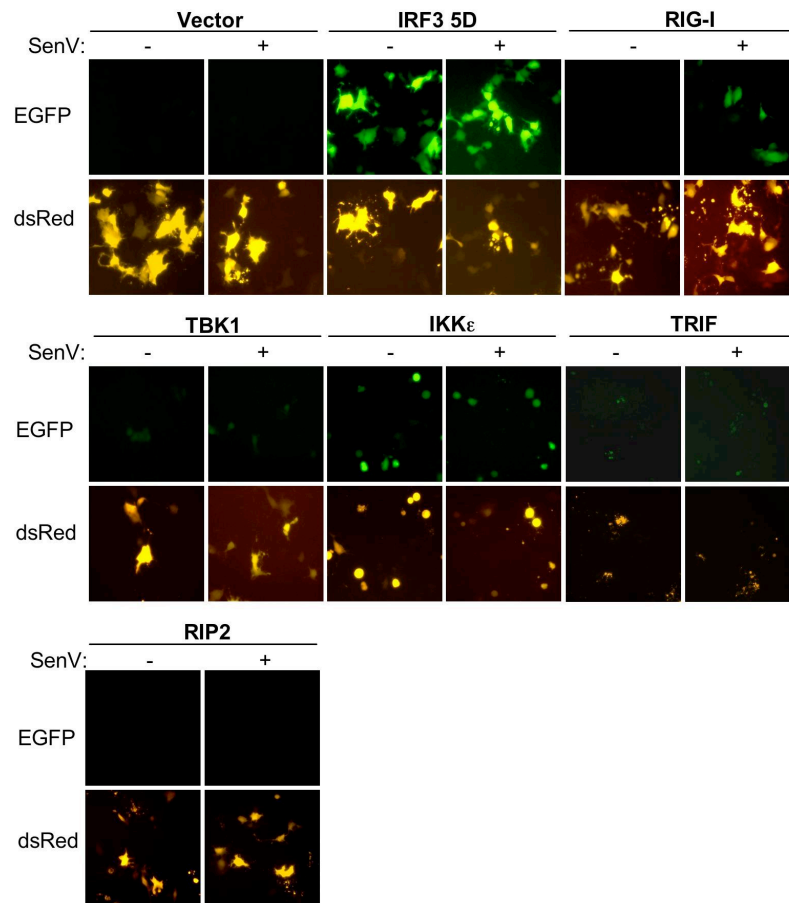
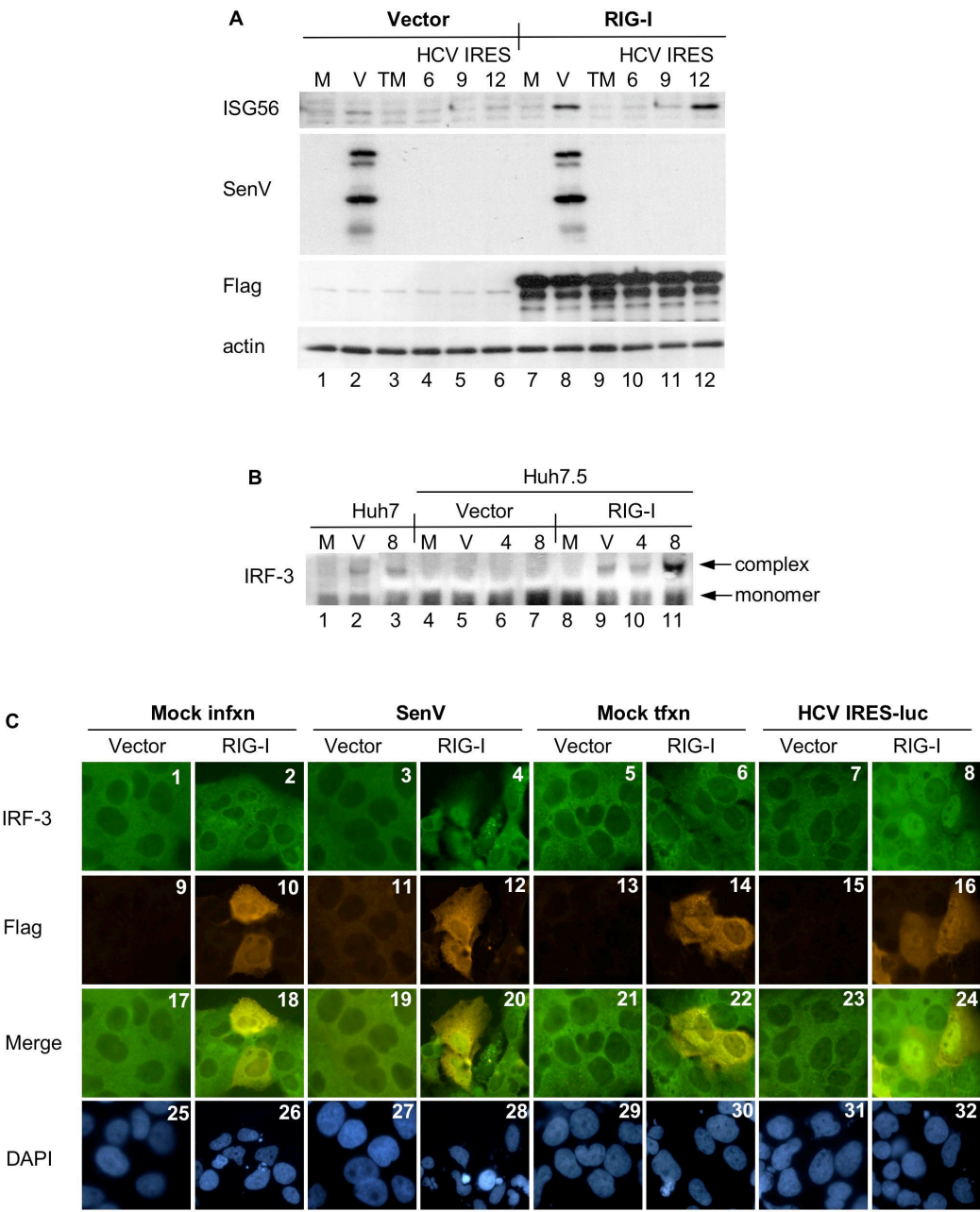


Fig 4-5. RIG-I specifically complements defective virus-induced IRF-3 reporter activation in Huh7.5 cells. Huh7.5 cells were cotransfected with inducible pF3-EGFP and constitutive pDsRed plasmids and vector control or plasmids directing the expression of IRF-3 5D, RIG-I, TBK1, IKK $\epsilon$ , TRIF or RIP2. 6 hr post transfection, cells were mock infected (-) or infected (+) with SenV (100 HAU/mL). Cells were observed by direct fluorescence imaging in FITC (EGFP) and TRITC (dsRed) channels 24 hr post infection.



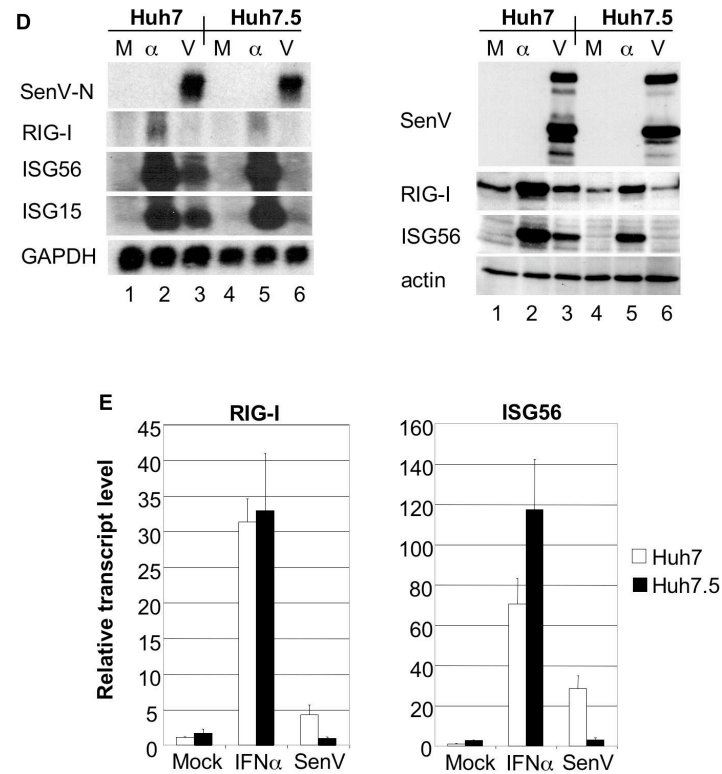


Fig 4-6. RIG-I restores the IRF-3 response to virus and HCV dsRNA in Huh7.5 cells. (A) Huh7.5 cells were transfected with vector control or a plasmid encoding full-length RIG-I and allowed to recover for 24 hr. Cells were then either mock infected (M) or infected with SenV (V) (lanes 1-2 and 7-8) and total cellular protein was collected after 24 hr. In addition, cells were mock transfected (TM) or transfected with *in vitro* transcribed HCV IRES-luciferase RNA (lanes 3-6 and 9-12) and total cellular protein was collected at 6, 9 or 12 hr post RNA transfection. Mock transfected samples were collected at 12 hr. 20  $\mu$ g of total cellular protein was resolved by SDS-PAGE and subjected to immunoblot analysis with polyclonal rabbit antisera specific for ISG56 or SenV, monoclonal anti-Flag (RIG-I) and goat polyclonal antiserum specific for  $\beta$ -actin. (B) Lanes 1-3: Huh7 cells were mock infected (M), infected with SenV (V, 100 HAU/mL; 24 hr) or transfected with HCV IRES-luc RNA

for 8 hr (8). Lanes 4-11: Huh7.5 cells were transfected with vector control or a plasmid encoding full-length RIG-I. 24 hr post transfection, cells were either mock infected (M), infected with SenV (V, 100 HAU/mL; 24 hr) or transfected with HCV IRES-luc RNA for 4 or 8 hr (4, 8). 20  $\mu$ g total cellular protein was resolved on a nondenaturing gel subjected to immunoblot analysis with rabbit polyclonal anti-IRF-3. (C) Huh7.5 cells were transfected with vector control or a plasmid encoding full-length RIG-I. 24 hr post transfection, cells were mock infected or infected with with SenV (100 HAU/mL; 24 hr) or mock transfected or transfected with *in vitro* transcribed HCV IRES-luciferase RNA (8 hr). Cells were then fixed, permeabilized and probed with rabbit polyclonal anti-IRF-3 and monoclonal anti-Flag followed by FITC-conjugated donkey anti-rabbit and Rhodamine-conjugated donkey anti-mouse secondary antibodies. Nuclei were visualized by staining with DAPI (lower panel set). Magnification was 40X. (D) Huh7 and Huh7.5 cells were mock treated (M) or treated with 100 IU/mL IFN- $\alpha$ 2a ( $\alpha$ ) for 12 hr or infected with 100 HAU/mL SenV (V) for 24 hr and total cellular RNA and protein were collected. 5  $\mu$ g of total cellular RNA was subjected to Northern blot analysis using probes specific for SenV, RIG-I, ISG56, ISG15 or GAPDH (left panel set). 20  $\mu$ g of total cellular protein was resolved by SDS-PAGE and subjected to immunoblot analysis with polyclonal rabbit anti-RIG-I, ISG56 or SenV and goat polyclonal anti- $\beta$ -actin (right panel set). (E) Real time PCR analysis of relative RIG-I (left graph) and ISG56 (right graph) transcript levels was performed in triplicate on reverse transcribed RNA from samples in Fig 4D. Bars show average GAPDH normalized IFN- $\beta$  transcript level and standard deviation.

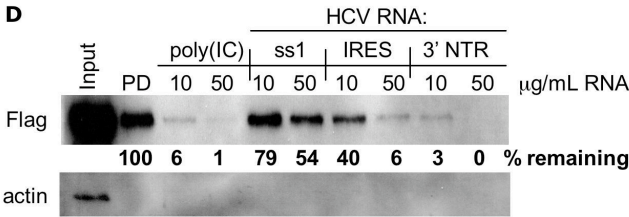
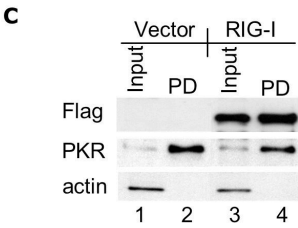
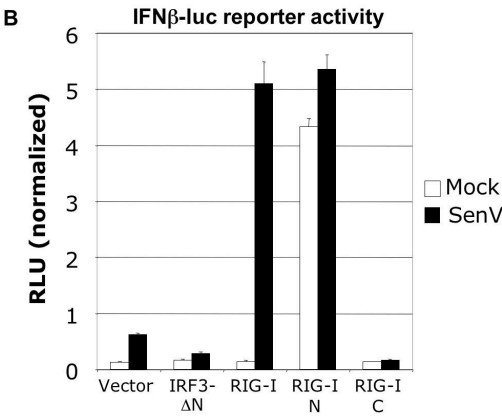
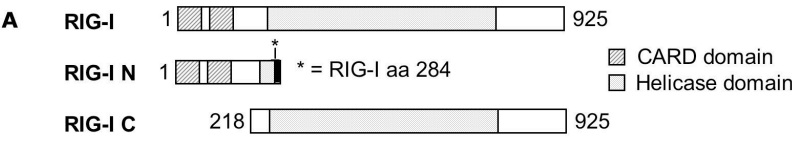
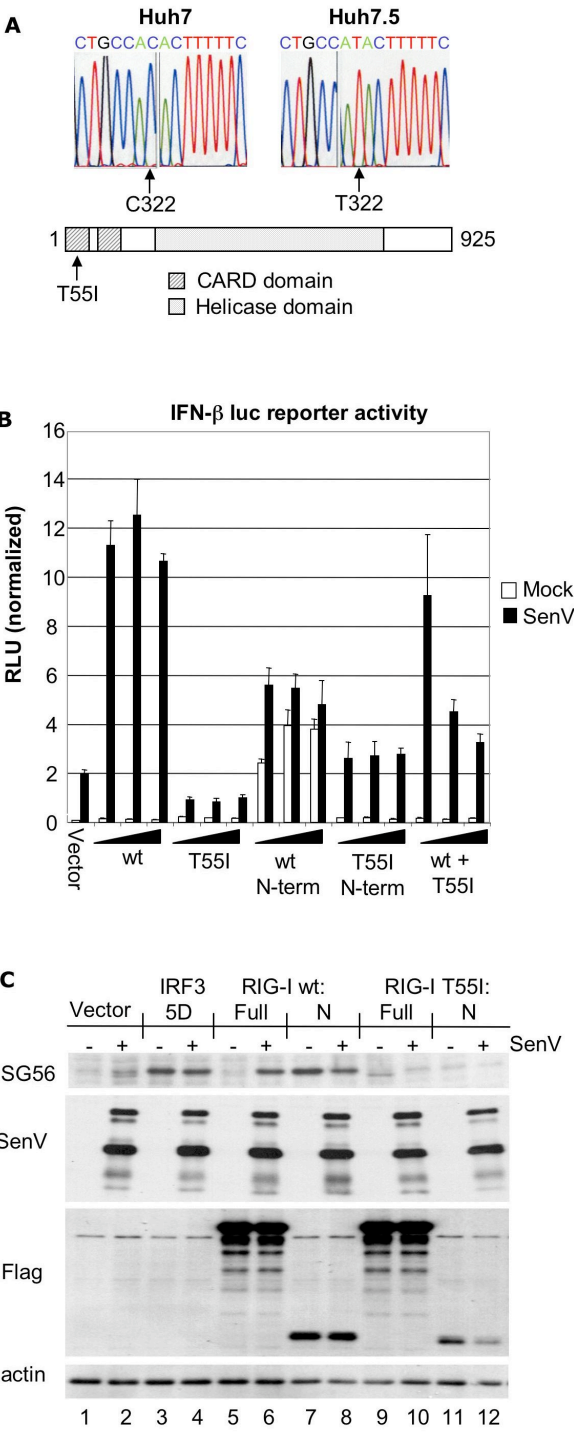


Fig 4-7. RIG-I controls the host response to HCV dsRNA. (A) Schematic representation of the domain structure of RIG-I, RIG-I N (containing the tandem CARD domains) and RIG-I C (containing the helicase domain) (B) Triplicate cultures of Huh7 cells were cotransfected with inducible IFN- $\beta$  firefly luciferase and constitutive pCMV-*Renilla* plasmids and plasmids directing the expression of IRF-3  $\Delta$ N (dominant negative), RIG-I full length, RIG-I N or RIG-I C. 24 hr post transfection, cells were either mock infected or infected with SenV (100 HAU/mL). Cells were harvested 24 hr post infection and extracts were subjected to dual luciferase assay. Bars show the average firefly luciferase value and standard deviation normalized for *Renilla* expression for each sample. (C) Huh7 cells were transfected with vector control or a plasmid directing the expression of full length RIG-I and total cellular protein was harvested 24 hr post transfection. 20  $\mu$ g total cellular protein was mixed with poly(I)(C) coated agarose beads. Input and bound (PD) proteins were subjected to immunoblot analysis with monoclonal anti-Flag and anti-PKR antibodies and a goat polyclonal anti- $\beta$ -actin antibody. (D) 3  $\mu$ g of the lysate from RIG-I transfected cells was mixed with poly(I)(C) coated agarose beads and the binding reactions were supplemented with 10 or 50  $\mu$ g/mL poly(I)(C) or HCV ss1, IRES or 3' NTR *in vitro* transcribed RNAs. Input and bound proteins were subjected to immunoblot analysis with monoclonal anti-Flag and goat polyclonal anti- $\beta$ -actin antibodies. Efficiency of competition was determined by densitometry and is expressed as percentage of initial pulldown signal remaining.



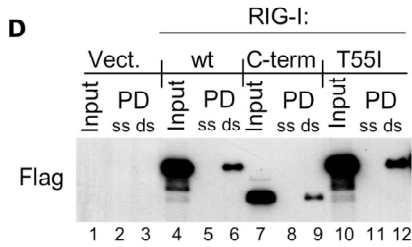


Fig 4-8. Identification and characterization of mutant RIG-I from Huh7.5 cells. (A) RT-PCR was performed on total RNA from Huh7 and Huh7.5 cells using RIG-I specific primers and PCR products were directly sequenced. The electropherograms demonstrating the C→T point mutation at position 322 in the RIG-I mRNA from Huh7.5 cells sequence are shown. A schematic representation of RIG-I with the position of the resultant single aa mutation (T55I) is shown below. (B) Triplicate cultures of Huh7 cells were cotransfected with inducible IFN- $\beta$  firefly luciferase and constitutive pCMV-*Renilla* plasmids and increasing amounts of plasmids encoding full length or N-terminal wild-type RIG-I (wt and wt N-term), full length or N-terminal RIG-I T55I (T55I and T55I N-term) or a constant amount of wild type RIG-I with increasing amounts of RIG-I T55I (wt + T55I). 24 hr post transfection, cells were either mock infected or infected with SenV (100 HAU/mL). Cells were harvested 24 hr post infection and extracts were subjected to dual luciferase assay. Bars show the average firefly luciferase value and standard deviation normalized for *Renilla* expression for each sample. (C) Huh7.5 cells were transfected with vector control or plasmids encoding IRF-3 5D, RIG-I, RIG-I N, RIG-I T55I or RIG-I T55I N and allowed to recover for 24 hr. Cells were then mock infected (-) or infected (+) with SenV (100 HAU/mL) and protein was collected 24 hr after infection. 20  $\mu$ g of total cellular protein was resolved by SDS-PAGE



and subjected to immunoblot analysis with polyclonal rabbit anti-ISG56 or SenV, monoclonal anti-Flag (RIG-I) and goat polyclonal anti- $\beta$ -actin. (D) Huh7 cells were transfected with vector control or a plasmid directing the expression of full length RIG-I (wt), RIG-I C (C-term) or RIG-I T55I (T55I) and total cellular protein was harvested 24 hr post transfection. 3  $\mu$ g total cellular protein was mixed with poly(C) (ss) or poly(I)(C) (ds) coated agarose beads. Input and bound (PD) proteins were subjected to immunoblot analysis with a monoclonal anti-Flag antibody.

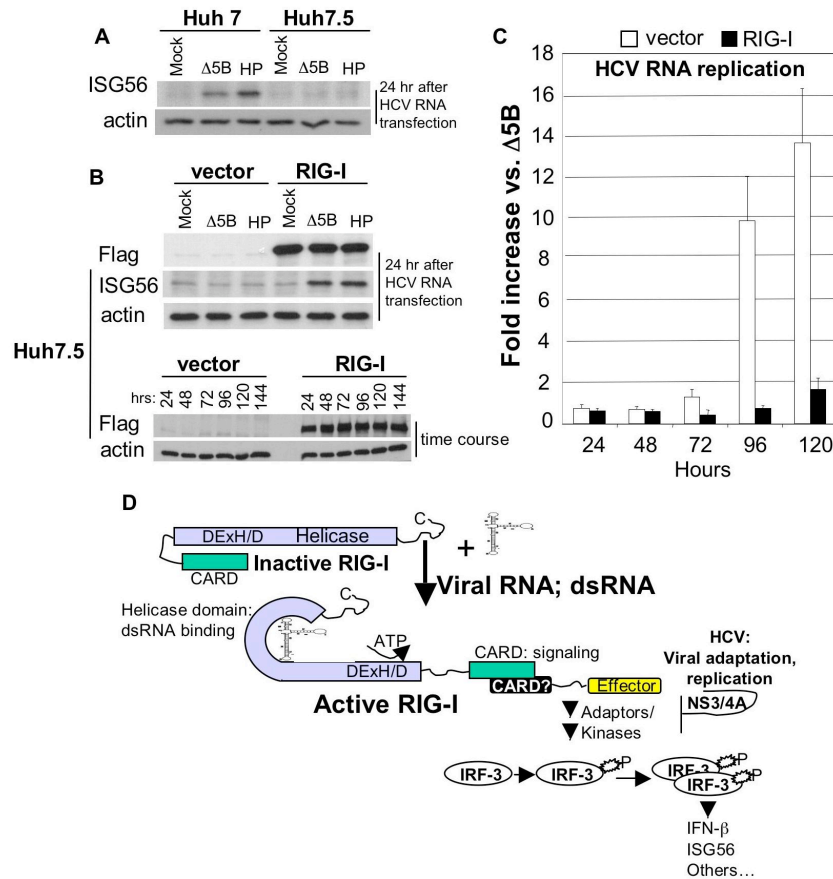


Fig 4-9. RIG-I defines host cell permissiveness to HCV RNA replication. (A) Huh7 and Huh7.5 cells were mock transfected or transfected with  $\Delta$ 5B-luc or HP-luc replicon RNAs and cells were harvested 24 hr post transfection. 20  $\mu$ g total cellular protein was resolved by SDS-PAGE and subjected to immunoblot analysis with rabbit polyclonal anti-ISG56 and goat polyclonal anti- $\beta$ -actin. (B) Top panel: Huh7.5 cells were transfected with control vector or a plasmid directing the expression of full-length RIG-I and allowed to recover for 24 hr. Cells were then transfected with  $\Delta$ 5B-luc or HP-luc replicon RNAs and cells were harvested 24 hr post RNA transfection. 20  $\mu$ g total cellular protein was resolved by SDS-

PAGE and subjected to immunoblot analysis with monoclonal anti-Flag, rabbit polyclonal anti-ISG56 and goat polyclonal anti- $\beta$ -actin. Bottom panel: Huh7.5 cells were transfected with control vector or a plasmid directing the expression of full-length RIG-I and total cellular protein was harvested at the indicated times post transfection. 20  $\mu$ g total cellular protein was resolved by SDS-PAGE and subjected to immunoblot analysis with monoclonal anti-Flag and goat polyclonal anti- $\beta$ -actin. (C) Huh7.5 cells were transfected with control vector or a plasmid directing the expression of full-length RIG-I and allowed to recover for 24 hr. Cells were then transfected with  $\Delta$ 5B-luc or HP-luc replicon RNAs and the initial HCV replication assay was performed as described in Materials and Methods. Bars show the average fold increase in HCV RNA replication and standard deviation for triplicate samples at each time point post HCV RNA transfection. (D) Model for RIG-I-mediated activation of the host antiviral response to HCV RNA.

## CHAPTER 5: GENERAL CONCLUSIONS AND FUTURE DIRECTIONS

### Molecular mechanisms of HCV resistance to IFN

The HP and K2040 HCV subgenomic RNA replicons described in this work represent the only model system currently available for the study of acquisition of IFN-resistance by HCV. With regard to the HP replicon, it has been very difficult to evaluate the relative contributions of mutations in individual HCV proteins to the IFN-resistant phenotype. However, recent improvements in experimental techniques have now made these studies possible. Identification of the HP mutations that contribute to IFN resistance will facilitate the evaluation of candidate cellular pathways targeted by HCV to allow for persistence in the face of IFN treatment. One of the HP mutations (S2236P) lies about 15 aa proximal to the recently mapped p85 $\alpha$  PI3K regulatory subunit interaction domain, which has been shown to be important for NS5A-mediated activation of PI3K, leading to increased levels of Akt activity (152). This may help to explain why levels of phosphorylated Akt are higher in Huh7 cells harboring the HP replicon than those harboring the K2040 replicon (see Fig 5-1). We have also observed that the IFN-resistant phenotype arises reproducibly upon long-term culture of cells harboring the L2198S replicon. By correlating IFN resistance to changes in aa sequence in parallel L2198S cultures over time, it may be possible to find additional mutations that are associated with the evolution to IFN resistance.

We have shown a correlation between decreased IFN-induced ISG56 levels and IFN resistance in our model system, and ISG56 is only one of hundreds of genes whose

expression is upregulated by IFN (32). It would be of interest in the future to perform RNA interference experiments to specifically knock down ISG56 expression, which would allow direct evaluation of the contribution of ISG56 to inhibition of HCV replication in the context of IFN treatment. While we focused our attention on ISG56 because of its ability to attenuate HCV IRES mediated translation, it is not the only ISG that is differentially regulated between IFN sensitive and IFN resistant replicons (Fig 5-2). In fact, there appears to be a “potentiation” of ISG expression by IFN sensitive replicons in the sense that many ISGs are induced much more rapidly, although we did not find any differences in ISGF3-mediated signaling that would explain this phenotype. An explanation for these results could lie in the differential regulation of alternative IFN signaling pathways. For example, the P38 MAPK pathway is constitutively activated in Huh7 cells harboring the IFN-sensitive K2040 replicon, and its activation in response to IFN treatment is both more rapid and intense than observed in control cells or cells harboring the IFN-resistant HP replicon (see Fig 5-1). Regulation of basal and IFN-induced P38 activation could contribute to potentiation of ISGs in a several ways. First, because binding sites for AP-1 family transcription factors are found in the promoters of many ISGs, they could potentially synergize with ISGF3 to potentiate ISG expression. Second, activation of P38 results in stimulation of chromatin remodeling by phosphorylating MSK1 and 2, which in turn phosphorylate histone H3 (150), and the resultant relaxation of chromatin structure around ISG loci might contribute to potentiation. This could help to resolve the discrepancy between our observations that transcription of ISGs from native promoters, but not luciferase reporters (which are episomal and thus not histone-associated), is potentiated.

Another possible explanation for ISG potentiation by HCV replicons is that IFN sensitive and IFN resistant replicons may differ in their ability to regulate an intracellular antiviral pathway that is stimulated by interferon. We have examined both PKR and IRF-3 for differential activation in IFN treated replicons, and found no differences that would explain resistance to IFN treatment *in vivo*. Recently, studies from several labs have demonstrated that TLR7 and TLR8 recognize U-rich regions from single stranded RNA viruses (33, 109), and the HCV 3' NTR contains a U-rich region that could be a ligand for these receptors. TLR7 is an ISG (122), and both TLR7 and TLR8 activate NF $\kappa$ B, MAPK (including P38) and IFN- $\alpha$  signaling (33, 65, 109). TLR7 is expressed at high levels in Huh7 cells, and differential regulation of its activity by HCV replicons might contribute to the IFN resistance. This could also help explain the differences observed in P38 activation mentioned above.

Another interesting observation regards the ability of HCV replicons to regulate IRF-5. Unfortunately, at this time no antibody is available to enable examination of endogenous IRF-5, so IRF-5 must be artificially overexpressed. When EGFP-tagged IRF-5 is ectopically expressed in parental Huh7 cells, it is almost exclusively localized to the cytoplasm, but in cells harboring the K2040 replicon IRF-5 is found in the nucleus of most cells (Fig 5-3A). Therefore, we conclude that HCV has the capacity to activate IRF-5 by an unknown mechanism. However, in cells harboring the HP replicon, nuclear accumulation of IRF-5 does not occur, despite similar levels of HCV RNA and protein, suggesting that the HP

replicon encodes a mechanism to block the activation of IRF-5. Infection with VSV results in the nuclear translocation of IRF-5 in each cell line, but cells harboring the HP replicon are refractory in this response. While IRF-5 is undetectable by RT-PCR in untreated Huh7 cells, its mRNA levels are increased by infection with Sendai virus (Fig 5-3B), demonstrating that these cells have the capacity to express IRF-5. SenV infection also induces IRF-5 expression in Huh7.5 cells, which do not activate IRF-3 or IFN- $\beta$  in response to SenV (156). Since IRF-5 appears to be expressed only at low levels in unstimulated cells, the ability to regulate IRF-5 may only become important in the context of IFN treatment or virus infection, and its activities may contribute to potentiation of the IFN response in cells harboring IFN-sensitive replicons. As mentioned earlier, the upstream pathways involved in IRF-5 activation are not known, and the viral stimulus has yet to be identified. Since Sendai virus infection results in the activation of IRF-3 but not IRF-5 (11), it appears unlikely that viral dsRNA will be the IRF-5 trigger. TLRs 7 and 8 are attractive candidates for virus-induced IRF-5 activation since they appear to have the capacity to directly induce IFN- $\alpha$  expression (65, 109).

#### Host permissiveness to HCV RNA replication

The RIG-I pathway is critical for regulating the host response to HCV RNA replication in our model systems, as demonstrated by the increased permissiveness of cells Huh7.5 cells, which are defective in RIG-I function. Due to their profound defects in the host antiviral response to dsRNA, Huh7.5 cells represent a potential substrate for the development of a native HCV replication system and can be used to evaluate the relative importance of RIG-I in initiating a host response to other viruses. Efforts are currently

underway to stably complement Huh7.5 cells with wild-type RIG-I and to create Huh7 cell line in which RIG-I expression is blocked by RNA interference.

While amplifying RIG-I to obtain its cDNA sequence, we found at least 3 splice variants of RIG-I mRNA in addition to the mRNA coding for full-length RIG-I (Fig 5-4). Two of the variants encode RIG-I isoforms that contain the CARD and helicase domains, but lack the DExH/D region that is responsible for ATP binding and hydrolysis and thus may act as dominant negative proteins (184). The DExH/D family helicases are involved in mRNA splicing (136), so it is possible that RIG-I could autoregulate its activity by alternatively splicing its own mRNA. Several ISGs are also DExH/D family helicases (32) that might be responsible for regulation of RIG-I mRNA splicing. Control of RIG-I splicing could play a key role in the antiviral response by rapidly increasing the levels of full-length RIG-I mRNA during viral infection or exposure to IFN and decreasing spurious activation of IRF-3 and NF $\kappa$ B in the uninfected cell. Indeed, ectopic expression of full-length RIG-I results in a small but potentially significant increase in the basal activity of an IFN- $\beta$  reporter construct (184), which could represent a type of “hypersensitive” state normally avoided by the splicing of RIG-I mRNA. Dysregulation of NOD2, a CARD-containing sensor that responds to bacterial products is associated with Crohn’s disease (74, 127), an inflammatory bowel disease in which the immune response is dysregulated. Future research may uncover a link between increased susceptibility to viral infections or autoimmunity and polymorphisms in RIG-I.



RIG-I is not the only RNA helicase involved in sensing viral infection. In fact, a related CARD-containing DExH/D box helicase protein, MDA-5, has recently been shown to activate the antiviral response (184). In addition to the T55I mutation in RIG-I from Huh7.5 cells, we also found two mutations (H460R and H843R) in MDA-5 from Huh7.5 cells. However, in contrast to the the RIG-I T55I mutation, the MDA-5 mutations were found in both Huh7 and Huh7.5 cells. It will be interesting to determine whether MDA-5 responds to HCV dsRNA, and if a potential lack of MDA-5 function due to these mutations contributes to the relative permissiveness of Huh7 cells to HCV RNA replication.

#### TLR signaling and NS5A

Huh7 cells have been known for some time to be defective in their response to extracellular dsRNA, presumably because of an unidentified lesion in the TLR3 pathway (98). However, PH5CH8 cells, which were derived by immortalization of primary human hepatocytes with SV40 large T antigen (76), have a robust response to extracellular dsRNA, suggesting that TLR3-mediated signaling may be intact in primary liver cells. Although a role for TLR3 in host defense against HCV infection has not yet been demonstrated, defective TLR3 signaling could be an additional “hit” increasing the permissiveness of Huh7 cells to HCV replication. HCV NS5A interacts with PKR (45), and PKR has been shown in several studies to be necessary for signaling in response to both extracellular dsRNA (70, 81, 182) and LPS (73). When ectopically expressed in 293T cells stably overexpressing TLR3, NS5A conferred an almost complete block to NF $\kappa$ B promoter activation and a reduction of IFN- $\beta$  promoter activation in response to dsRNA treatment (Fig 5-5A). NS5A conferred a

partial block to NF $\kappa$ B activation in 293T/TLR4 (Fig 5-5B) cells treated with LPS, which is not surprising due to the use of several unique adapter proteins by TLR4 (126). Although PKR kinase activity is activated during TLR3-mediated signaling (73), it is unclear whether this is required for signal transduction or if PKR is acting as an adapter molecule for assembly of downstream signaling components (177). PKR is rapidly recruited to the activated signalosome after ligand binding by TLR3 (81), so its sequestration by binding to NS5A, which is associated with the ER due to its interaction with a prenylated host cell protein (183), may prevent its participation in TLR3-mediated signaling. Since PKR has been implicated in TLR signaling via the adapter proteins TIRAP and MyD88 (which is utilized by all TLRs) (71), the effects of the NS5A:PKR interaction could modulate signaling through many other TLRs, including the other “antiviral” TLRs 7 and 8. In addition, many TLRs are ISGs (122), and therefore inhibition of TLR signaling by NS5A may be an important factor in the ability of HCV to control the antiviral response and the evolution of viral resistance to IFN.

### Final thoughts

Our work has established that Huh7 cells used in the replicon system to model HCV infection are not merely inert substrates for HCV RNA replication. In fact, they are capable of mounting an innate antiviral response to HCV dsRNA despite several defects that may contribute to their relative overall permissiveness. We have shown that the HCV replicon system can be used to model both the acquisition of IFN resistance in chronic HCV infection and virus/host interactions critical for determining the outcome of exposure to HCV. These

observations will contribute to future efforts to understand HCV persistence and pathogenesis.

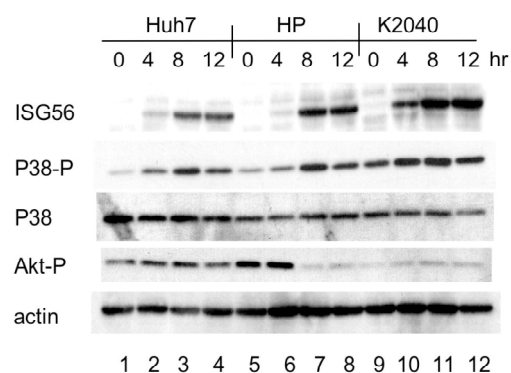


Fig 5-1. Differential regulation of P38 and Akt phosphorylation in Huh7 and replicon-bearing cell lines. Huh7, Huh7-HP and Huh7-K2040 cells cultured in medium alone or medium containing 10 U/ml IFN $\alpha$ 2a and cells were harvested at 0, 4, 8 and 12 hr post-IFN treatment as indicated above each lane. 20  $\mu$ g total cellular protein from was then resolved by SDS-PAGE and subjected to immunoblot analysis with rabbit polyclonal antisera specific for ISG56, phospho-Thr180/Tyr182-P38, total P38, phospho-Ser473-Akt and goat polyclonal anti- $\beta$ -actin.

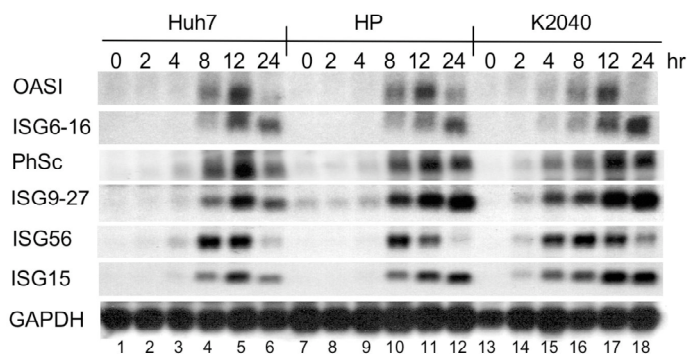


Fig 5-2. Potentiation of IFN-induced ISG expression in IFN sensitive K2040 replicon. Huh7, Huh7-HP and Huh7-K2040 cells were cultured in medium alone or medium containing 10 U/ml IFN $\alpha$ 2a and total RNA was harvested at 0, 2, 4, 8, 12 or 24 hr post-IFN treatment as indicated above each lane. 5  $\mu$ g of total RNA was then subjected to Northern blot analysis using cDNA probes specific for OASI, ISG6-16, phospholipid scramblase (PhSc), ISG9-27, ISG56, ISG15 or GAPDH.

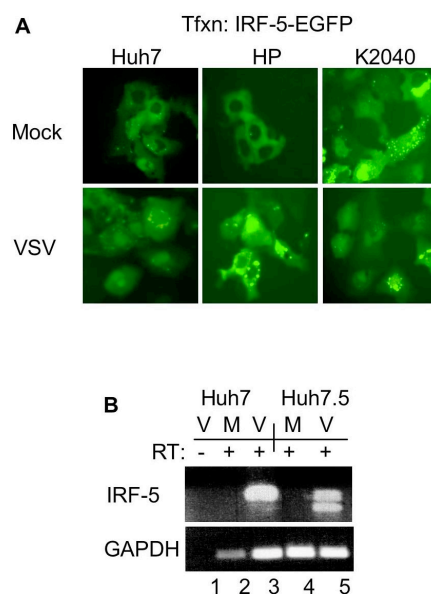


Fig 5-3. Regulation of IRF-5 localization and expression. (A) Huh7, Huh7-HP and Huh7-K2040 cells were transfected with pIRF-5-EGFP and allowed to recover for 24 hr. Cells were then infected with VSV (MOI = 10) and 6 hr post-infection cells were visualized by fluorescence microscopy. Magnification was 40X. (B) Huh7 and Huh7.5 cells were mock infected or infected with SenV (100 HAU/mL; 24 hr) and total RNA was extracted. RT-PCR was performed with primers specific for IRF-5 (40 cycles) or GAPDH (30 cycles) and PCR products were visualized by agarose gel electrophoresis. The identity of the IRF-5 PCR product was confirmed by automated sequencing of TA clones.

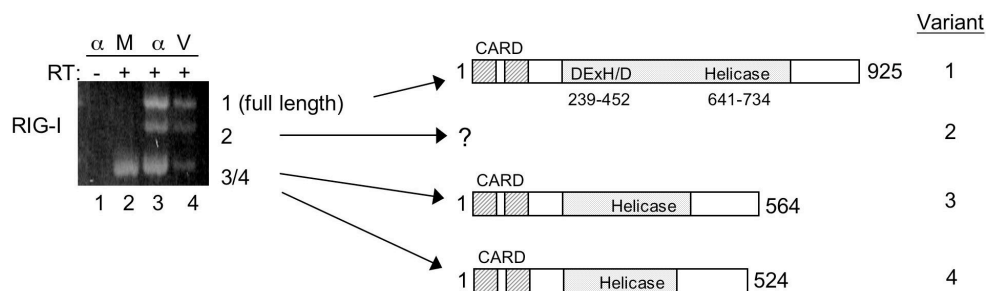


Fig 5-4. RIG-I is alternatively spliced. Huh7 cells were mock treated, treated with IFN- $\alpha$  (100 IU/mL; 8 hr) or infected with SenV (100 HAU/mL; 24 hr) and total RNA was extracted. RT-PCR was performed on total RNA and PCR products were separated by agarose gel electrophoresis, TA cloned and sequenced. Schematic representations of full length RIG-I and two of its splice variants are shown on the right.

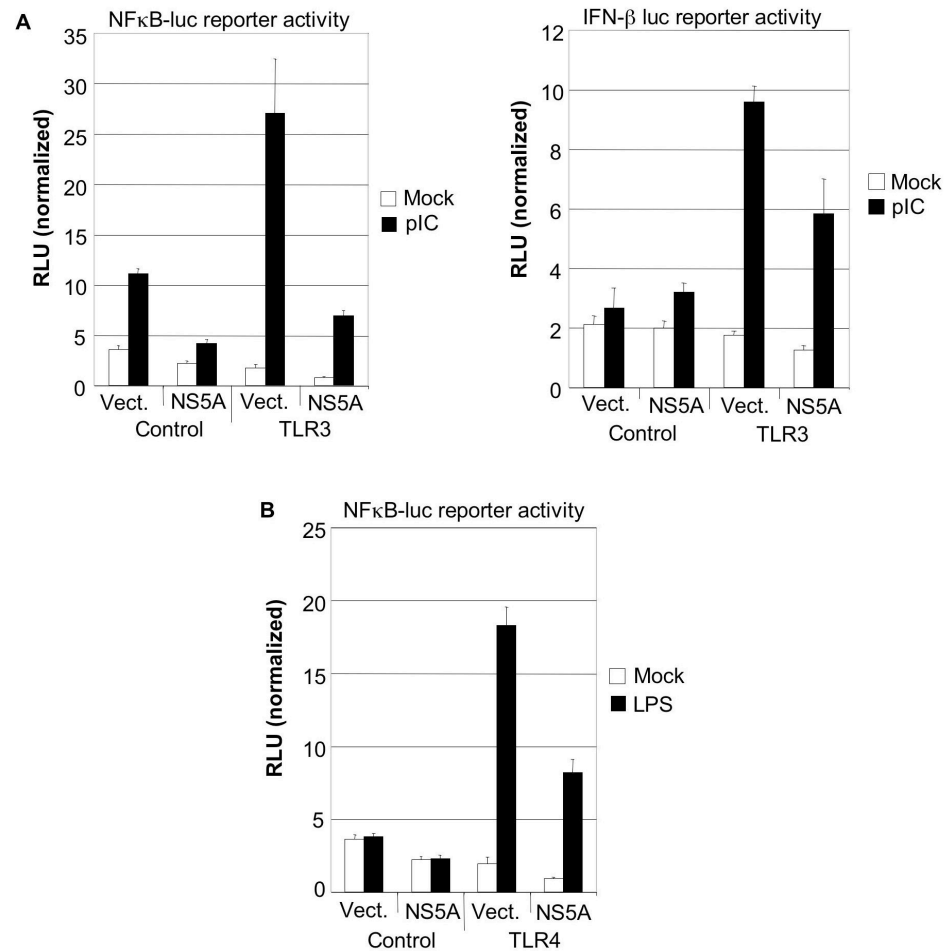


Fig 5-5. HCV NS5A regulates TLR3 and TLR4 signaling. (A) Triplicate cultures of 293T/Neo (control) or 293T/TLR3 (TLR3) cells were cotransfected with inducible NFκB- or IFN-β firefly luciferase and constitutive pCMV-*Renilla* plasmids plus either vector alone or pFlag NS5A 1b-1 followed by mock treatment or treatment with poly(I)(C) (50 μg/mL; 8 hr). Cells were then harvested and extracts were subjected to dual luciferase assay. Bars show the average firefly luciferase value and standard deviation normalized for *Renilla* expression for each sample. (B) Triplicate cultures of 293T/Neo (control) or 293T/TLR3 (TLR4) cells were cotransfected with inducible NFκB- or IFN-β firefly luciferase and constitutive pCMV-



*Renilla* plasmids plus either vector alone or pFlag NS5A 1b-1 followed by mock treatment or treatment with LPS (100 ng/mL; 8 hr). Cells were then harvested and extracts were subjected to dual luciferase assay. Bars show the average firefly luciferase value and standard deviation normalized for *Renilla* expression for each sample.

## BIBLIOGRAPHY

1. **Adolf, G. R.** 1990. Monoclonal antibodies and enzyme immunoassays specific for human interferon (IFN) omega 1: evidence that IFN-omega 1 is a component of human leukocyte IFN. *Virology* **175**:410-7.
2. **Akira, S.** 2003. Mammalian Toll-like receptors. *Curr Opin Immunol* **15**:238.
3. **Alexopoulou, L., A. C. Holt, R. Medzhitov, and R. A. Flavell.** 2001. Recognition of double-stranded RNA and activation of NF-kappaB by Toll-like receptor 3. *Nature* **413**:732-8.
4. **Ali, N., C. Wang, and A. Siddiqui.** 1995. Translation of hepatitis C virus genome. *Princess Takamatsu Symposia* **25P99-110**:99-110.
5. **Anderson, J. C., J. Simonetti, D. G. Fisher, J. Williams, Y. Yamamura, N. Rodriguez, D. G. Sullivan, D. R. Gretch, B. McMahon, and K. J. Williams.** 2003. Comparison of different HCV viral load and genotyping assays. *J Clin Virol* **28**:27-37.
6. **Appay, V., and S. L. Rowland-Jones.** 2001. RANTES: a versatile and controversial chemokine. *Trends Immunol* **22**:83-7.
7. **Balachandran, S., P. C. Roberts, L. E. Brown, H. Truong, A. K. Pattnaik, D. R. Archer, and G. N. Barber.** 2000. Essential role for the dsRNA-dependent protein kinase PKR in innate immunity to viral infection. *Immunity* **13**:129-41.
8. **Barnes, B., B. Lubyova, and P. M. Pitha.** 2002. On the role of IRF in host defense. *J. Interferon Cytokine Res.* **22**:59-71.

9. **Barnes, B. J., A. E. Field, and P. M. Pitha-Rowe.** 2003. Virus-induced Heterodimer Formation between IRF-5 and IRF-7 Modulates Assembly of the IFNA Enhanceosome in Vivo and Transcriptional Activity of IFNA Genes. *J Biol Chem* **278**:16630-16641.
10. **Barnes, B. J., M. J. Kellum, A. E. Field, and P. M. Pitha.** 2002. Multiple regulatory domains of IRF-5 control activation, cellular localization, and induction of chemokines that mediate recruitment of T lymphocytes. *Mol Cell Biol* **22**:5721-40.
11. **Barnes, B. J., P. A. Moore, and P. M. Pitha.** 2001. Virus-specific activation of a novel interferon regulatory factor, IRF-5, results in the induction of distinct interferon alpha genes. *J Biol Chem* **276**:23382-90.
12. **Bartenschlager, R., A. Kaul, and S. Sparacio.** 2003. Replication of the hepatitis C virus in cell culture. *Antiviral Res* **60**:91-102.
13. **Beard, M. R., G. Abell, M. Honda, A. Carroll, M. Gartland, B. Clarke, K. Suzuki, R. Lanford, D. V. Sangar, and S. M. Lemon.** 1999. An infectious molecular clone of a Japanese genotype 1b hepatitis C virus. *Hepatology* **30**:316-324.
14. **Beattie, E., E. B. Kauffman, H. Martinez, M. E. Perkus, B. L. Jacobs, E. Paoletti, and J. Tartaglia.** 1996. Host-range restriction of vaccinia virus E3L-specific deletion mutants. *Virus Gene* **12**:89-94.
15. **Bertin, J., L. Wang, Y. Guo, M. D. Jacobson, J. L. Poyet, S. M. Srinivasula, S. Merriam, P. S. DiStefano, and E. S. Alnemri.** 2001. CARD11 and CARD14 are novel caspase recruitment domain (CARD)/membrane-associated guanylate kinase

- (MAGUK) family members that interact with BCL10 and activate NF-kappa B. *J Biol Chem* **276**:11877-82.
16. **Blight, K. J., A. A. Kolykhalov, and C. M. Rice.** 2000. Efficient initiation of HCV RNA replication in cell culture. *Science* **290**:1972-1974.
  17. **Blight, K. J., J. A. McKeating, and C. M. Rice.** 2002. Highly permissive cell lines for subgenomic and genomic hepatitis C virus RNA replication. *J Virol* **76**:13001-14.
  18. **Blight, K. J., and C. M. Rice.** 1997. Secondary structure determination of the conserved 98-base sequence at the 3' terminus of hepatitis C virus genome RNA. *J Virol* **71**:7345-7352.
  19. **Booth, J. C.** 1998. Chronic hepatitis C: the virus, its discovery and the natural history of the disease. *J Viral Hepat* **5**:213-22.
  20. **Borowski, P., M. Heiland, H. Feucht, and R. Laufs.** 1999. Characterisation of non-structural protein 3 of hepatitis C virus as modulator of protein phosphorylation mediated by PKA and PKC: evidences for action on the level of substrate and enzyme. *Arch Virol* **144**:687-701.
  21. **Bouchier-Hayes, L., and S. J. Martin.** 2002. CARD games in apoptosis and immunity. *EMBO Rep* **3**:616-21.
  22. **Brown, E. A., H. Zhang, L. H. Ping, and S. M. Lemon.** 1992. Secondary structure of the 5' nontranslated regions of hepatitis C virus and pestivirus genomic RNAs. *Nucleic Acids Res* **20**:5041-5.

23. **Bukh, J., R. H. Purcell, and R. H. Miller.** 1993. At least 12 genotypes of hepatitis C virus predicted by sequence analysis of the putative E1 gene of isolates collected worldwide. *Proc Natl Acad Sci U S A* **90**:8234-8.
24. **Carneiro, L. A., L. H. Travassos, and D. J. Philpott.** 2004. Innate immune recognition of microbes through Nod1 and Nod2: implications for disease. *Microbes Infect* **6**:609-16.
25. **Chamaillard, M., M. Hashimoto, Y. Horie, J. Masumoto, S. Qiu, L. Saab, Y. Ogura, A. Kawasaki, K. Fukase, S. Kusumoto, M. A. Valvano, S. J. Foster, T. W. Mak, G. Nunez, and N. Inohara.** 2003. An essential role for NOD1 in host recognition of bacterial peptidoglycan containing diaminopimelic acid. *Nat Immunol* **4**:702-7.
26. **Chen, Z., T. B. Gibson, F. Robinson, L. Silvestro, G. Pearson, B. Xu, A. Wright, C. Vanderbilt, and M. H. Cobb.** 2001. MAP kinases. *Chem Rev* **101**:2449-76.
27. **Cheney, I. W., S. Naim, V. C. Lai, S. Dempsey, D. Bellows, M. P. Walker, J. H. Shim, N. Horscroft, Z. Hong, and W. Zhong.** 2002. Mutations in NS5B polymerase of hepatitis C virus: impacts on in vitro enzymatic activity and viral RNA replication in the subgenomic replicon cell culture. *Virology* **297**:298-306.
28. **Choo, Q. L., G. Kuo, A. J. Weiner, L. R. Overby, D. W. Bradley, and M. Houghton.** 1989. Isolation of a cDNA clone derived from a blood-borne non-A, non-B viral hepatitis genome. *Science* **244**:359-362.

29. **Chu, W. M., D. Ostertag, Z. W. Li, L. Chang, Y. Chen, Y. Hu, B. Williams, J. Perrault, and M. Karin.** 1999. JNK2 and IKKbeta are required for activating the innate response to viral infection. *Immunity* **11**:721-31.
30. **Crozat, K., and B. Beutler.** 2004. TLR7: A new sensor of viral infection. *Proc Natl Acad Sci U S A* **101**:6835-6.
31. **Der, S. D., Y.-L. Yang, C. Weissman, and B. R. G. Williams.** 1997. A double-stranded RNA-activated protein kinase-dependent pathway mediating stress-induced apoptosis. *Proc Natl Acad Sci U S A* **94**:3279-3283.
32. **Der, S. D., A. Zhou, B. R. G. Williams, and R. H. Silverman.** 1998. Identification of genes differentially regulated by interferon alpha, beta, or gamma using oligonucleotide arrays. *Proc Natl Acad Sci U S A* **95**:15623-15628.
33. **Diebold, S. S., T. Kaisho, H. Hemmi, S. Akira, and C. Reis e Sousa.** 2004. Innate antiviral responses by means of TLR7-mediated recognition of single-stranded RNA. *Science* **303**:1529-31.
34. **Donze, O., J. Deng, J. Curran, R. Sladek, D. Picard, and N. Sonenberg.** 2004. The protein kinase PKR: a molecular clock that sequentially activates survival and death programs. *EMBO J* **23**:564-571.
35. **Dunne, A., and L. A. O'Neill.** 2003. The interleukin-1 receptor/Toll-like receptor superfamily: signal transduction during inflammation and host defense. *Sci STKE* **2003**.

36. **Egger, D., B. Wolk, R. Gosert, L. Bianchi, H. E. Blum, D. Moradpour, and K. Bienz.** 2002. Expression of hepatitis C virus proteins induces distinct membrane alterations including a candidate viral replication complex. *J Virol* **76**:5974-5984.
37. **Feng, G.-S., K. L. Chong, A. Kumara, and B. R. G. Williams.** 1992. Identification of double-stranded RNA-binding domains in the interferon-induced double-stranded RNA-activated p68 kinase. *Proc Natl Acad Sci U S A* **89**:5447-5451.
38. **Fitzgerald, K. A., S. M. McWhirter, K. L. Faia, D. C. Rowe, E. Latz, D. T. Golenbock, A. J. Coyle, S. M. Liao, and T. Maniatis.** 2003. IKKepsilon and TBK1 are essential components of the IRF3 signaling pathway. *Nat Immunol* **4**:491-496.
39. **Foster, G. R., and N. B. Finter.** 1998. Are all type I human interferons equivalent? *J Viral Hepat* **5**:143-52.
40. **Foy, E., Li, K., C. Wang, R. Sumpter, M. Ikeda, S. M. Lemon, and M. Gale, Jr.** 2003. Regulation of interferon regulatory factor-3 by the hepatitis C virus serine protease. *Science* **300**:1145-1148.
41. **Fredericksen, B., G. Akkaraju, E. Foy, C. Wang, J. Pflugheber, Z. J. Chen, and M. Gale, Jr.** 2001. Activation of the inteferon-beta promoter during hepatitis C virus RNA replication. *Viral Immunol.* **15**:29-40.
42. **Fried, M. W., M. L. Shiffman, K. R. Reddy, C. Smith, G. Marinos, F. L. Goncales, Jr., D. Haussinger, M. Diago, G. Carosi, D. Dhumeaux, A. Craxi, A. Lin, J. Hoffman, and J. Yu.** 2002. Peginterferon alfa-2a plus ribavirin for chronic hepatitis C virus infection. *N Engl J Med* **347**:975-982.

43. **Fujita, T., L. F. Reis, N. Watanabe, Y. Kimura, and T. Taniguchi.** 1986. Induction of the transcription factor IRF-1 and interferon-beta mRNAs by cytokines and activators of second-messenger pathways. *Proc Natl Acad Sci U S A* **86**:9936-9940.
44. **Gale, M., Jr., C. M. Blakely, B. Kwieciszewski, S.-L. Tan, M. Dossett, M. J. Korth, S. J. Polyak, D. R. Gretch, and M. G. Katze.** 1998. Control of PKR protein kinase by hepatitis C virus nonstructural 5A protein: molecular mechanisms of kinase regulation. *Mol Cell Biol* **18**:5208-5218.
45. **Gale, M., Jr., and M. G. Katze.** 1998. Molecular mechanisms of interferon resistance mediated by viral-directed inhibition of PKR, the interferon-induced protein kinase. *Pharmacol Ther* **78**:29-46.
46. **Gale, M., Jr., M. J. Korth, N. M. Tang, S.-L. Tan, D. A. Hopkins, T. E. Dever, S. J. Polyak, D. R. Gretch, and M. G. Katze.** 1997. Evidence that hepatitis C virus resistance to interferon is mediated through repression of the PKR protein kinase by the nonstructural 5A protein. *Virology* **230**:217-227.
47. **Gale, M., Jr., B. Kwieciszewski, M. Dossett, H. Nakao, and M. G. Katze.** 1999. Anti-apoptotic and oncogenic potentials of hepatitis C virus are linked to interferon resistance by viral repression of the PKR protein kinase. *J Virol* **73**:6506-6516.
48. **Garcia-Sastre, A.** 2002. Mechanisms of inhibition of the host interferon alpha/beta-mediated antiviral responses by viruses. *Microbes Infect* **4**:647-55.



49. **Garcia-Sastre, A., A. Egorov, D. Matassov, S. Brandt, D. E. Levy, J. E. Durbin, P. Palese, and T. Muster.** 1999. Influenza A virus lacking the NS1 gene replicates in interferon-deficient systems. *Virology* **252**:324-330.
50. **Geiss, G. K., V. S. Carter, Y. He, B. K. Kwieciszewski, T. Holzman, M. J. Korth, C. A. Lazaro, N. Fausto, R. E. Bumgarner, and M. G. Katze.** 2003. Gene expression profiling of the cellular transcriptional network regulated by alpha/beta interferon and its partial attenuation by the hepatitis C virus nonstructural 5A protein. *J Virol* **77**:6367-6375.
51. **Ghosh, S., and M. Karin.** 2002. Missing pieces in the NF-kappaB puzzle. *Cell* **109**:S81-96.
52. **Girardin, S. E., I. G. Boneca, L. A. Carneiro, A. Antignac, M. Jehanno, J. Viala, K. Tedin, M. K. Taha, A. Labigne, U. Zahringer, A. J. Coyle, P. S. DiStefano, J. Bertin, P. J. Sansonetti, and D. J. Philpott.** 2003. Nod1 detects a unique muropeptide from gram-negative bacterial peptidoglycan. *Science* **300**:1584-7.
53. **Goh, K. C., M. J. deVeer, and B. R. Williams.** 2000. The protein kinase PKR is required for p38 MAPK activation and the innate immune response to bacterial endotoxin. *EMBO J* **19**:4292-7.
54. **Goh, K. C., S. J. Haque, and B. R. Williams.** 1999. p38 MAP kinase is required for STAT1 serine phosphorylation and transcriptional activation induced by interferons. *EMBO J* **18**:5601-8.

55. **Goodbourn, S., L. Didcock, and R. E. Randall.** 2000. Interferons: cell signaling, immune modulation, antiviral responses and virus countermeasures. *J Gen Virol* **81**:2341-2364.
56. **Grandvaux, N., M. J. Servant, B. tenOever, G. C. Sen, S. Balachandran, G. N. Barber, R. Lin, and J. Hiscott.** 2002. Transcriptional profiling of interferon regulatory factor 3 target genes: direct involvement in the regulation of interferon-stimulated genes. *J Virol* **76**:5532-5539.
57. **Guo, J., V. Bichko, and C. Seeger.** 2001. Effect of alpha interferon on the hepatitis C virus replication. *J Virol* **75**:8516-8523.
58. **Guo, J., D. J. Hui, W. C. Merrick, and G. C. Sen.** 2000. A new pathway of translational regulation mediated by eukaryotic initiation factor 3. *EMBO J* **19**:6891-6899.
59. **Guo, J., K. L. Peters, and G. C. Sen.** 2000. Induction of the human protein p56 by interferon, double-stranded RNA, or virus infection. *Virology* **267**:209-219.
60. **Harada, H., T. Fujita, M. Miyamoto, Y. Kimura, M. Maruyama, A. Furia, T. Miyata, and T. Taniguchi.** 1989. Structurally similar but functionally distinct factors, IRF-1 and IRF-2, bind to the same regulatory elements of IFN and IFN-inducible genes. *Cell* **58**:729-739.
61. **Harada, H., E. Takahashi, S. Itoh, K. Harada, T. A. Hori, and T. Taniguchi.** 1994. Structure and regulation of the human interferon regulatory factor 1 (IRF-1) and IRF-2 genes: implications for a gene network in the interferon system. *Mol Cell Biol* **14**:1500-9.

62. **He, B., M. Gross, and B. Roizman.** 1997. The gamma(1)34.5 protein of herpes simplex virus I complexes with protein phosphatase 1 alpha to dephosphorylate the alpha subunit of the eukaryotic translation initiation factor 2 and preclude the shutoff of protein synthesis by double-stranded RNA-activated protein kinase. *Proc Natl Acad Sci U S A* **94**:843-848.
63. **He, Y., and M. G. Katze.** 2002. To interfere and to anti-interfere: the interplay between hepatitis C virus and interferon. *Viral Immunol* **15**:95-119.
64. **He, Y., H. Nakao, S. L. Tan, S. J. Polyak, P. Neddermann, S. Vijaysri, B. L. Jacobs, and M. G. Katze.** 2002. Subversion of cell signaling pathways by hepatitis C virus nonstructural 5A protein via interaction with Grb2 and P85 phosphatidylinositol 3-kinase. *J Virol* **76**:9207-9217.
65. **Heil, F., H. Hemmi, H. Hochrein, F. Ampenberger, C. Kirschning, S. Akira, G. Lipford, H. Wagner, and S. Bauer.** 2004. Species-specific recognition of single-stranded RNA via toll-like receptor 7 and 8. *Science* **303**:1526-9.
66. **Hermine, O., F. Lefrere, J. P. Bronowicki, X. Mariette, K. Jondeau, V. Eclache-Saudreau, B. Delmas, F. Valensi, P. Cacoub, C. Brechot, B. Varet, and X. Troussard.** 2002. Regression of splenic lymphoma with villous lymphocytes after treatment of hepatitis C virus infection. *N Engl J Med* **347**:89-94.
67. **Hertzog, P. J., L. A. O'Neill, and J. A. Hamilton.** 2003. The interferon in TLR signaling: more than just antiviral. *Trends Immunol* **24**:534-539.
68. **Hoebe, K., E. M. Janssen, S. O. Kim, L. Alexopoulou, R. A. Flavell, J. Han, and B. Beutler.** 2003. Upregulation of costimulatory molecules induced by

- lipopolysaccharide and double-stranded RNA occurs by Trif-dependent and Trif-independent pathways. *Nat Immunol* **4**:1223-1229.
69. **Holland-Staley, C. A., L. C. Kovari, E. M. Golenberg, K. J. Pobursky, and D. L. Mayers.** 2002. Genetic diversity and response to IFN of the NS3 protease gene from clinical strains of the hepatitis C virus. *Arch Virol* **147**:1385-1406.
  70. **Honda, K., S. Sakaguchi, C. Nakajima, A. Watanabe, H. Yanai, M. Matsumoto, T. Ohteki, T. Kaisho, A. Takaoka, S. Akira, T. Seya, and T. Taniguchi.** 2003. Selective contribution of IFN-alpha/beta signaling to the maturation of dendritic cells induced by double-stranded RNA or viral infection. *Proc Natl Acad Sci U S A* **100**:10872-7.
  71. **Horng, T., G. M. Barton, and R. Medzhitov.** 2001. TIRAP: an adapter molecule in the Toll signaling pathway. *Nat Immunol* **2**:835-41.
  72. **Horvath, C. M.** 2004. Silencing STATs: lessons from paramyxovirus interferon evasion. *Cytokine Growth Factor Rev* **15**:117-27.
  73. **Hsu, L. C., J. M. Park, K. Zhang, J. L. Luo, S. Maeda, R. J. Kaufman, L. Eckmann, D. G. Guiney, and M. Karin.** 2004. The protein kinase PKR is required for macrophage apoptosis after activation of Toll-like receptor 4. *Nature* **428**:341-5.
  74. **Hugot, J. P., M. Chamaillard, H. Zouali, S. Lesage, J. P. Cezard, J. Belaiche, S. Almer, C. Tysk, C. A. O'Morain, M. Gassull, V. Binder, Y. Finkel, A. Cortot, R. Modigliani, P. Laurent-Puig, C. Gower-Rousseau, J. Macry, J. F. Colombel, M. Sahbatou, and G. Thomas.** 2001. Association of NOD2 leucine-rich repeat variants with susceptibility to Crohn's disease. *Nature* **411**:599-603.

75. **Hui, D. J., C. R. Bhasker, W. C. Merrick, and G. C. Sen.** 2003. Viral stress-inducible protein p56 inhibits translation by blocking the interaction of eIF3 with the ternary complex eIF2.GTP.Met-tRNAi. *J Biol Chem* **278**:39477-39482.
76. **Ikeda, M., K. Sugiyama, T. Mizutani, T. Tanaka, K. Tanaka, H. Sekihara, K. Shimotohno, and N. Kato.** 1998. Human hepatocyte clonal cell lines that support persistent replication of hepatitis C virus. *Virus Res* **56**:157-67.
77. **Ikeda, M., M. Yi, K. li, and S. M. Lemon.** 2002. Selectable subgenomic and genome-length dicistronic RNAs derived from an infectious molecular clone of the HCV-N strain of hepatitis C virus replicate efficiently in cultured Huh7 cells. *J Virol* **76**:2997-3006.
78. **Inohara, N., and G. Nunez.** 2003. NODs: intracellular proteins involved in inflammation and apoptosis. *Nat Rev Immunol* **3**:371-82.
79. **Inohara, N., Y. Ogura, A. Fontalba, O. Gutierrez, F. Pons, J. Crespo, K. Fukase, S. Inamura, S. Kusumoto, M. Hashimoto, S. J. Foster, A. P. Moran, J. L. Fernandez-Luna, and G. Nunez.** 2003. Host recognition of bacterial muramyl dipeptide mediated through NOD2. Implications for Crohn's disease. *J Biol Chem* **278**:5509-12.
80. **Iordanov, M. S., J. M. Paranjape, A. Zhou, J. Wong, B. R. Williams, E. F. Meurs, R. H. Silverman, and B. E. Magun.** 2000. Activation of p38 mitogen-activated protein kinase and c-Jun NH(2)-terminal kinase by double-stranded RNA and encephalomyocarditis virus: involvement of RNase L, protein kinase R, and alternative pathways. *Mol Cell Biol* **20**:617-27.

81. **Jiang, Z., M. Zamanian-Daryoush, H. Nie, A. M. Silva, B. R. Williams, and X. Li.** 2003. Poly(I-C)-induced Toll-like receptor 3 (TLR3)-mediated activation of NFkappa B and MAP kinase is through an interleukin-1 receptor-associated kinase (IRAK)-independent pathway employing the signaling components TLR3-TRAF6-TAK1-TAB2-PKR. *J Biol Chem* **278**:16713-9.
82. **Johnson, G. L., and R. Lapadat.** 2002. Mitogen-activated protein kinase pathways mediated by ERK, JNK, and p38 protein kinases. *Science* **298**:1911-2.
83. **Kaneko, T., Y. Tanji, S. Satoh, M. Hijikata, S. Asabe, K. Kimura, and K. Shimotohno.** 1994. Production of two phosphoproteins from the NS5A region of the hepatitis C viral genome. *Biochem Biophys Res Commun* **205**:320-326.
84. **Karin, M., Y. Yamamoto, and Q. M. Wang.** 2004. The IKK NF-kappa B system: a treasure trove for drug development. *Nat Rev Drug Discov* **3**:17-26.
85. **Kerkmann, M., S. Rothenfusser, V. Hornung, A. Towarowski, M. Wagner, A. Sarris, T. Giese, S. Endres, and G. Hartmann.** 2003. Activation with CpG-A and CpG-B oligonucleotides reveals two distinct regulatory pathways of type I IFN synthesis in human plasmacytoid dendritic cells. *J Immunol* **170**:4465-74.
86. **Khakoo, S., P. Glue, L. Grellier, B. Wells, A. Bell, C. Dash, I. Murray-Lyon, D. Lypnyj, B. Flannery, K. Walters, and G. M. Dusheiko.** 1998. Ribavirin and interferon alfa-2b in chronic hepatitis C: assessment of possible pharmacokinetic and pharmacodynamic interactions. *Br J Clin Pharmacol* **46**:563-570.

87. **Kim, T., T. Y. Kim, Y. H. Song, I. M. Min, J. Yim, and T. K. Kim.** 1999. Activation of interferon regulatory factor 3 in response to DNA-damaging agents. *J Biol Chem* **274**:30686-9.
88. **Kimura, T., K. Nakayama, J. Penninger, M. Kitagawa, H. Harada, T. Matsuyama, N. Tanaka, R. Kamijo, J. Vilcek, T. W. Mak, and T. Taniguchi.** 1994. Involvement of the IRF-1 transcription factor in antiviral responses to interferons. *Science* **264**:1921-1924.
89. **Koch, J. O., and R. Bartenschlager.** 1997. Determinants of substrate specificity in the NS3 serine proteinase of the hepatitis C virus. *Virology* **237**:78-88.
90. **Kolykhalov, A. A., E. V. Agapov, K. J. Blight, K. Mihalik, S. M. Feinstone, and C. M. Rice.** 1997. Transmission of hepatitis C by intrahepatic inoculation with transcribed RNA. *Science* **277**:570-574.
91. **Kolykhalov, A. A., K. Mihalik, S. M. Feinstone, and C. M. Rice.** 2000. Hepatitis C virus-encoded enzymatic activities and conserved RNA elements in the 3' nontranslated region are essential for virus replication in vivo. *J Virol* **74**:2046-51.
92. **Kotenko, S. V., G. Gallagher, V. V. Baurin, A. Lewis-Antes, M. Shen, N. K. Shah, J. A. Langer, F. Sheikh, H. Dickensheets, and R. P. Donnelly.** 2003. IFN-lambdas mediate antiviral protection through a distinct class II cytokine receptor complex. *Nat Immunol* **4**:69-77.
93. **Kreiger, N., V. Lohmann, and R. Bartenschlager.** 2001. Enhancement of hepatitis C virus RNA replication by cell culture-adaptive mutations. *J Virol* **75**:4614-4654.

94. **Kroger, A., M. Koster, K. Schroeder, H. Hauser, and P. P. Mueller.** 2002. Activities of IRF-1. *J Interferon Cytokine Res* **22**:5-14.
95. **Kuhen, K. L., and C. E. Samuel.** 1999. Mechanism of interferon action: functional characteristics of positive and negative regulatory domains that modulate transcriptional activation of the human RNA-dependent protein kinase Pkr promoter. *Virology* **254**:182-195.
96. **Kumar, A., Y.-L. Yang, V. Flati, S. Der, S. Kadereit, A. Deb, J. Haque, L. Reis, C. Weissmann, and B. R. G. Williams.** 1997. Deficient cytokine signaling in mouse embryo fibroblasts with a targeted deletion in the PKR gene: role of IRF-1 and NF- $\kappa$ B. *EMBO J* **16**:406-416.
97. **Kumar, S., J. Boehm, and J. C. Lee.** 2003. p38 MAP kinases: key signalling molecules as therapeutic targets for inflammatory diseases. *Nat Rev Drug Discov* **2**:717-26.
98. **Lanford, R. E., B. Guerra, H. Lee, D. R. Averett, B. Pfeiffer, D. Chavez, L. Notvall, and C. Bigger.** 2003. Antiviral effect and virus-host interactions in response to alpha interferon, gamma interferon, poly(i)-poly(c), tumor necrosis factor alpha, and ribavirin in hepatitis C virus subgenomic replicons. *J Virol* **77**:1092-1104.
99. **Lauer, G. M., and B. D. Walker.** 2001. Hepatitis C virus infection. *N Engl J Med* **345**:41-52.
100. **Levy, D. E., and C. K. Lee.** 2002. What does Stat3 do? *J Clin Invest* **109**:1143-1148.
101. **Lin, C., K. Lin, Y. P. Luong, B. G. Rao, Y. Y. Wei, D. L. Brennan, J. R. Fulghum, H. M. Hsiao, S. Ma, J. P. Maxwell, K. M. Cottrell, R. B. Perni, C. A.**



- Gates, and A. D. Kwong.** 2004. In vitro resistance studies of hepatitis C virus serine protease inhibitors, VX-950 and BILN 2061: structural analysis indicates different resistance mechanisms. *J Biol Chem* **279**:17508-14.
102. **Lin, R., C. Heylbroeck, P. M. Pitha, and J. Hiscott.** 1998. Virus-dependent phosphorylation of the IRF-3 transcription factor regulates nuclear translocation, transactivation potential, and proteasome-mediated degradation. *Mol Cell Biol* **18**:2986-2996.
103. **Lin, R., Y. Mamane, and J. Hiscott.** 1999. Structural and functional analysis of interferon regulatory factor 3: localization of the transactivation and autoinhibitory domains. *Mol Cell Biol* **19**:2465-2474.
104. **Lohmann, V., S. Hoffmann, U. Herian, F. Penin, and R. Bartenschlager.** 2003. Viral and Cellular Determinants of Hepatitis C Virus RNA Replication in Cell Culture. *J Virol* **77**:3007-3019.
105. **Lohmann, V., F. Korner, J.-O. Kock, L. Theilmann, and R. Bartenschlager.** 1999. Replication of subgenomic hepatitis C virus RNAs in a hepatoma cell line. *Science* **285**:110-113.
106. **Look, D. C., W. T. Roswit, A. G. Frick, Y. Gris-Alevy, D. M. Dickhaus, M. J. Walter, and M. J. Holtzman.** 1998. Direct suppression of Stat1 function during adenoviral infection. *Immunity* **9**:871-80.
107. **Lu, R., W. C. Au, W. S. Yeow, N. Hageman, and P. M. Pitha.** 2000. Regulation of the promoter activity of interferon regulatory factor-7 gene. Activation by interferon and silencing by hypermethylation. *J Biol Chem* **275**:31805-31812.

108. **Lund, J., A. Sato, S. Akira, R. Medzhitov, and A. Iwasaki.** 2003. Toll-like receptor 9-mediated recognition of Herpes simplex virus-2 by plasmacytoid dendritic cells. *J Exp Med* **198**:513-20.
109. **Lund, J. M., L. Alexopoulou, A. Sato, M. Karow, N. C. Adams, N. W. Gale, A. Iwasaki, and R. A. Flavell.** 2004. Recognition of single-stranded RNA viruses by Toll-like receptor 7. *Proc Natl Acad Sci U S A* **101**:5598-603.
110. **Mamane, Y., C. Heylbroeck, P. Genin, M. Algarte, M. J. Servant, C. LePage, C. DeLuca, H. Kwon, R. Lin, and J. Hiscott.** 1999. Interferon regulatory factors: the next generation. *Gene* **237**:1-14.
111. **Martell, M., J. I. Esteban, J. Quer, J. Genesca, A. Weiner, R. Esteban, J. Guardia, and J. Gomez.** 1992. Hepatitis C virus (HCV) circulates as a population of different but closely related genomes: quasispecies nature of HCV genome distribution. *J Virol* **66**:3225-3229.
112. **Martinez-Moczygemba, M., M. J. Gutch, D. L. French, and N. C. Reich.** 1997. Distinct STAT structure promotes interaction of STAT2 with the p48 subunit of the interferon-alpha-stimulated transcription factor ISGF3. *J Biol Chem* **272**:20070-6.
113. **Matsumoto, M., K. Funami, M. Tanabe, H. Oshiumi, M. Shingai, Y. Seto, A. Yamamoto, and T. Seya.** 2003. Subcellular localization of Toll-like receptor 3 in human dendritic cells. *J Immunol* **171**:3154-62.
114. **Matsuyama, T., T. Kimura, M. Kitagawa, K. Pfeffer, T. Kawakami, N. Watanabe, T. M. Kundig, R. Amakawa, K. Kishihara, A. Wakeham, and et al.**

1993. Targeted disruption of IRF-1 or IRF-2 results in abnormal type I IFN gene induction and aberrant lymphocyte development. *Cell* **75**:83-97.
115. **Mayo, M. J.** 2003. Extrahepatic manifestations of hepatitis C infection. *Am J Med Sci* **325**:135-48.
  116. **McHutchison, J. G., and A. T. Dev.** 2004. Future trends in managing hepatitis C. *Gastroenterol Clin North Am* **33**:S51-61.
  117. **McHutchison, J. G., S. C. Gordon, E. R. Schiff, M. L. Shiffman, W. M. Lee, Z. D. Goodman, M. H. Ling, S. Cort, J. K. Albrecht, and f. t. I. I. T. Group.** 1998. Interferon alfa-2b alone or in combination with ribavirin as initial treatment for chronic hepatitis C. *N Engl J Med* **339**:1485-1492.
  118. **McWhirter, S. M., K. A. Fitzgerald, J. Rosains, D. C. Rowe, D. T. Golenbock, and T. Maniatis.** 2004. IFN-regulatory factor 3-dependent gene expression is defective in Tbk1-deficient mouse embryonic fibroblasts. *Proc Natl Acad Sci U S A* **101**:233-8.
  119. **Medzhitov, R.** 2001. Toll-like receptors and innate immunity. *Nat Rev Immunol* **1**:135-45.
  120. **Mercer, D. F., D. E. Schiller, J. F. Elliott, D. N. Douglas, C. Hao, A. Rinfret, W. R. Addison, K. P. Fischer, T. A. Churchill, J. R. Lakey, D. L. Tyrrell, and N. M. Kneteman.** 2001. Hepatitis C virus replication in mice with chimeric human livers. *Nat Med* **7**:927-33.
  121. **Merrick, W. C., and J. W. B. Hershey.** 1996. The pathway and mechanism of eukaryotic protein synthesis, p. 31-70. *In* J. Hershey, M. Mathews, and N. Sonenberg

- (ed.), Translational control. Cold Spring Harbor Laboratory Press, Cold Spring Harbor, N.Y.
122. **Miettinen, M., T. Sareneva, I. Julkunen, and S. Matikainen.** 2001. IFNs activate toll-like receptor gene expression in viral infections. *Genes Immun* **2**:349-55.
  123. **Miyamoto, M., T. Fujita, Y. Kimura, M. Maruyama, H. Harada, Y. Sudo, T. Miyata, and T. Taniguchi.** 1988. Regulated expression of a gene encoding a nuclear factor, IRF-1, that specifically binds to IFN-beta gene regulatory elements. *Cell* **54**:903-13.
  124. **Mori, M., M. Yoneyama, T. Ito, K. Takahashi, F. Inagaki, and T. Fujita.** 2003. Identification of Ser 386 of interferon regulatory factor 3 as critical targets for inducible phosphorylation that determines activation. *J Biol Chem* **279**:9698-702.
  125. **Nakaya, T., M. Sato, N. Hata, M. Asagiri, H. Suemori, S. Noguchi, N. Tanaka, and T. Taniguchi.** 2001. Gene induction pathways mediated by distinct IRFs during viral infection. *Biochem Biophys Res Commun* **283**:1150-1156.
  126. **O'Neill, L. A., K. A. Fitzgerald, and A. G. Bowie.** 2003. The Toll-IL-1 receptor adaptor family grows to five members. *Trends Immunol* **24**:286-289.
  127. **Ogura, Y., D. K. Bonen, N. Inohara, D. L. Nicolae, F. F. Chen, R. Ramos, H. Britton, T. Moran, R. Karaliuskas, R. H. Duerr, J. P. Achkar, S. R. Brant, T. M. Bayless, B. S. Kirschner, S. B. Hanauer, G. Nunez, and J. H. Cho.** 2001. A frameshift mutation in NOD2 associated with susceptibility to Crohn's disease. *Nature* **411**:603-6.

128. **Ozato, K., H. Tsujimura, and T. Tamura.** 2002. Toll-like receptor signaling and regulation of cytokine gene expression in the immune system. *BioTechniques Suppl*:66-8, 70, 72.
129. **Panteva, M., H. Korkaya, and S. Jameel.** 2003. Hepatitis viruses and the MAPK pathway: is this a survival strategy? *Virus Res* **92**:131-40.
130. **Parekh, B. S., and T. Maniatis.** 1999. Virus infection leads to localized hyperacetylation of histones H3 and H4 at the IFN-beta promoter. *Mol Cell* **3**:125-129.
131. **Petska, S., J. A. Langer, K. Zoon, and C. E. Samuel.** 1987. Interferons and their actions. *Annual Review Of Biochemistry* **56**:727-777.
132. **Pfeifer, U., R. Thomssen, K. Legler, U. Bottcher, W. Gerlich, E. Weinmann, and O. Klinge.** 1980. Experimental non-A, non-B hepatitis: four types of cytoplasmic alteration in hepatocytes of infected chimpanzees. *Virchows Arch B Cell Pathol Incl Mol Pathol*:233-43.
133. **Pflugheber, J., B. Fredericksen, R. Sumpter, C. Wang, F. Ware, D. Sodora, and M. Gale, Jr.** 2002. Regulation of PKR and IRF-1 during hepatitis C virus RNA replication. *Proc Natl Acad Sci U S A* **99**:4650-4655.
134. **Platanias, L. C., and E. N. Fish.** 1999. Signaling pathways activated by interferons. *Exp Hematol* **27**:1583-92.
135. **Rebouillat, D., and A. G. Hovanessian.** 1999. The human 2',5'-oligoadenylate synthetase family: interferon-induced proteins with unique enzymatic properties. *J Interferon Cytokine Res* **19**:295-308.

136. **Rocak, S., and P. Linder.** 2004. DEAD-box proteins: the driving forces behind RNA metabolism. *Nat Rev Mol Cell Biol* **5**:232-41.
137. **Rothwarf, D. M., and M. Karin.** 1999. The NF-kappa B activation pathway: a paradigm in information transfer from membrane to nucleus. *Sci STKE* **1999**.
138. **Ruan, H., C. Y. Brown, and D. R. Morris.** 1997. Analysis of ribosome loading onto mRNA species: implications for translational control, p. 305-321. *In* J. D. Richter (ed.), mRNA formation and function. Academic Press, New York.
139. **Samuel, C. E.** 2001. Antiviral actions of interferons. *Clin Microbiol Rev* **14**:778-809, table.
140. **Santoro, M. G., A. Rossi, and C. Amici.** 2003. NF-kappaB and virus infection: who controls whom. *EMBO J* **22**:2552-60.
141. **Sato, M., H. Suemori, N. Hata, M. Asagiri, K. Ogasawara, K. Nakao, T. Nakaya, M. Katsuki, S. Noguchi, N. Tanaka, and T. Taniguchi.** 2000. Distinct and essential roles of transcription factors IRF-3 and IRF-7 in response to viruses for IFN-alpha/beta gene induction. *Immunity* **13**:539-548.
142. **Schaeffer, H. J., and M. J. Weber.** 1999. Mitogen-activated protein kinases: specific messages from ubiquitous messengers. *Mol Cell Biol* **19**:2435-2444.
143. **Sen, G. C.** 2001. Viruses and interferons. *Ann Rev Microbiol* **55**:255-281.
144. **Servant, M. J., N. Grandvaux, and J. Hiscott.** 2002. Multiple signaling pathways leading to the activation of interferon regulatory factor 3. *Biochem Pharmacol* **64**:985-992.

145. **Sharma, S., R. Benjamin, B. tenOever, N. Grandvaux, G.-P. Zhou, R. Lin, and J. Hiscott.** 2003. Triggering the interferon antiviral response through a novel IKK-related pathway. *Science* **300**:1148-1151.
146. **Sheridan, I., O. G. Pybus, E. C. Holmes, and P. Klennerman.** 2004. High-resolution phylogenetic analysis of hepatitis C virus adaptation and its relationship to disease progression. *J Virol* **78**:3447-3454.
147. **Shimizu, Y. K., A. J. Weiner, J. Rosenblatt, D. C. Wong, M. Shapiro, T. Popkin, M. Houghton, H. J. Alter, and R. H. Purcell.** 1990. Early events in hepatitis C virus infection of chimpanzees. *Proc Natl Acad Sci U S A* **87**:6441-6444.
148. **Shors, S. T., E. Beattie, K. Paoletti, J. Tartaglia, and B. L. Jacobs.** 1998. Role of the vaccinia virus E3L and K3L gene products in rescue of VSV and EMCV from the effects of IFN-alpha. *J Interferon Cytokine Res* **18**:721-729.
149. **Smith, M. W., Z. N. Yue, M. J. Korth, H. A. Do, L. Boix, N. Fausto, J. Bruix, R. L. Carithers, Jr., and M. G. Katze.** 2003. Hepatitis C virus and liver disease: global transcriptional profiling and identification of potential markers. *Hepatology* **38**:1458-1467.
150. **Soloaga, A., S. Thomson, G. R. Wiggin, N. Rampersaud, M. H. Dyson, C. A. Hazzalin, L. C. Mahadevan, and J. S. Arthur.** 2003. MSK2 and MSK1 mediate the mitogen- and stress-induced phosphorylation of histone H3 and HMG-14. *EMBO J* **22**:2788-97.

151. **Stark, G. R., I. M. Kerr, B. R. G. Williams, R. H. Silverman, and R. D. Schreiber.** 1998. How cells respond to interferons. *Annual Review Of Biochemistry* **67**:227-264.
152. **Street, A., A. Macdonald, K. Crowder, and M. Harris.** 2004. The Hepatitis C virus NS5A protein activates a phosphoinositide 3-kinase-dependent survival signaling cascade. *J Biol Chem* **279**:12232-41.
153. **Su, A. I., J. P. Pezacki, L. Wodicka, A. D. Brideau, L. Supekova, R. Thimme, S. Wieland, J. Bukh, R. H. Purcell, P. G. Schultz, and F. V. Chisari.** 2002. Genomic analysis of the host response to hepatitis C virus infection. *Proc Natl Acad Sci U S A* **99**:15669-15674.
154. **Su, L., and M. David.** 2000. Distinct mechanisms of STAT phosphorylation via the interferon-alpha/beta receptor. Selective inhibition of STAT3 and STAT5 by piceatannol. *J Biol Chem* **275**:12661-6.
155. **Sudhakar, A., A. Ramachandran, S. Ghosh, S. E. Hasnain, R. J. Kaufman, and K. V. Ramaiah.** 2000. Phosphorylation of serine 51 in initiation factor 2 alpha (eIF2 alpha) promotes complex formation between eIF2 alpha(P) and eIF2B and causes inhibition in the guanine nucleotide exchange activity of eIF2B. *Biochemistry* **39**:12929-38.
156. **Sumpter, R., Y.-M. Loo, E. Foy, M. Yoneyama, T. Fujita, and M. Gale.** 2004. RIG-I defines host cell permissiveness to HCV RNA replication. Submitted.



157. **Sumpter, R., C. Wang, E. Foy, Y.-M. Loo, and M. Gale.** 2004. Viral evolution and interferon resistance of hepatitis C virus RNA replication in a cell culture model. *J Virol* **In press**.
158. **Taha, C., Z. Liu, J. Jin, H. Al-Hasani, N. Sonenberg, and A. Klip.** 1999. Opposite translational control of GLUT1 and GLUT4 glucose transporter mRNAs in response to insulin. *J Biol Chem* **274**:33085-33091.
159. **Taki, S., T. Sato, K. Ogasawara, T. Fukuda, M. Sato, S. Hida, G. Suzuki, M. Mitsuyama, E. H. Shin, S. Kojima, T. Taniguchi, and Y. Asano.** 1997. Multistage regulation of Th1-type immune responses by the transcription factor IRF-1. *Immunity* **6**:673-9.
160. **Tan, S.-L., H. Nakao, Y. He, V. Vijaysri, P. Neddermann, B. L. Jacobs, B. J. Mayer, and M. G. Katze.** 1999. NS5A, a nonstructural protein of hepatitis C virus, binds growth factor receptor-bound protein 2 adaptor protein in a Src homology 3 domain/ligand-dependent manner and perturbs mitogenic signaling. *Proc Natl Acad Sci U S A* **96**:5533-5538.
161. **Taniguchi, T., M. S. Lamphier, and N. Tanaka.** 1997. IRF-1: the transcription factor linking the interferon response and oncogenesis. *Biochimica Et Biophysica Acta* **1333**:9-17.
162. **Taylor, D. R., S. T. Shi, P. R. Romano, G. N. Barber, and M. M. C. Lai.** 1999. Inhibition of the interferon-inducible protein kinase PKR by HCV E2 protein. *Science* **285**:107-110.

163. **TenOever, B. R., M. J. Servant, N. Grandvaux, R. Lin, and J. Hiscott.** 2002.  
Recognition of the measles virus nucleocapsid as a mechanism of IRF-3 activation. *J Virol* **76**:3659-3669.
164. **Thanos, D., and T. Maniatis.** 1992. The high mobility group protein HMG I(Y) is required for NF-kappa B-dependent virus induction of the human IFN-beta gene. *Cell* **71**:777-89.
165. **Thimme, R., D. Oldach, K. M. Chang, C. Steiger, S. C. Ray, and F. V. Chisari.** 2001. Determinants of viral clearance and persistence during acute hepatitis C virus infection. *J Exp Med* **194**:1395-1406.
166. **Trachsel, H.** 1996. Binding of initiator methionyl-tRNA to ribosomes, p. 113-138. *In* J. W. B. Hershey, M. B. Mathews, and N. Sonenberg (ed.), *Translational control*. Cold Spring Harbor Laboratory Press, Plainview, N.Y.
167. **Tuplin, A., J. Wood, D. J. Evans, A. H. Patel, and P. Simmonds.** 2002.  
Thermodynamic and phylogenetic prediction of RNA secondary structures in the coding region of hepatitis C virus. *RNA* **8**:824-41.
168. **Turner, N. C., G. Dusheiko, and A. Jones.** 2003. Hepatitis C and B-cell lymphoma. *Ann Oncol* **14**:1341-5.
169. **von Kobbe, C., J. M. van Deursen, J. P. Rodrigues, D. Sitterlin, A. Bachi, X. Wu, M. Wilm, M. Carmo-Fonseca, and E. Izaurralde.** 2000. Vesicular stomatitis virus matrix protein inhibits host cell gene expression by targeting the nucleoporin Nup98. *Mol Cell* **6**:1243-52.

170. **Wang, C., J. Pflugheber, R. Sumpter, D. Sodora, D. Hui, G. C. Sen, and M. Gale, Jr.** 2003. Alpha interferon induces distinct translational control programs to suppress hepatitis C virus RNA replication. *J Virol* **77**:3898-912.
171. **Wang, L., Y. Guo, W. J. Huang, X. Ke, J. L. Poyet, G. A. Manji, S. Merriam, M. A. Glucksmann, P. S. DiStefano, E. S. Alnemri, and J. Bertin.** 2001. Card10 is a novel caspase recruitment domain/membrane-associated guanylate kinase family member that interacts with BCL10 and activates NF-kappa B. *J Biol Chem* **276**:21405-9.
172. **Wang, X., M. Li, H. Zheng, T. Muster, P. Palese, A. A. Beg, and A. Garcia-Sastre.** 2000. Influenza A virus NS1 protein prevents activation of NF-kappaB and induction of alpha/beta interferon. *J Virol* **74**:11566-73.
173. **Wathelet, M. G., C. H. Lin, B. S. Parekh, L. V. Ronco, P. M. Howley, and T. Maniatis.** 1998. Virus infection induces the assembly of coordinately activated transcription factors on the IFN-beta enhancer in vivo. *Mol Cell* **1**:507-518.
174. **Weaver, B. K., K. P. Kumar, and N. C. Reich.** 1998. Interferon regulatory factor 3 and CREB-binding protein/p300 are subunits of double-stranded RNA-activated transcription factor DRAF1. *Mol Cell Biol* **18**:1359-1368.
175. **Weiner, A. J., H. M. Geysen, C. Christopherson, J. E. Hall, T. J. Mason, G. Saracco, F. Bonino, K. Crawford, C. D. Marion, K. A. Crawford, and et al.** 1992. Evidence for immune selection of hepatitis C virus (HCV) putative envelope glycoprotein variants: potential role in chronic HCV infections. *Proc Natl Acad Sci U S A* **89**:3468-72.

176. **Wek, R. C.** 1994. eIF-2 kinases: regulators of general and gene-specific translation initiation. *Trends Biochem Sci* **19**:491-496.
177. **Williams, B. R.** 2001. Signal integration via PKR. *Sci STKE* **2001**.
178. **Witherell, G. W., and P. Beibeke.** 2000. Statistical analysis of combined substitutions in nonstructural 5A region of hepatitis C virus and interferon response. *J Med Virol* **63**:8-16.
179. **Xiang, Y., R. C. Condit, S. Vijaysri, B. Jacobs, B. R. Williams, and R. H. Silverman.** 2002. Blockade of interferon induction and action by the E3L double-stranded RNA binding proteins of vaccinia virus. *J Virol* **76**:5251-5259.
180. **Yamamoto, M., S. Sato, H. Hemmi, K. Hoshino, T. Kaisho, H. Sanjo, O. Takeuchi, M. Sugiyama, M. Okabe, K. Takeda, and S. Akira.** 2003. Role of adaptor TRIF in the MyD88-independent toll-like receptor signaling pathway. *Science* **301**:640-643.
181. **Yang, C. H., W. Shi, L. Basu, A. Murti, S. N. Constantinescu, L. Blatt, E. Croze, J. E. Mullersman, and L. M. Pfeffer.** 1996. Direct association of STAT3 with the IFNAR-1 chain of the human type I interferon receptor. *J Biol Chem* **271**:8057-61.
182. **Yang, Y.-L., L. F. L. Reis, J. Pavlovic, A. Aguzzi, R. Sch.,fer, A. Kumar, B. R. G. Williams, M. Aguet, and C. Weissmann.** 1995. Deficient signaling in mice devoid of double-stranded RNA-dependent protein kinase. *EMBO J* **14**:6095-6106.
183. **Ye, J., C. Wang, R. Sumpter, Jr., M. S. Brown, J. L. Goldstein, and M. Gale, Jr.** 2003. Disruption of hepatitis C virus RNA replication through inhibition of host protein geranylgeranylation. *Proc Natl Acad Sci U S A* **100**:15865-15870.

184. **Yoneyama, M., M. Kikuchi, T. Natsukawa, N. Shinobu, T. Imaizumi, M. Miyagishi, K. Taira, S. Akira, and T. Fujita.** 2004. The RNA helicase RIG-I has an essential function in double-stranded RNA-induced innate antiviral responses. *Nat Immunol* **5**:730-7.
185. **Yoneyama, M., W. Suhara, and T. Fujita.** 2002. Control of IRF-3 activation by phosphorylation. *J Interferon Cytokine Res* **22**:73-76.
186. **Yoneyama, M., W. Suhara, Y. Fukuhara, M. Fukuda, E. Nishida, and T. Fujita.** 1998. Direct triggering of the type I interferon system by virus infection: activation of a transcription factor complex containing IRF-3 and CBP/p300. *EMBO J* **17**:1087-1095.
187. **Young, K., R. Resnick, and T. Myers.** 1993. Detection of hepatitis C virus RNA by a combined reverse transcription-polymerase chain reaction assay. *J Clin Microbiol* **31**:882-886.
188. **Zhou, A., J. Paranjape, T. L. Brown, H. Nie, S. Naik, B. Dong, A. Chang, B. Trapp, R. Fairchild, C. Colmenares, and R. H. Silverman.** 1997. Interferon action and apoptosis are defective in mice devoid of 2',5'-oligoadenylate-dependent RNase L. *EMBO J* **16**:6355-6363.
189. **Zhu, H., H. Zhao, C. D. Collins, S. E. Eckenrode, Q. Run, R. A. McIndoe, J. M. Crawford, D. R. Nelson, J. X. She, and C. Liu.** 2003. Gene expression associated with interferon alfa antiviral activity in an HCV replicon cell line. *Hepatology* **37**:1180-1188.

190. **Zhu, Q., J. T. Guo, and C. Seeger.** 2003. Replication of hepatitis C virus subgenomes in nonhepatic epithelial and mouse hepatoma cells. *J Virol* **77**:9204-9210.

## VITAE

Rhea Myers Sumpter, Jr. was born in Atlanta, Georgia on February 15, 1975, the son of Anne Diveley Sumpter and Rhea Myers Sumpter, Sr. After graduating from Marist High School, Atlanta, Georgia in 1993, he entered Rice University in Houston, Texas, where he received a degree of Bachelor of Arts with a major in Biochemistry in 1997. He was awarded a Fulbright Fellowship to study at the University of Buenos Aires in Argentina and returned to Dallas to begin work for his M.D. and Ph.D. degrees at the University of Texas Southwestern Medical School in the summer of 1998. In 2001 he married Kathryn Maria Noack of St. Petersburg, Florida. They have two dogs, Lyle and Willie.

Permanent address: 9946 Mixon Dr.  
Dallas, TX 75220